# Plasma assisted conversion of biogas at atmospheric pressure supported by a DBD and the influence of additives on the product distribution

Von der Fakultät für Lebenswissenschaften

der Technischen Universität Carolo-Wilhelmina

zu Braunschweig

zur Erlangung des Grades eines

Doktors der Naturwissenschaften

(Dr. rer. nat.)

genehmigte

**D i s s e r t a t i o n**

von Torsten Kolb
aus Salzwedel

1. Referent: Professor Dr. Karl-Heinz Gericke
2. Referent: Privatdozent Dr. Christof Maul
Eingereicht am: 24.10.2012
mündliche Prüfung (Disputation) am: 07.12.2012

Druckjahr 2012

## Vorveröffentlichungen der Dissertation

Teilergebnisse aus dieser Arbeit wurden mit Genehmigung der Fakultät für Lebenswissenschaften, vertreten durch den Mentor der Arbeit, in folgenden Beiträgen vorab veröffentlicht:

### Publikationen

[1] Kolb, T., Voigt, J.H., & Gericke, K.-H. Conversion of methane and carbon dioxide in a DBD reactor – influence of oxygen. Plasma Chemistry and Plasma Processing, submitted (2012).

[2] Kolb, T., Kroker T., Voigt, J. H. & Gericke, K.-H. Wet conversion of methane and carbon dioxide in a DBD reactor. Plasma Chemistry and Plasma Processing, DOI: 10.1007/s11090-012-9411-y (2012).

[3] Kolb, T., Kroker T. & Gericke, K.-H. Conversion of biogas like mixtures to C2 hydrocarbon in a plug flow reactor supported by a DBD at atmospheric pressure. Vacuum 88:144-148 (2013).

### Tagungsbeiträge

[1] Kolb, T., Voigt, J. H. & Gericke, K.-H.: Affect of water and oxygen on the Conversion of Methane and Carbon Dioxide in a Plug Flow Reactor Supported by a DBD. (Vortrag) Hakone XIII, Kazimierz Dolny (Polen) (2012).

[2] Kolb, T., & Gericke, K.-H.: Influence of Water on the Conversion of Methane and Carbon Dioxide in a Plug Flow Reactor Supported by a DBD. (Vortrag) DPG-Tagung , Stuttgart (2012).

[3] Kolb, T., Kroker T. & Gericke, K.-H.: Conversion of methane and carbon dioxide to C-2 hydrocarbon in a plug flow reactor supported by a DBD at atmospheric pressure. (Vortrag) ISAPS, Hakone (Japan) (2011).

[4] Kroker, T., Kolb, T., Schenk, A., Gericke, K.-H., Młotek, M., Krawczyk, K. & Schmidt-Szałowski, K.: Catalytic Conversion of Biogas to Synthesis Gas in a Fluidised Bed Reactor Supported by a DBD. DPG-Tagung, Hannover (2010).

# Table of Content

Table of Figures ..... VIII

List of Tables ..... IX

1 Introduction ..... 1

1.1 Regenerative sources for methane and carbon dioxide ..... 2

1.2 State of the research, scope of work and target of this thesis ..... 4

2 Theory ..... 7

2.1 Introduction to plasma ..... 7

2.2 Generation of a plasma ..... 8

2.3 Paschen Law ..... 11

2.4 Dielectric Barrier Discharge ..... 12

3 Experimental Setup ..... 17

3.1 Gas supply ..... 17

3.2 Reaction chamber with the DBD reactor and the plasma generator ..... 18

3.3 Analysis range ..... 20

3.3.1 FTIR spectrometer ..... 20

3.3.2 QMS ..... 21

3.4 Generation of the vacuum ..... 21

4 Performance of the experiments ..... 23

4.1 Different plasma power ..... 23

4.2 Different concentration of the additives ..... 23

5 Qualitative analysis ..... 25

6 Calibration of the FTIR spectrometer and the QMS ..... 28

6.1 Gaseous substances ..... 28

6.2 Methanol and formaldehyde ..... 30

7 References for section 1 to 6 ..... 32

8 Conversion of biogas like mixtures to $C_2$ hydrocarbon in a plug flow reactor supported by a DBD at atmospheric pressure ..... 35
8.1 Introduction ..... 36
8.2 Experimental procedure ..... 36
8.3 Results and discussion ..... 38
8.4 Conclusion ..... 44
8.5 References for section 8 ..... 45
9 Wet conversion of methane and carbon dioxide in a DBD reactor ..... 46
9.1 Introduction ..... 47
9.2 Experimental setup ..... 48
9.3 Results and discussion ..... 50
9.3.1 Conversion of the starting material ..... 51
9.3.2 Oxygenated hydrocarbons ..... 54
9.3.3 Synthesis gas ..... 58
9.3.4 C2 hydrocarbons ..... 62
9.3.5 Total consumed energy ..... 63
9.4 References for section 9 ..... 66
10 Conversion of methane and carbon dioxide in a DBD reactor – influence of oxygen ..... 68
10.1 Introduction ..... 69
10.2 Experimental Setup ..... 70
10.3 Results and discussion ..... 70
10.3.1 Influence of oxygen on the conversion of methane and on the product distribution ..... 72
10.3.2 Influence of methane, carbon dioxide, and plasma power on the product distribution. ..... 79
10.4 Conclusion ..... 86
10.5 References for section 10 ..... 88
11 Conclusion ..... 89

12 Acknowledgement ..... 91

# Table of Figures

Figure 1.1: Regenerative sources for methane and carbon dioxide and its feed stock ..... 2
Figure 2.1: Voltage-current characteristic of DC low pressure electrical discharge and the corresponding circuit diagram ..... 9
Figure 2.2: Paschen curves for different gases ..... 11
Figure 2.3: Configuration of dielectric barrier discharges ..... 13
Figure 2.4: Development and processing of a dielectric barrier discharge ..... 14
Figure 3.1: Schematic setup of the current experiment. ..... 17
Figure 3.2: The DBD reactor. ..... 18
Figure 5.1: Spectra of the inlet flow consisting of 2% methane, 0.5% carbon dioxide, 0.5% oxygen and 97% helium and after igniting 70 W plasma ..... 25
Figure 5.2: QMS spectra after igniting a 70 W plasma ..... 26
Figure 6.1: Graphs for the calibration of the analysis devices (left: FTIR with CO; right: QMS with $H_2$) ..... 28
Figure 6.2: Schematic setup to calibrate the FTIR spectrometer with methanol and formaldehyde. ..... 30
Figure 8.1: Schematic setup ..... 37
Figure 8.2: Spectra of the inlet flow (7 sccm $CH_4$, 3 sccm $CO_2$, 390 sccm He) and the product stream (generator power: 65 W). ..... 38
Figure 8.3: Produced amount of C2 hydrocarbons as a function of the adjusted generator power. ..... 39
Figure 8.4: Conversion of methane as a function of the adjusted generator power 41
Figure 8.5: Influence of the flow velocity on the ethane yield ..... 42
Figure 8.6: Produced amount of ethane as a function of the adjusted generator power for different inlet mixtures at a flow rate of 200 sccm. ..... 42
Figure 8.7: Selectivity of this reactor for the three C2 hydrocarbons as a function of the inlet power ..... 43
Figure 9.1: Schematic setup of the current experiment. ..... 48
Figure 9.2: The DBD reactor used in this experiment ..... 49

Figure 9.3: Conversion of methane and carbon dioxide as a function of the water proportion ..... 52
Figure 9.4: Conversion of methane as a function of plasma power and $CH_4$ composition of the inlet flow. ..... 53
Figure 9.5: Conversion of carbon dioxide as a function of plasma power and $CH_4$ composition of the inlet flow. ..... 53
Figure 9.6: Methanol and formaldehyde yield as a function of added water. ..... 55
Figure 9.7: Selectivity of the two oxygenated hydrocarbons for different amounts of water ..... 56
Figure 9.8: Methanol yield for different plasma powers and $CH_4$ composition of the inlet flow ..... 56
Figure 9.9: Formaldehyde yield for different plasma powers and $CH_4$ composition of the inlet flow. ..... 57
Figure 9.10: Dependency of the yield of the synthesis gas components on the amount of water and the ratio of hydrogen to carbon monoxide. ..... 58
Figure 9.11: Selectivity of the synthesis gas components for different amounts of water ..... 60
Figure 9.12: Yield of the synthesis gas components and their ratio ($H_2$:CO) on the plasma power for different composition of the inlet flow at a fixed amount of water (17%). ..... 61
Figure 9.13: Yield of C2 hydrocarbons in a DBD reactor.. ..... 62
Figure 9.14: Total consumed energy for the conversion in this DBD reactor for different water amounts. ..... 63
Figure 10.1: Conversion of methane and oxygen as a function of the oxygen portion. ..... 72
Figure 10.2: Product distribution of the synthesis gas components ($H_2$ and CO), left scale, and their ratio ($H_2$:CO), right scale, for different amounts of oxygen in the inlet gas ..... 73
Figure 10.3: Yield of C2 hydrocarbons as a function of the amount of oxygen ..... 75
Figure 10.4: Methanol and formaldehyde yields as a function of the amount of oxygen ..... 76
Figure 10.5: Above: Selectivity calculated from C balance as a function of the added oxygen. Below: Selectivity of methane to hydrogen. ..... 77
Figure 10.6: Total consumed energy for different concentration of oxygen ..... 78

Figure 10.7: Conversion of methane as a function of the concentration of the starting material ($CH_4$, $CO_2$ and $O_2$) and the plasma power ..... 79
Figure 10.8: Conversion of carbon dioxide as a function of the concentration of the starting material ($CH_4$, $CO_2$ and $O_2$) and the plasma power ..... 80
Figure 10.9: Formaldehyde yield for different compositions of the inlet gas and plasma power ..... 82
Figure 10.10: Influence of the plasma power and the composition of the inlet gas on the concentration of methanol.. ..... 83
Figure 10.11: Yield of the synthesis gas components as a function of the power and the composition of the inlet gas at a fixed amount of oxygen ..... 84
Figure 10.12: Influence of the plasma power and the composition of the inlet gas on the ethane yield.. ..... 86

## List of Tables

Table 1.1: Distribution of the compounds in biogas, sewage gas, and landfill gas .... 2
Table 2.1: Characteristic micro discharge properties. ..... 15
Table 2.2: Ionization and dissociation processes for the experiment performed in this work ..... 15
Table 5.1: Distribution of higher hydrocarbons. ..... 27
Table 6.1: Summary of the calibration of the FTIR spectrometer ..... 29
Table 6.2: Summary of the calibration of the QMS. ..... 30
Table 9.1: Summery of the wet conditions. ..... 65
Table 10.1: Conversion of oxygen as a function of the concentration of the starting material ($CH_4$, $CO_2$) and the plasma power ..... 81

# 1 Introduction

Nowadays, most basic organic chemicals as saturated and unsaturated hydrocarbons are manufactured from crude oil or natural gas. These fossil fuels will run out in the future. The end of the crude oil extraction will be reached in about 50 years [1] and for natural gas in over 100 years [2]. This information is only valid in the case of a moderate increase of the consumption of such fuels. Thus, new techniques are required to produce organic chemicals. One possibility could be the conversion of methane and carbon dioxide. Both gases are not very reactive. The Hydrogen atoms in the tetrahedral structure of methane protect the molecule for reactions with other molecules at ambient temperature and pressure. Carbon dioxide is a stable product of the compete combustion of carbonaceous compounds. Therefore, the reactivity of both components has to be increased in order to convert them to other useful products. Thermal heating or/and the use of a catalyst [3-6] are well-known opportunities to convert methane and carbon dioxide, thereby, steam reforming of methane [7] is the most important activation process. The main products are synthesis gas, a mixture of hydrogen and carbon monoxide. The following formula explains the process:

$$CH_4 + H_2O \rightarrow 3H_2 + CO \qquad (1.1)$$

A temperature of 975 to 1375 K, a nickel catalyst and high pressure (3-25 bar) are required to obtain the products for the reaction (1.1).

However, igniting plasma at low temperature and atmospheric presure is an alternative route to activate methane and carbon dioxide. To this end, different plasma sources are mentioned in the literature [8, 9], examples are corona discharges, gliding arcs, dielectric barrier discharges (DBD) and microwave discharges. Here, the conversion of a molecule in a plasma reactor occurs through plasma electrons. The molecules are ionized on the one hand or dissociated to radicals on the other hand while the reactive species recombine to new products. Thus, synthesis gas, saturated and unsaturated hydrocarbons or oxygenates are generated in the case of using methane and carbon dioxide as a starting material.

Natural gas is the main source for starting material methane which has an amount of up to 99% [10]. It is also generated in agriculture. Examples are rice fields during the plant growth and the digestion of ruminants as cows, cattle and harts. The complete combustion of fossil fuels as crude oil, natural gas as well as coal is a main source to produce carbon dioxide.

In summary, both gases originate mainly from fossil fuels running out in the future. But, why is the use of methane and carbon dioxide an alternative route to generate basic organic chemicals after the fossil fuels will be consumed? There are two reasons:

Firstly, both compounds are renewable, being generated in an anaerobe digestion of biomass. The resulting gas mixture is called bio-, landfill- or digester gas, depending on the starting material. Further details are discussed in section 1.1. Secondly, $CO_2$ as well as methane are potent greenhouse gases. Both gases leave the surface of the earth and attain the Earth's atmosphere. The Earth emits IR radiation which is absorbed by the greenhouse gases. Thereby, the average temperature on the surface of our planet increases. Due to its total amount, carbon dioxide is the main greenhouse gas. One third of the artificially generated $CO_2$ is produced commercially in power stations generating electricity [11]. The artificial greenhouse effect will be reduced if the amount of these gases blowing through chimneys into the environment is reduced by industrial conversion, for example in a plasma reactor. Methane is the second important greenhouse gas, having a 25 times stronger heat trapping ability per molecule than carbon dioxide.

## 1.1 Regenerative sources for methane and carbon dioxide

The first sections of paragraph one give a short introduction into the topic of this thesis. This subsection deals with methane and carbon dioxide as a regenerative source. A detailed discussion about the starting material, the development, and the contribution for this process is given in the next paragraphs.

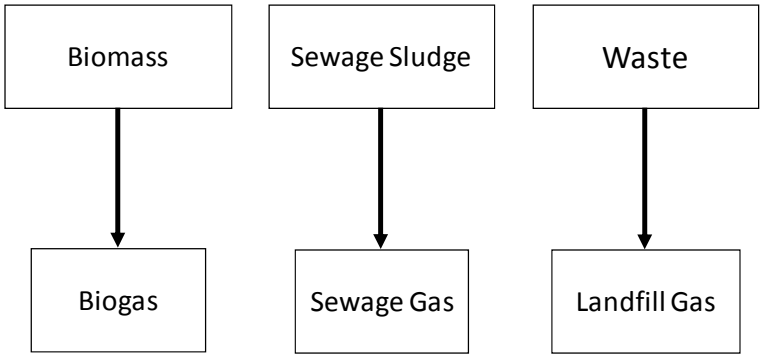


**Figure 1.1:** Regenerative sources for methane and carbon dioxide and its feed stock.

Renewable sources as biomass, organic waste and sewage sludge are converted to gases consisting mostly of methane and carbon dioxide. These gas mixtures are

called biogas, sewage gas or landfill gas, depending on the process parameter. Figure 1.1 illustrates the connection of different types of gases to its basic material.
The starting material for biogas is biomass, consisting of plants as corn, crops and sugar beets and often slurry [12]. A high methane production is the requirement for plants, thereby, corn has the best yield (340-360 l/(g of organic dry matter) [13]). In landfills, herbal and animalistic organic waste is converted. Byrne [14] defined waste as a “material, which has no direct value to the producer and so must be disposed of”. Urban sewage water is purified in a sewage plant. The result is clean drinking water and sludge. The latter one is transferred to sewage gas.

**Table 1.1:** Distribution of the compounds in biogas, sewage gas, and landfill gas [1,15,16].

| Compound | Biogas | Sewage Gas | Landfill Gas |
|---|---|---|---|
| Methane [vol. %] | 50 - 75 | 61 – 65 | 40 – 60 |
| Carbon dioxide [vol. %] | 25 – 50 | 36 – 38 | 20 – 40 |
| Nitrogen [vol. %] | 0 – 5 | 0 – 2 | 2 – 20 |
| Oxygen [vol. %] | 0 – 2 | 0 – 1 | 0 – 1 |
| Hydrogen [vol. %] | 0 – 1 | 0 | 0 – 1,5 |
| Hydrogen Sulfide [ppm] | 50 – 6000 | 10 - 80 | 20 – 200 |
| Ammonia [vol. %] | 0 - 1 | 0 | 0 |

In general, the processes to receive a mixture of methane and carbon dioxide are nearly the same. The anaerobic digestion occurs in the absence of air and is typically carried out over a period of a few weeks [1]. Four steps [13] are required to transfer the starting material to methane and carbon dioxide:

- hydrolysis
- acidogenesis
- acetogenesis
- methanogenesis

Different kinds of bacteria break the organic macromolecules as polysaccharides, proteins and lipids to mainly methane and carbon dioxide. Other products in a lower concentration are nitrogen, oxygen, hydrogen, water vapor, hydrogen sulfide, and ammonia. This typical product distribution is shown in Table 1.1.
All of these gas mixtures are mainly applied in order to produce electricity and heat. It would be best to use only sewage and landfill gas, but no biogas because the latter is generated from plants which are needed as a food source while the former two are produced from waste.

Methane and carbon dioxide originating from biomass, sludge, and waste will be referred to as biogas in the following for simplicity seasons.

## 1.2 State of the research, scope of work and target of this thesis

Different sources of biogas have been discussed in the previous subsection. This part will focus on the use of simulated biogas consisting only of methane and carbon dioxide.

The state of the technology to use a DBD reactor for the conversion of methane and carbon dioxide will be summarized below.

Intense research has been performed to convert methane and carbon dioxide inside a DBD reactor. The measurements occurred at atmospheric pressure, low temperature, for discharge frequencies in the range of a few Hertz, at high frequencies and at different velocities of the flow and different concentrations of methane and carbon dioxide. Thereby, synthesis gas [11,17-22] (hydrogen and carbon monoxide), hydrocarbons [20,23-28] (especially with two carbons) and oxygenates [20,23, 24] such as methanol and formaldehyde have been the main products. The plasma process is often supported by catalysts [18-22,25]. The temperature [11,19-21,25,28] in the DBD reactor is measured to maintain the best operating range for the catalysts.

In short, low flow rates and high wall temperatures of the reactor have a positive effect on the conversion of methane and carbon dioxide. Methane rich feed generates hydrogen and hydrocarbons in high concentrations. A carbon dioxide rich inlet flow has a positive effect on the yield of carbon monoxide. A catalyst consisting of palladium on aluminum oxide increases the produced concentration of C2 hydrocarbons and hydrogen. If zeolite is used as a catalyst, the yield of hydrocarbons rises. All catalysts have a negative effect on the conversion of the starting material.

Several working groups have analyzed the influence of additives such as helium [17], oxygen [23,28,30,31,32] and water vapor [31,33] on the conversion of methane and carbon dioxide. Helium generally increases the conversion of the starting material. Oxygen increases, not only the conversion of methane, but also the concentration of oxygenates being generated in lower concentration without oxygen. Finally, additional water in the reaction chamber decreases the conversion of methane and raises the yield of carbon monoxide and hydrogen.

In contrast to the references mentioned above ([11,17-33]), the current experiments are driven at radio frequency (13.56 MHz) instead of using a frequencies between a few hertz and some hundred kilohertz. The essential difference between the radio

frequency (rf) and lower frequencies is that for rf ions do not move very far during a half cycle and, therefore, the source of the initially formed radicals are electron collisions only with neutral molecules. This different process might lead to a different chemistry.

Previously work with the current rf setup was performed by Kroker [34]. In this work the setup was developed and characterized, and experiments at 100 mbar and at atmospheric pressure were carried out. Gas mixtures consisting of methane and carbon dioxide were converted in a DBD reactor at different plasma power, catalysts and temperatures with the form of the studies centered on investigating the role of catalyst. Helium was used to dilute the gas mixture. Synthesis gas and ethane are the main products for all pressure ranges studied. The conversion of the starting material and the yield of the synthesis gas components at atmospheric pressure where studied [35, 36].

One objective of this thesis is to optimize and refine the apparatus being used by Kroker. The main focus, however, is to investigate the influence of water and oxygen an as an additive on the product distribution and the improvement of the conversion to the inlet gas mixture. All this experiments are done under the aspect of reducing the amount of consumed energy.

The current work focuses on the conversion of a simulated biogas mixture in a cylindrical DBD reactor at atmospheric pressure with a frequency of 13.56 MHz. The inlet flows are diluted with helium to 2.5%. The starting material and the product stream are analyzed in a Fourier transform infrared spectrometer (FTIR) and a quadrupole mass spectrometer (QMS).

Three different topics are researched in this thesis:

1) Analysis of the conversion of methane and carbon dioxide to C2 hydrocarbons
2) Influence of water on the conversion of the starting material
3) Impact of oxygen on the conversion of simulated biogas

Therefore, the contribution of methane and carbon dioxide in the inlet flow is altered in the first part of this thesis. At different plasma power and flow rates, the conversion of this material is investigated. Conversion of the starting material, yield and selectivity of ethane, ethylene and ethine are herein the main focus. In parts, data were obtained by Bruchmann [37], Haak [38], Schmidt [39] and Schäfer [40] for their bachelor theses under the author’s guidance.

The second and the third part of this thesis have many similarities follow a similar experimental strategy for the two additives water and oxygen. The influence of the additives (water and oxygen) on the plasma assisted conversion of methane and carbon dioxide is analyzed. To begin with, the concentrations of water and oxygen are varied.

In the second step, the amount of the additives is fixed to 17% and the concentration of methane and carbon dioxide is altered. Here, product distributions as well as the conversion of the starting material are in the focus of intrest. A VI probe is used for these experiments to calculate the total consumed energy. In parts, data were obtained by Wilharm [41], Song [42] and Homolya [43] for their bachelor theses under the author's guidance.

Previous work of Wang et al. [31] and Mfopara et al. [33] were performed for a different frequency range and for selected compositions of inlet gas mixture. In this work, the role of water and oxygen were comparatively studied for a large variation of gas mixtures.

# 2 Theory

The first part of this chapter gives a short introduction about plasma chemistry and the special possibility to convert molecules. The second part of the theory section will focus on the DBD reactor being used in this research.

## 2.1 Introduction to plasma

Irving Langmuir introduced the term plasma first in 1928 [44]. Plasma is defined as a partly or completely ionized gas [45-49] being generated through heating up a gas to a few thousand Kelvin. Therefore, this condition is often named as the fourth state of aggregation beside solid, liquid and gaseous. The plasma state is quasi neutral because the number of electrons is equal to the number of charged particles. Nevertheless, the electrons and ions move in the plasma volume and form negative or positive charged regions on the molecular scale. An external magnetic or electric field increases the volume having more ions or electrons.

There are numerous examples for naturally occurring plasmas. The sun is a well-known example. The surface temperature of about 6000 K is generated through nuclear fusion of hydrogen atoms to helium. The matter at the surface reaches the plasma state because of high temperature. Another example is lightning resulting from a potential difference within clouds or between clouds and the surface of the earth producing a discharge.

The above mentioned plasmas can be allocated to the category of a hot plasma. There, neutral particles, ions and electrons are in a thermal equilibrium. The exchange of the temperature occurs through collisions. This kind of plasma is called thermal, equilibrium or isothermal plasma. The opposite is a nonthermal plasma where the electrons and ions/neutral particles are not in a thermal equilibrium. This is achieved at low pressure, where the probability of a collision is lower and the mass difference is too large to exchange the energy effectively. Here, the temperature of the ions and neutral particles is several hundred Kelvin while the electrons have a temperature of some 10,000 K. As an advantage, a reaction with large activation temperature will be activated in such a plasma. Fluorescent tubes, plasma TV sets, and modification of surfaces are examples for applications at low temperatures.

A plasma is characterized by the degree of ionization X as the following equation shows:

$$x = \frac{n_e}{n_e + n_0} \tag{2.1}$$

$n_e$ ..... number density of electrons [$1/m^3$]
$n_0$ ..... number density of neutrals [$1/m^3$]

A thermal plasma has a high degree of ionization; the matter is nearly complete ionized. A weakly ionized plasma is typical for a non-thermal plasma with an ionization rate of typically less than $10^{-2}$. Another important parameter is the density of the ions ($n_i$) which has the same value as $n_e$. The plasma in the DBD reactor used in this work is weakly ionized, with a degree of ionization of about $10^{-4}$ [50].

## 2.2 Generation of a plasma

This section deals with the different possibilities of igniting a plasma: Collision of particles, electromagnetic radiation; or strong electric field are examples to generate ions beside the thermal energy already mentioned above. Common to all these sources is that they need to provide a certain energy to ionize a molecule or an atom which is called the ionization energy. The values to remove one electron range between ca. 4 eV and 25 eV [51]. Much more energy is required for a multiple ionization of a molecule or atom. In the experiments performed in this work, the ignition of the plasma occurs through controlling the current and the voltages in the DBD reactor. Thus, the following paragraphs focus only on electrically ignited plasma.

An anode and a cathode are required for an electrical gas discharge. A parallel plate type capacitor is the easiest application. The following parameters are important to ignite a plasma:

- Number of free electrons
- Mean free path of electrons

It is not possible to generate plasma electrically without initially present free charges. Therefore, at least a small part of the gas has to be ionized e.g. through natural radioactivity or cosmic radiation in the absence of plasma. If a significantly strong electronic field is applied, electrons all be accelerated in the electric field to reach the ionization energy of the neutral particles.

The mean free path of the electrons is given by the following equation:

$$\lambda = \frac{k \cdot T}{\sqrt{2}\sigma p} \tag{2.2}$$

k ..... Boltzmann constant [$1.381 \cdot 10^{-23}\,J/K$]
T ..... Temperature [K]
σ ..... Collision cross section [$m^2$]
p ..... Pressure [Pa]

Equation (2.2) displays the average distance travelled by an electron between two collisions. The electron is accelerated over this distance if a voltage is applied. In order to ignite a plasma, the mean free path has to be long enough for the kinetic energy of the electron to reach the ionization energy of the molecules and atoms. The ignition of the plasma is controllable by increasing the applied voltage until the electric field is high enough to generate secondary electrons after a collision of a primary electron with a particle.

The voltage / current characteristic of a discharge and the coresponding circuit diagram are shown in Figure 2.1. This graph is divided into three parts: the dark, glow and arc discharge. The circuit diagram for all processes is shown on the top right. It consists of an external voltage source, the plasma, a resistance, and devices to measure the current and the voltage across the plasma zone.

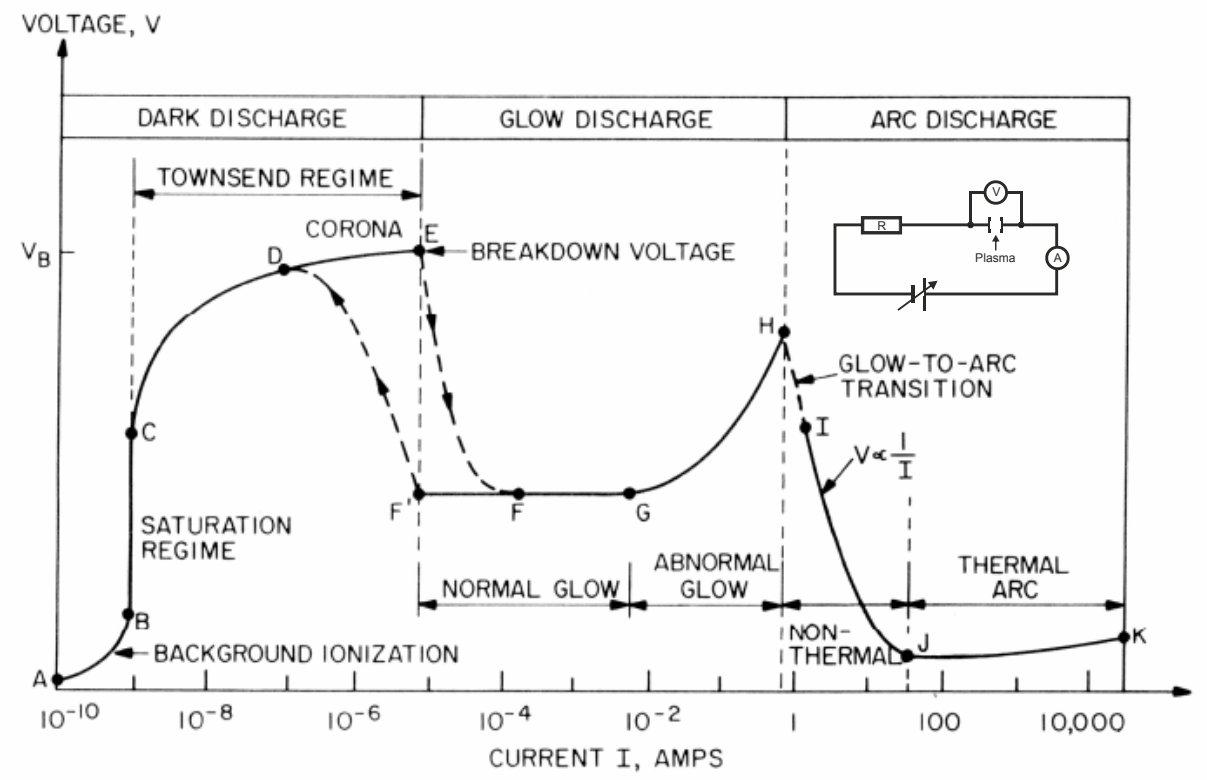


**Figure 2.1:** Voltage-current characteristic of the DC low pressure electrical discharge and the corresponding circuit diagram (top right) [52] (A: background ionization, B: saturation regime, C: begin of the Townsend regime, D: corona discharge, E: electrical breakdown, F – G: normal glow discharge, G – H: abnormal discharge, H – I: glow to arc transition, I – J: non thermal arcs, I – K: thermal arcs).

The dark discharge is invisible to the eye and is divided into the background ionization (A → C) and the Townsend (C → E) regimes. The free charge carriers in the for-

mer are produced through background ionization due to cosmic rays, e.g. these carriers are in equilibrium of ionization and recombination reactions. The charged particles are accelerated to the oppositely charged electrode after a voltage is applied because of the electric field. Therefore, not all ions and electrons can recombine to form the neutral particles resulting in an increase of the voltage between the plasma electrodes. Simultaneously, the resulting electrons are moving towards the positive part of the power supply unit resulting in a measurable electron flow. After changing the voltage at the adjustable power-supply such that the current increases from A to C, the potential difference between the plasma electrodes increases, because the resistance in the plasma area increases.

After reaching point C, the current approaches a limit. At this stage, the electric field becomes high enough to accelerate the free electrons to an energy being longer than the ionization energy of the particles. Now, secondary electrons are created before the primary electrons reach the anode, and the resistance in the plasma area decreases. In contrast to the ionization, the recombination process is dominated in the region C → E. Therefore, this part is called the dependent discharge in the Townsend regime. The secondary electrons are accelerated in the electric field. If the mean free path is long enough, the electrons can ionize other particles. The electrons are proliferated similar to avalanche. In point E, the voltages is high enough to generate many electrons to ignite the plasma. The voltage at that point is called ignition voltage.

Between E and H the plasma is in the glow discharge region, where the DBD reactor used in this work operates. The plasma is luminous there and the number of electrons proliferates now like an avalanche. The electron number density and energy are high enough to excite molecules and atoms in the visible region. This region is well-known in everyday live. Examples are plasma TVs, the yellow light of the street lights (sodium vapor lamp) and fluorescent tubes in different colors. The voltage decreases after igniting plasma at point E and increasing the current because the resistance in the plasma zone decreases. Thereafter, the voltage is over several orders of magnitude independent of the current. At point G, the normal discharges change over to the abnormal glow discharge and the potential difference between the plasma electrodes increases again. The electrodes are heated up through the continuous bombardment of electrons and ions. Thus, electrons are emitted thermally out of the electrode.

An arc discharge is created for currents higher than point H. High temperatures of the electrodes, local discharge spots on the electrode, higher discharge currents and a smaller voltage are characteristics of arcs. This kind of plasma is for instance used to generate ethine and for electric arc welding.

## 2.3 Paschen law

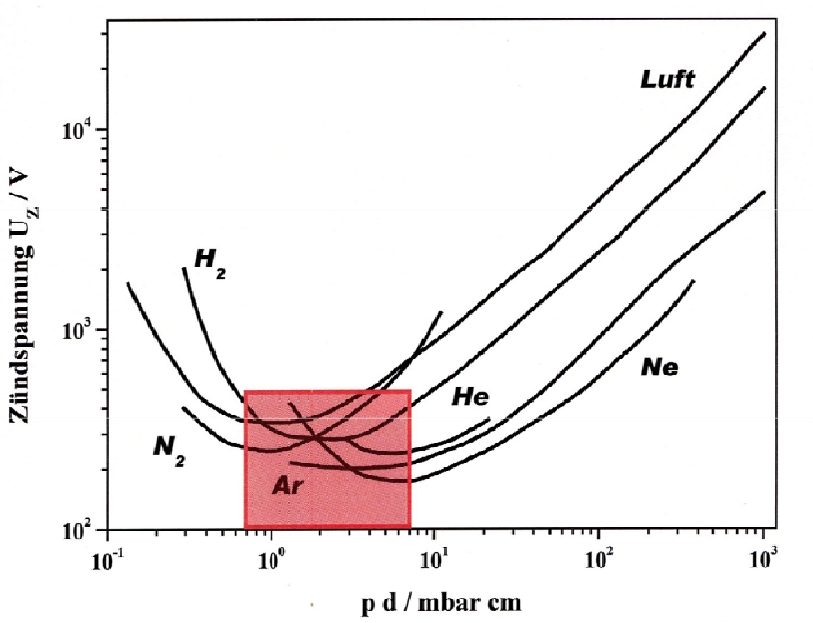


**Figure 2.2:** Paschen curves for different gases [34, 54].

Friedrich Paschen [53] developed in 1889 the relationship between igniting voltage and the coefficient of pressure (p) and distance of the electrodes (d). The ignition voltages ($U_I$) as a function of the product of $p \cdot d$ for different gases are shown in Figure 2.2 being calculated by using the Paschen formula:

$$U_I = \frac{B \cdot (p \cdot d)}{C + \ln\left(\frac{p}{p^0} \cdot \frac{d}{d^0}\right)} \tag{2.3}$$

C ..... gas characteristic constant
B ..... Stoljetow constant
$p^0$ ..... Reference pressure
$d^0$ ..... Reference distance

The constant B represents the minimal ionization energy and depends on the gas:

$$B = \left(\frac{E}{p}\right)_{min} = \left(\frac{U_I}{p \cdot d}\right)_{min} \tag{2.4}$$

E ..... Electric field [V/m]

As shown in Figure 2.2, all gases have a characteristic minimum for the ionization voltage. The curves rise continuously on both sides of the minimum.

The slopes on the left side of the maximum are explainable with the reduced gas pressure. Thus, the mean free path of an electron increases and the number of collision decreases. As a result, the energy of the electrons is high enough to ionize the particles but an electron particle collision has a lower probability. A higher voltage is required to ignite the plasma. The ignition is not possible for too low values of $p \cdot d$.

The contrary is observed on the right side of the Paschen minimum in comparison to the left side. Here, the particle density is very large, therefore, the number of collision increases and the free mean path decreases. The electrons cannot reach the required ionization energy. The deficit in energy is balanced by increasing the electric field to higher values.

In summary, secondary electrons being generated through primary electrons are the source for generating plasma. They are produced through a collision of a neutral particle with primary electron. The electrons receive their energy through electric fields. A gas with low ionization energy will be ionized at lower electric fields than a particle with higher ionization energy. As a result, the ignition voltage is lower for the former than for the latter. Helium has a lower Paschen minimum in comparison to methane and carbon dioxide, because its cross section is lower, resulting in a larger mean free path of the electrons. For easier ignition of the plasma, the inlet flow of our experiment is therefore diluted with helium.

## 2.4 Dielectric Barrier Discharge

The plasma assisted conversion of methane and carbon dioxide to other useful chemicals is the subject of this dissertation. Here, initiating a non thermal plasma and the avoidance of arcs are two important requirements. There are different ways for igniting of the plasma. Tao et al.[8] analyzed the advantages and disadvantages of common plasma sources in their review article. Corona discharge, dielectric barrier discharge, microwave discharge, atmospheric pressure discharge and the gliding arc are listed there. He found that the first two are non uniform plasma sources with low electron density. The uniform microwave discharge needs to complicated and expensive equipment for industrial applications. The last two are difficult to enlarge.

In this work, a DBD reactor was used to convert the starting material. On the one hand, a wide range of the electron energy (1 – 10 eV) by avoiding the formation of sparks and arcs and the electron density of $10^{14}$ – $10^{15}$ $cm^{-3}$ are advantages of this

technique. Its flexibility with respect to geometrical configuration, operating medium and operating parameters is unprecedented as well as a scale up to large industrial installations and the low cost for power supplies [55]. On the other hand, inhomogeneous discharge space resulting in a limited reaction region and a low energy efficiency are the disadvantages.

A dielectric barrier discharge (DBD) is also known as silent discharge or barrier discharge. Siemens [56] reported the first experimental investigations in 1857. He developed a process to generate ozone from oxygen or air in a DBD reactor. The novel feature of Siemens discharge apparatus is the fact that electrodes were positioned outside the chamber and came not in contact with the plasma [57].

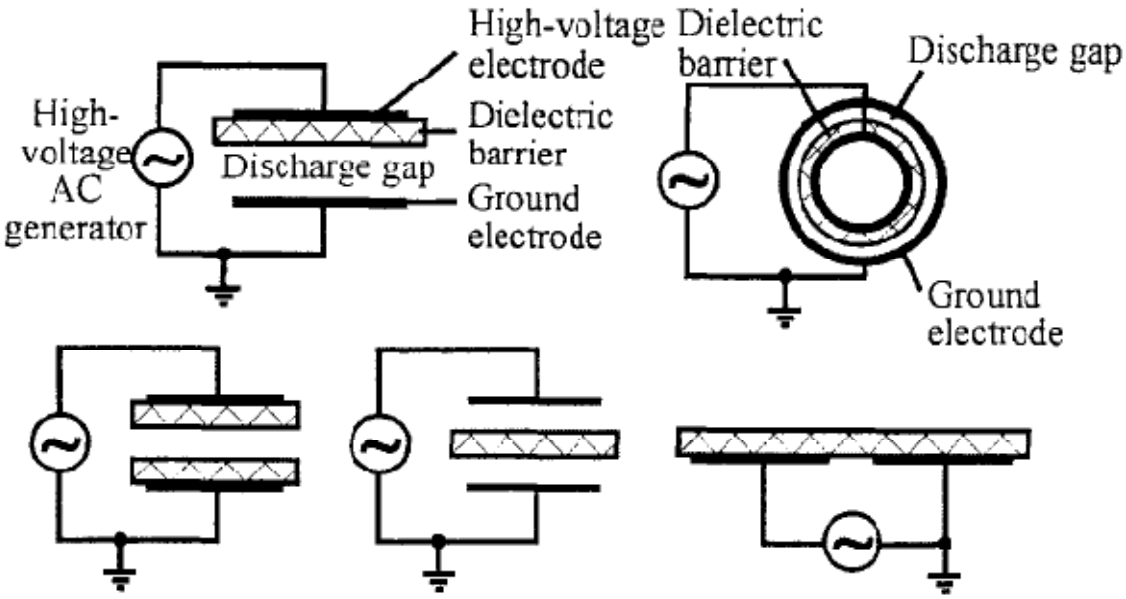


**Figure 2.3:** Configuration of dielectric barrier discharges [48].

At least one electrode is covered with a dielectric in a DBD. Common dielectric materials are glass, enamel, ceramic, silica glasses, plastic and Teflon. Therefore, alternating voltages are required to operate a DBD reactor. Thus, the electric field in the discharge gap has to be high enough to cause a breakdown. Typical electrode configurations are shown in Figure 2.3. The electrodes and dielectrics can be arranged in a planar or cylindrical configuration. Generally, one electrode is grounded while the other electrode is supplied with an alternating current.

A cylindrical design is used in the experimental setup used in this work. The outer ground electrode is covered with Duran glass. There are numerous industrial applications [57] for such a plasma source. Surface treatment of plastic foils and other poly-

mer material, $CO_2$ Lasers, ultraviolet excimer lamps and plasma display panels are examples for DBDs beside the generations of ozone.

Micro filaments are formed in the discharge zone of a DBD reactor, thereby, the plasma is not homogenous. The ionization rate is low outside the filaments. Figure 2.4 illustrates the development of the plasma in one filament. The process is divided into three parts:

(1) Triggered avalanche

(2) Creation of a microfilament and an electron cluster

(3) Termination of discharge

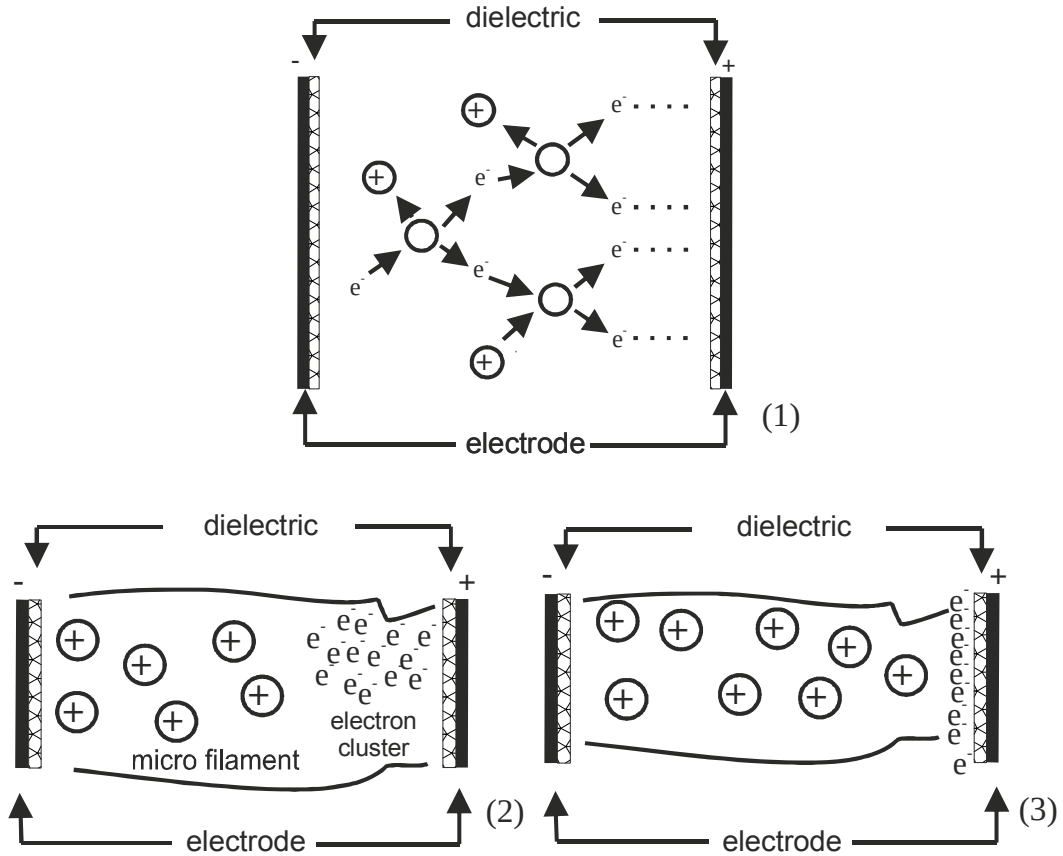


**Figure 2.4:** Development and processing of a dielectric barrier discharge, (1) triggered avalanche, (2) creation of a micro filament and an electron cluster, (3) termination of discharge.

Free electrons are required to start a triggered avalanche. They are generated by cosmic radiation and natural radioactivity. Thus, the electrons get accelerated after applying a high voltage to reach at least the ionization energy of the inlet gas. As a result, the primary electron detaches another electron after a collision with a neutral particle. Both electrons are then accelerated and repeat this ionization process another time to generate two more electrons. This process continues so that the number of free electrons rises exponentially. Therefore, the electrons create an ava-

lanche in which the number of electrons doubles with each generation of ionizing collisions [58].

In comparison to the electrons, the ions are less mobile, therefore, the former form a cluster. The electron swarm moves to the anode leaving the slower ions, and excited active species behind that can induce further chemical reactions. The micro filament is formed at that stage.

**Table 2.1:** Characteristic micro discharge properties [55].

| | |
|---|---|
| duration | 1-10 ns |
| filament radius | about 0.1 mm |
| peak current | 0.1 A |
| Current density | 100 – 1000 A/cm$^2$ |
| total charge | 0.1 – 1 nC |
| electron density | $10^{14}$ – $10^{15}$ cm$^{-3}$ |
| electron energy | 1 – 10 eV |
| gas temperature | A few hundred Kelvin |

**Table 2.2:** Ionization and dissociation processes for the experiment performed in this work.

| Process | Reaction | Energy [59],[60] |
|---|---|---|
| Ionization | $CH_4 \xrightarrow{e^-} CH_4^+ + e^-$ | 12.6 eV |
| Ionization | $CO_2 \xrightarrow{e^-} CO_2^+ + e^-$ | 13.7 eV |
| Ionization | $O_2 \xrightarrow{e^-} O_2^+ + e^-$ | 12.1 eV |
| Ionization | $H_2O \xrightarrow{e^-} H_2O^+ + e^-$ | 12.6 eV |
| Dissociation | $CH_4 \xrightarrow{e^-} CH_3 + H$ | 4.5 eV |
| Dissociation | $CO_2 \xrightarrow{e^-} CO + O$ | 5.5 eV |
| Dissociation | $O_2 \xrightarrow{e^-} O + O$ | 5.2 eV |
| Dissociation | $H_2O \xrightarrow{e^-} OH + H$ | 5.2 eV |

In the next step, an electron cluster spreads out over the whole surface of the dielectric after reaching the electrode. The positive charge of the anode gets counterbalanced through the surface layer of electrons. The combination of surface electrons

with slower electrons being left behind reduces the electric field in the micro filament and terminates the discharge in this area for some tens of nanoseconds.

Those filaments have a diameter of a few ten to a few hundred micrometers. At the point, where their roots contact the dielectric surface pitting or pinholing of a work-piece can be the consequences [58]. The creations of filaments are improved through dust, irregularities in thickness, or abrasiveness on the surface of the dielectric. Typical values of a micro discharge are shown in Table 2.1

Two competing processes occur in the DBD reactor. The neutral particles are either ionized or dissociated in the discharge region through energy rich electrons. The latter process requires lower energy than the former ant therefore a higher probability because the free plasma electrons are accelerated only to a maximum of 10 eV. Higher energies are required to ionize methane, carbon dioxide, oxygen or hydrogen which are the reactants used in the current project. Therefore, products are mainly formed through reactions where radicals are involved. Table 2.2 summarizes the primary reaction and the required energy for the experimental setup discussed in this section.

# 3 Experimental Setup

The experimental setup is divided into two parts, the processing and the analysis part, as shown in Figure 3.1. The former operates at atmospheric pressure and consists of a cubic reaction chamber and the DBD reactor. A Fourier transform infrared spectrometer (FTIR) and a quadrupole mass spectrometer (QMS) are used in the latter one. All components of the experimental setup will be described in detail in the following. The description follows the way of the gases.

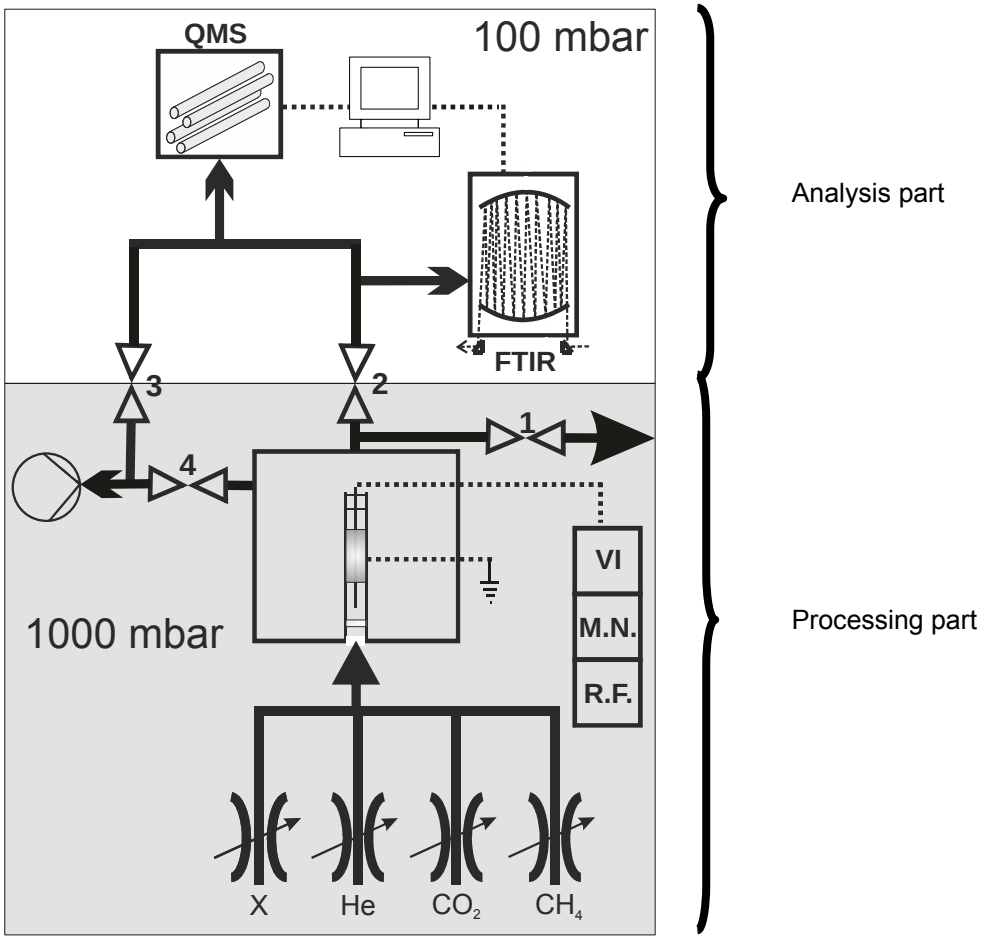


**Figure 3.1:** Schematic setup of the current experiment; QMS: quadrupole mass spectrometer; FTIR: Fourier transform infrared spectrometer; VI: VI probe; M.N.: matching network; R.F.: radio frequency generator; X: oxygen, helium/water or unused; 1, 4: valves; 2,3: precision valves; ●●● electrical feed in; → gas flow.

## 3.1 Gas supply

Four mass flow controllers (MKS Instruments Germany) with different control ranges are used to adjust the gas mixture. Two of them are used to regulate the flow of methane and carbon dioxide. This gas mixture is diluted with helium (third mass flow controller) to 2.5%. The volume of a helium atom is smaller in comparison to the size

of biogas components. Thus, the ignition of plasma occurs at a lower plasma power because of the high energy levels of helium whereby there is no dissipation of energy. The additives water and oxygen are introduced by the last mass flow controller for the measurements with water at vapor pressure is used by bubbling helium through a tank of water. The cylindrical water tank has a height of 145 mm and an inner diameter of 70 mm, where half of the overall volume of ≈560 ml is filled with distilled water. The concentration of water in the reactor is dependent on the helium pressure and the water temperature. The water amount in the gas mixture is adjusted by changing the flow rate of the third and the fourth mass flow controller.

A multi gas controller (MKS, type: 647B) is used to adjust the four mass flow controller at a total flow rate of 200 sccm. Thus, different compositions of methane, carbon dioxide and additives are obtained.

## 3.2 Reaction chamber with the DBD reactor and the plasma generator

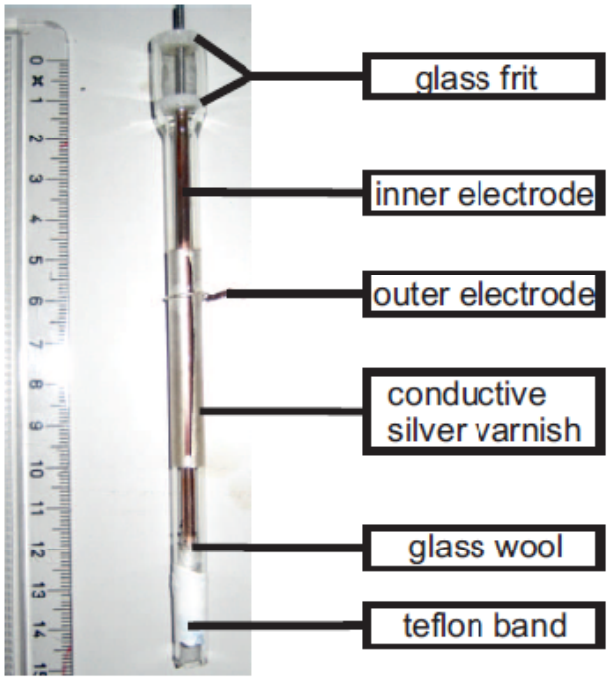


**Figure 3.2:** The DBD reactor.

All gases are mixed before they reach the bottom of the cubic reaction chamber having a dimension of 10 cm. The chamber is made of stainless steel. One side is covered with Plexiglas to monitor the process and the bottom is made from brass. Two

current feed throughs are integrated in one side wall and save to ignite the plasma. Another side wall has a vacuum part to evacuate the chamber (see section 3.4).

The DBD reactor is the centerpiece of the apparatus used in this work. The reactor is shown in Figure 3.2 and consists of a 140 mm long Duran glass tube with an outer diameter of 8 mm and an inner diameter of 5.9 mm. Therefore, the dielectric has a thickness of 1.05 mm. To ignite the plasma, the reactor is covered over a length of 50 mm on the outer side with conductive silver varnish to create the grounded electrode. A slit of around 1 mm is left free over the whole length to monitor the plasma inside the reactor. A 3 mm thick welding rod is used as the inner electrode being centered on the bottom with glass wool and on the top with two glass frits which have a hole in the middle. The glass tube was widened on the top over a length of about 20 mm to the diameter of 13.2 mm to fix the frits.

A high frequency generator (ENI ACG-6B) is used to generate the plasma at a frequency of 13.56 MHz. The power can be adjusted from 1 W to a maximum of 600 W in steps of 1 W. A matching network (ENI MW 10D) with control unit (ENI RFC 5M) is applied to minimize the reflection from load and to maximize the power transfer. Reflections originate from impedance mismatch. The network device is a tunable electrical oscillating circuit consisting of an inductor and two adjustable capacitors. During the measurement, the total impedance is adjusted to the required 50 Ω.

Between the reactor and the generator unit an Octiv Single Frequency VI Probe (Impedans) is located to measure voltage, current and the phase between them. This device has an accuracy for the voltage of ±0.25 V, for the current of ±5.0 mA, and for the phase of ±0.01°. The measured data are transferred to a computer and analyzed by the Octiv Meter software calculating the power and impedance.

The DBD reactor is located vertically in the reaction chamber. A hole is drilled in the bottom to fix the reactor and to introduce the starting material. The reactor is covered with Teflon band at the bottom to convey the complete gas stream through the DBD reactor. The top of the reaction chamber is expanded with a reducing flange and is covered with Teflon to locate the DBD reactor and to prevent plasma outside the reactor.

Mainly reactive radicals and some cations are created after igniting the plasma. These reactive particles recombine to molecules with lower energy after a collision among themselves or with the neutral particles. The process occurs in the plasma

zone or the afterglow region. The inlet flow and the product stream leave the reaction chamber on the top through valve 1 in Figure 3.1.
All parts of the apparatus are wrapped with a heating wire to prevent the condensation of the liquid components. To this end, the temperature is adjusted to 80°C.

## 3.3 Analysis range

The previous two subsections have dealt with the description of devices to convert the starting material. This paragraph focuses on the analysis of the inlet and the product stream. A short part of the gas stream is sidelined through the precision valve 2 (of Figure 3.1) in the analysis region. All IR active substances are analyzed in a FTIR spectrometer and molecules having no characteristic IR peak or being IR inactive are researched in the QMS. Both devices are discussed in detail in the following subsections.

### 3.3.1 FTIR spectrometer

An Equinox 55 FTIR spectrometer (Bruker) supported by a long pass cell according to White was used to analyze all IR active species at a total pressure of 100 mbar. The IR beam is coupled into the cell by 90° prism. Inside the cell, the beam is reflected back and forth up to 30 times through two mirrors. Afterwards, the beam leaves the cell and is redirected back to the original direction through another 90° prism. The number of reflection in the cell and therefore the optical path of the beam in the cell is adjustable by three adjustment screws on the bottom of the cell and another one on the top of the cell. The distance of the two mirrors is 20 cm, therefore the beam path in the cell is at maximum 6 m. The intensity loss of the IR beam after every reflection is a general disadvantage of the White cell, but this is unimportant for the conducted experiments as it can be compensated for by increasing the power of the beam.
A Globar consisting of silicon carbide is used for all experiments as a radiation source. This source radiates between 7500 and 100 $cm^{-1}$. The transmitted radiation after the interaction with a sample is detected with a MCT (mercury cadmium telluride) detector which has a sensitivity range between 420 and 12000 $cm^{-1}$. Liquid nitrogen is used to cool down the detector. All windows and the beam splitter consist of potassium bromide.
In the performed experiments, the resolution of the detector was adjusted to 0.5 $cm^{-1}$. Every measurement is accumulated over 16 scans between 500 and 5000 $cm^{-1}$. The

forward backward method has been applied to collect data. The software Opus (version 3.1) was used to control the spectrometer.

The FTIR spectrometer has for ethene and ethine a detection limit of about 5 ppm for all gases relevant in this process[34]. The values have been confirmed during this thesis. Since the concentration of the products and the starting material is at least a few hundred ppm, the signal to noise ratio is generally quite large.

### 3.3.2 QMS

Molecules and atoms heaving no characteristic IR peak or being IR inactive are researched in the QMS (QME 200, Pfeiffer Vacuum). Since a QMS operates at a very low pressure of $10^{-5}$ mbar, therefore, a precision valve is used to introduce only a very small part of the stream into the QMS.

All molecules and atoms reaching the quadrupole mass spectrometer are ionized and fragmented through energy rich electrons; this process is called electron impact ionization. The resulting ions are focused with lenses to the quadrupole where they are filtered by the mass to charge ratio (m/z). The filtered ions reach a Faraday detector and get neutralized by electrons. The resulting voltage drop at the detector is measured, collected and analyzed by the software Quadstar 422 (Balzer).

The data are recorded between 1 and 90 amu. Every mass is collected for two seconds. The detection limit of this device has been determined in former studies [34] to 3 ppm. Since this value is also much lower than the concentration of every compound being used or generated during the experiments, QMS detection is an appropriate method for the detection of IR inactive species.

The QMS is utilized to determine the conversion of the starting material (methane, carbon dioxide and oxygen) and the yield of hydrogen and ethane.

## 3.4 Generation of the vacuum

The whole experimental setup is evacuated by a dry scroll vacuum pump (XDS 10, BOC Edwards). Therefore, precision valve 3 and ball valve 4 are opened while the valves 1 and 2 are closed. The required pressure of 100 mbar in the analysis region is adjusted by the valves 2 and 3 (Figure 3.1).

The pressure of $10^{-7}$ and $10^{-4}$ mbar in the QMS is adjusted by a precision valve and a turbo pumping station (Hi Cube 80 Eco, Pfeiffer Vacuum) consisting of turbo molecular pump (TPS 110) and a membrane backing pump (MVP 015-2).

Three pressure gauges are used to measure the pressure in every part of the experiments. The pressure in the analysis and the working region is measured by two compact pirani gauges (Pfeiffer) and a compact full range gauge is used in the QMS. The pressure is displayed on a digital pressure gauge (Pfeiffer).

# 4 Performance of the experiments

The experimental setup has described in detail in the last section. This paragraph will give an overview of the performance of the experiments; the details are explained in Section 8, 9 and 10. All experiments have been repeated three times in order to access their reproducibility.

The whole apparatus is evacuated with the dry scroll vacuum pump before starting any experiments. Two different kinds of experiments are performed:

a) Changing the plasma power

b) Changing the concentration of the additives

Both experiments are explained in detail in the following.

## 4.1 Different plasma power

Initially, the whole apparatus is flushed with helium to collect a background spectrum. The reactor is filled up with helium to atmospheric pressure and valve 1 (at Figure 3.1)is opened in the first step. Then, valve 2 is opened until the pressure reaches 6 mbar in the analysis region. Then, the pressure is increased to a value between 95 and 99 mbar by closing valve 3. After collecting the background sample, the gas flow is changed from pure helium to a mixture of methane, carbon dioxide, additives and helium as a buffer gas. The concentration of $CH_4$ was altered between 1.25% and 2.50%, 0% to 1.25% $CO_2$ was added and the amount of water or oxygen was fixed to 0.5%. The missing part to 100% was filled up with helium. For the measurement without an additive, the missing 0.5% is also filled up with helium. Two IR spectra of the inlet flow are measured after 15 and 18 minutes. Mass spectra are collected continuously. 3 min are required to collect one spectrum; therefore, the delay time is a multiple of 3 min.

The plasma is ignited to 30 W in the next step and two IR spectra are collected after 9 and 12 min. This time is required to reach the chemical equilibrium. After the second IR spectra had been recorded, the power was increased by 5 W and after 9 and 12 min, two spectra are collected. This procedure was continued until the power of 70 W had been reached.

## 4.2 Different concentration of the additives

The proceedings for this experiment are nearly the same as discussed in section 4.1. Here, the concentration of the additives was altered instead of the power.

The gas flow without an additive is adjusted after collecting the background spectrum. The inlet flow consisted of 2.5% methane and 97.5% helium for the measurement with oxygen as an additive and 2% methane, 0.5% carbon dioxide and 97.5% helium is used for the research with water. After 15 and 18 minutes, two IR spectra are collected and the plasma is ignited at 35 W (oxygen) or 60 W (water). After reaching chemical equilibrium (nine to twelve minutes), two IR spectra are recorded and the flow of the additives is turned on. The flow rate of helium is reduced to maintain a total flow speed of 200 sccm. Two more spectra are recorded 9 and 12 min after taking the previous two IR spectra. The concentration of the additives is increased and that of helium decreased. The procedure is stopped if the water concentration reached 0.7% or the oxygen amount achieved 1%. The former one is limited by the vapor pressure of water depending on the pressure and the temperature inside the water tank.

# 5 Qualitative Analysis

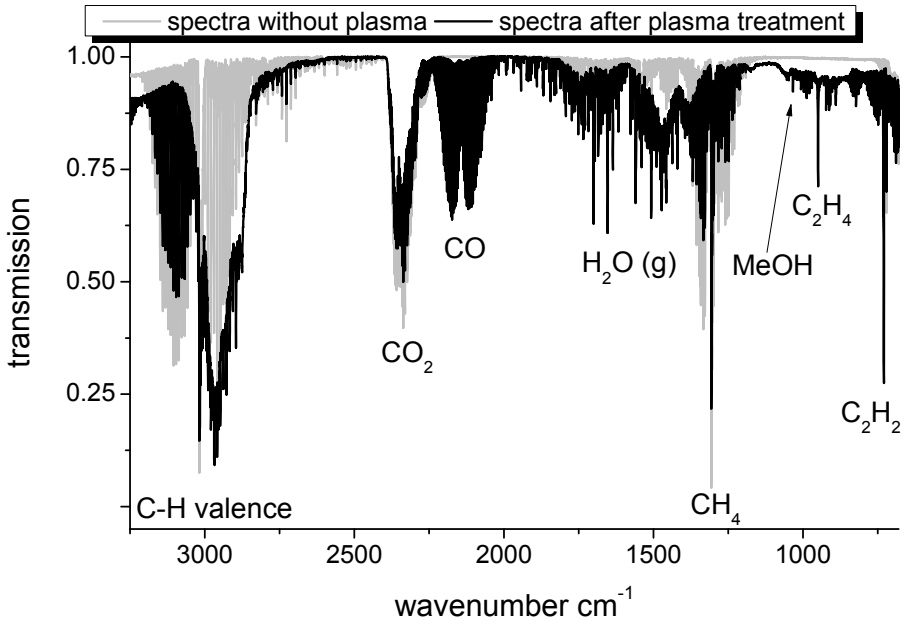


**Figure 5.1:** Spectra of the inlet flow consisting of 2% methane, 0.5% carbon dioxide, 0.5% oxygen and 97% helium and after igniting 70 W plasma.

The inlet flow and the product stream have to be analyzed qualitatively before discussing the conversion of the starting material and the yield of the products. This section deals with the qualitative analysis of the inlet and the product stream.

Figure 5.1 displays the IR spectra without plasma (light gray) and after igniting a 70 W plasma (black). The inlet flow consists of 2% methane, 0.5% carbon dioxide, 0.5% oxygen and 97% helium. The gray spectrum shows three characteristic peaks of the inlet flow. The C-H valence stretch vibration of methane is located at around 3000 $cm^{-1}$. Methane has at 1315 $cm^{-1}$ the triple degenerated bending mode. The P and R branches of the asymmetric stretch of carbon dioxide are located between 2395 and 2240 $cm^{-1}$.

After igniting the plasma, the transmission values of the starting material increase which is evidence of the conversion of these molecules. Four products are identified unequivocally with the help of the black spectra. The vibration rotational structure of carbon monoxide is shown between 2238 and 2020 wave numbers. The C-O stretch vibration of methanol (≈1033 $cm^{-1}$), the out of plane stretch vibration for ethene (≈949 $cm^{-1}$) and the bending mode of ethine (≈729 $cm^{-1}$) are clearly identified.

Water (2000 - 1400 $cm^{-1}$) is a product if oxygen has been added. For that reason, the peak for formaldehyde at ≈1745 $cm^{-1}$ is not discernable in this spectrum because it

overlaps with water. There is only a single peak belonging to formaldehyde, if the spectrum is scaled up.

IR peaks characteristic for only one component are required to calculate the conversion of the starting material and the yield of the products. On the contrary, the cross sensitivity has to be small, which is the case for the previously discussed components. The C-H valence stretch between 3050 and 2850 $cm^{-1}$ has a high cross sensitivity of all hydrocarbons [34]. For this reason, it is not possible to analyze ethane quantitatively via IR spectroscopy.

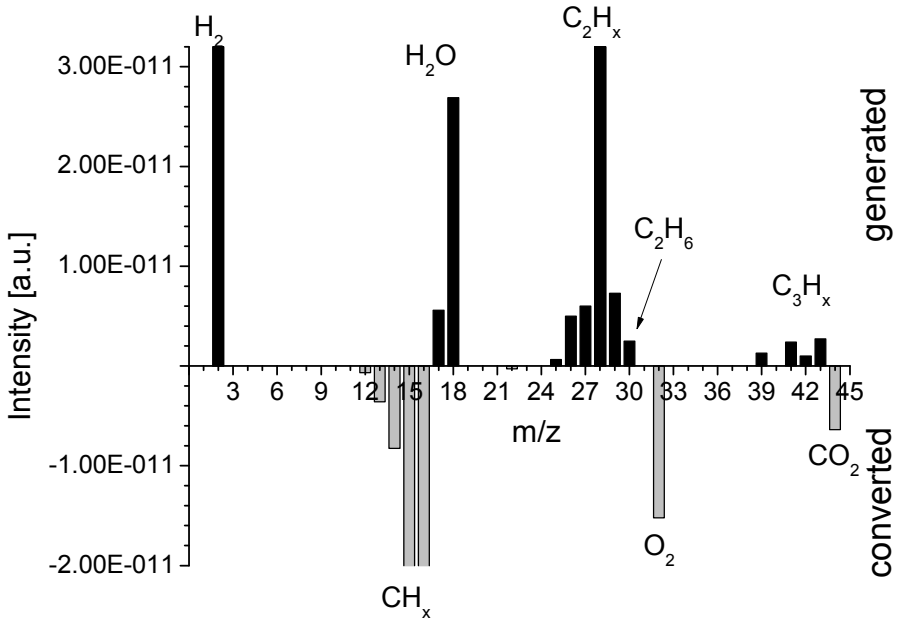


**Figure 5.2:** QMS differential spectra after igniting a 70 W plasma. The black peaks show the produced compounds and the gray peaks display the conversion of the starting material. The flow consisted of 2% methane, 0.5% carbon dioxide, 0.5% oxygen and 97% helium The peaks at m/z=2, 15 and 16 are cut off for clearness reasons.

A differential spectrum which is recorded in the mass spectrometer is shown in Figure 5.2. Two raw spectra are required to obtain the displayed differential spectrum. The first one is collected from the inlet flow consisting of 2% methane, 0.5% carbon dioxide, 0.5% oxygen and 97% helium and the second one is recorded after igniting the 70 W plasma.

Hydrogen (m/z=2) and ethane (m/z=30) are exactly identified products via mass spectroscopy. The conversion of the starting material is also calculated with the data from the mass spectra. All other products are identified via mass spectroscopy. Every compound is ionized and fragmented in the spectrometer. Hence, the intensity of one peak is often the sum of the intensity of multiple components. The peak at m/z=28 is

used to explain the overlap in detail. This peak is generated from carbon dioxide ($CO^+$), carbon monoxide ($CO^+$), ethane ($C_2H_4^+$) or ethene ($C_2H_4^+$). Therefore, no quantitative calculations are possible for these compounds at m/z=28.

**Table 5.1:** Distribution of higher hydrocarbons. The inlet flow consisted of 2.5% methane and 97.5% helium and the power was adjusted to 70 W. The values are transferred as they are listed by the "Fraunhofer Institut für Holzforschung in Braunschweig". No experimental error was specified.

| Substance | Concentration [µg/m$^3$] | Substance | Concentration [µg/m$^3$] |
|---|---|---|---|
| Propane | 26.004 | iso-Hexane | 7.819 |
| 1,2-Propadiene | 6.789 | iso-Hexene | 41.780 |
| Butane | 9.766 | 2-Methylpentane | 16.127 |
| iso-Butene | 11.117 | Methylcyclopentane | 3.878 |
| iso-Pentene | 9.801 | iso-Heptane | 20.653 |
| iso-Pentane | 42.496 | Benzene | 3.886 |
| n-Pentane + Pentene | 48.654 | 2-Methylhexane | 4.118 |
| iso-Hexene | 8.277 | 2-Methylhexane | 5.599 |
| Dimethylcyclopropane | 22.175 | iso-Heptene | 10.009 |
| iso-Hexene | 17.145 | Toluene | 4.201 |

Figure 5.2 shows peaks between m/z=39 to m/z=43 which are characteristic for the fragment $C_3H_x^+$ being formed from all higher hydrocarbons. These hydrocarbons are neither detectable by IR nor by mass spectroscopy. For this reason, the product stream consisting of 2.5% methane and 97.5% helium was analyzed at the "Fraunhofer Institut für Holzforschung in Braunschweig" via gas chromatography. The results are summarized in Table 5.1. The used DBD reactor generates also higher hydrocarbons with three to seven carbons beside the exact identified products. The main products having three and more carbons are iso-pentane, n-pentane, pentene, and iso-hexane.

# 6 Calibration of the FTIR Spectrometer and the QMS

Both devices used for analysis have to be calibrated with the particular substances to calculate the yield and selectivity of the products and the conversion of starting material. The procedure and the results for the calibration process are shown in the following section.

## 6.1 Gaseous substances

The whole apparatus is filled up with helium in the same way as described in section 4 “performance of the experiment”, and a background spectrum is collected for calibration of the FTIR spectrometer. Then the flow of the substance under investigation is turned on. Two IR spectra or ten mass spectra are collected after reaching the chemical equilibrium conditions. In the next step, the concentration of the substance is increased. The range of calibration concentrations is chosen such that it completely covers the concentrations of the experimentally measured amounts.

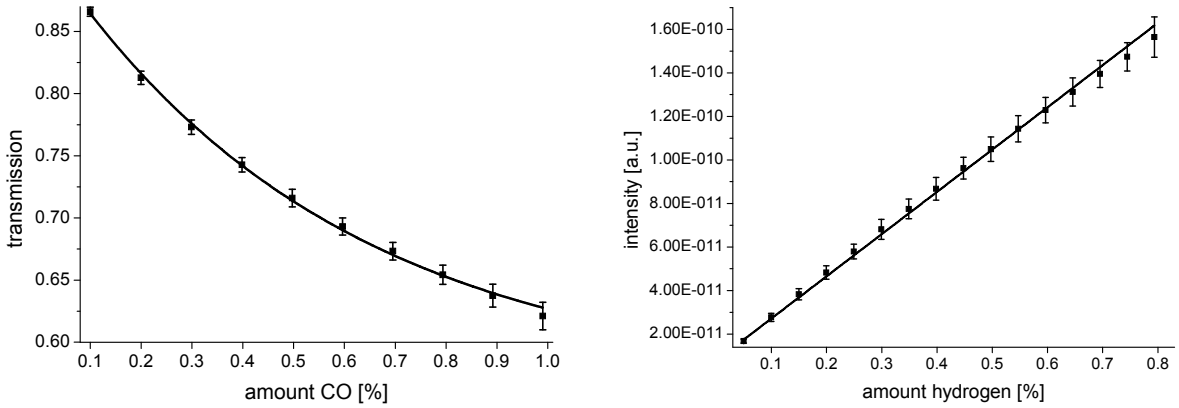


**Figure 6.1:** Graphs for the calibration of the analysis devices (left: FTIR with CO; right: QMS with $H_2$).

Transmission values as a function of the amount of carbon monoxide are plotted on the left of Figure 6.1. The measured data points are fitted to the following equation:

$$T = Y + Ae^{-\frac{C}{B}} \tag{6.1}$$

T ….. transmission
C ….. concentration [%]
Y, A, B ….. constant

This function originates from the Lambert-Beer law being given by equation 6.2. Theoretically, the constant Y should be zero and A should have a value of one after comparison of equation 6.1 and 6.2. This is not the case for the performed experiments because the resolution (0.5 $cm^{-1}$) of the IR spectrometer is insufficient to re-

solve the measured lines. Thus, part of the IR light always reaches the detector resulting in a non-zero value for Y and a value for A smaller than one.

$$T = \frac{I}{I_0} = e^{-\varepsilon \cdot C \cdot d} \tag{6.2}$$

T ….. transmission
I ….. intensity of the transmitted light [$W / m^2$]
$I_0$ ….. intensity of the incident light [$J / (s \cdot m^2)$]
$\varepsilon$ ….. molar absorption coefficient [$l / (mol \cdot cm)$]
C ….. concentration [mol/l]
d ….. path length [cm]

For background correction, the reference is chosen at 2417.33 $cm^{-1}$. At this wave number, the background noises are very low and the identified substances have no characteristic peak there.

There is a linear relationship between the intensity of the peaks and the concentration for the calibration of the QMS spectrometer as shown on the right in Figure 6.1. All molecules which are introduced to the spectrometer are ionized by energy rich electrons. The set of data is fitted using the following equation:

$$I_{QMS} = mC + n \tag{6.3}$$

$I_{QMS}$ ….. intensity of the peak
C ….. concentration [%]
m, n ….. constant

The average mean values over all calibration are shown by the error bars in Figure 6.1 which displays a good reproducibility of the measurements. All the other calibrations have nearly the same values for the errors.

**Table 6.1:** Summary of the calibration of the FTIR spectrometer.

| Substance | Wave number [$cm^{-1}$] | Y | ΔY | A | ΔA | B [1/%] | ΔB [1/%] | $R^2$ |
|---|---|---|---|---|---|---|---|---|
| Carbon monoxide | 2165.4 | 0.568 | 0.011 | 0.353 | 0.009 | 0.585 | 0.038 | 0.999 |
| Formaldehyde | 1745.7 | 0.723 | 0.019 | 0.255 | 0.015 | 278,3 | 46.6 | 0.993 |
| Methanol | 1033.4 | 0.781 | 0.037 | 0.235 | 0.030 | 116.6 | 35.0 | 0.989 |
| Ethene | 949.5 | 0.745 | 0.018 | 0.384 | 0.041 | 0.007 | 0.002 | 0.973 |
| Ethine | 729.4 | 0.169 | 0.016 | 1.105 | 0.011 | 0.0103 | 0.0005 | 0.999 |

The results for the calibration of the FTIR spectrometer and the QMS are summarized in Tables 6.1 and 6.2.

**Table 6.2:** Summary of the calibration of the QMS.

| Substance | m/z | m [1/%] | Δm [1/%] | n [%] | Δn [%] | $R^2$ |
|---|---|---|---|---|---|---|
| Hydrogen | 2 | 1.94E-10 | 1.26E-12 | 6.86E-12 | 2.77E-13 | 0.999 |
| Methane | 14 | 6.42E-11 | 1.18E-12 | -1.25E-14 | 3.03E-14 | 0.999 |
| Ethane | 30 | 1.66E-11 | 1.66E-13 | -9.60E-14 | 2.03E-14 | 0.999 |
| Oxygen | 32 | 4.25E-11 | 5.08E-13 | -5.25E-12 | 2.32E-13 | 0.999 |
| Carbon dioxide | 44 | 6.34E-11 | 3.81E-13 | -5.43E-13 | 1.72E-13 | 0.999 |

## 6.2 Methanol and formaldehyde

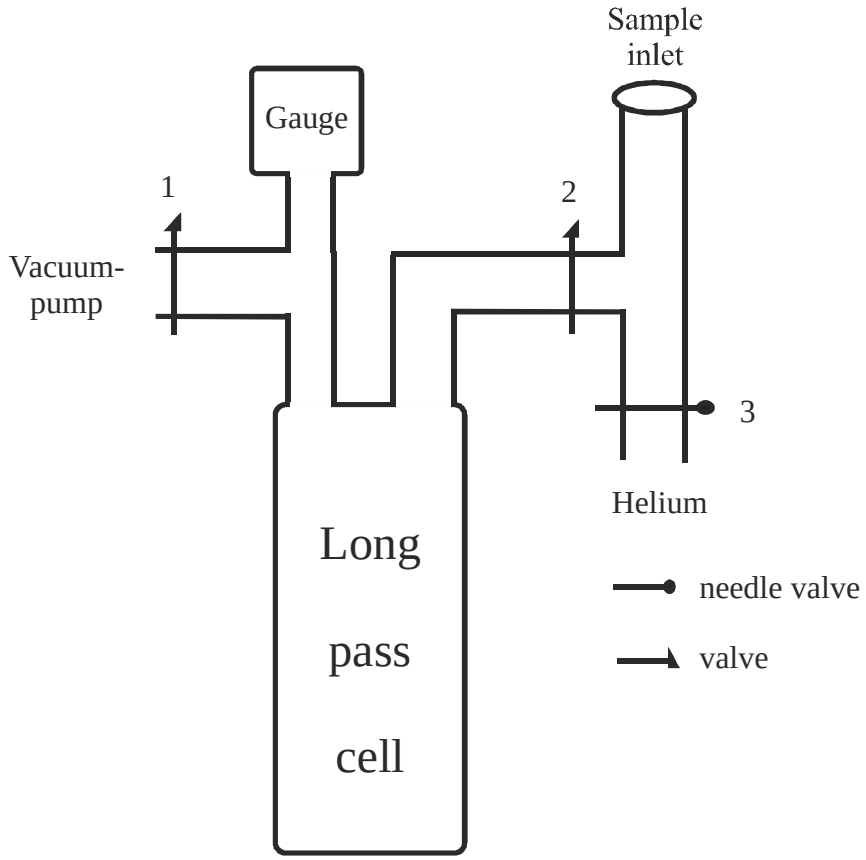


**Figure 6.2:** Schematic setup to calibrate the FTIR spectrometer with methane and formaldehyde.

The FTIR spectrometer is calibrated with methanol and formaldehyde by the setup shown in Figure 6.2. The whole apparatus is evacuated and flushed with helium to collect a background spectrum at the beginning. After that the apparatus is evacuated. In the next step, valve 1 and 2 are closed and the pressure in the tee is increased to atmospheric pressure by opening the needle valve 3. Shortly after that, the liquid sample is injected by a Hamilton syringe through a septum. Both liquids are produced in the DBD reactor in low concentration. For this reason, methanol is di-

luted with acetone to 1:99 and the 36.5% solution of formaldehyde in water and methanol as a stabilizer is diluted to 2:23 with methanol. Between 0.5 and 5 µl of the diluted sample is injected and valve 2 is opened to introduce the liquids in the long pass cell. To accelerate the process, the whole apparatus is heated up to 60 °C through a heating wire. Before measuring the IR spectra, the pressure in the apparatus is adjusted with helium to 100 mbar.

The concentration of methanol and formaldehyde in the cell is calculated by the ideal gas law. The required volume of the cell is 2.2 l which has been determined in previous work [61]. The analysis of the measurements is the same as discussed in section 6.1.

# 7 References for section 1 to 6


1. Demirbas A, (2009) Biofuels – Securing the Planet's Future Energy Needs, Springer-Verlag, London.
2. Andruleit H, Babies HG, Meßner J, Rehder S, Schauer M, Schmidt S (2011) Reserven, Ressourcen und Verfügbarkeit von Energierohstoffen 2011, Deutsche Rohstoffagentur (DERA) in der Bundesanstalt für Geowissenschaften und Rohstoffe (BGR), Hannover.
3. Alizadeh R, Jamshidi E, Zhang G (2009) Transformation of methane to synthesis gas over metal oxides without using catalyst, Journal of Natural Gas Chemistry 18:124–130.
4. Schwarz H (1991) Aktivierung von Methan, Angew. Chem. 103:837-838.
5. Choudhary TV, Goodman DW (2000) Methane activation on Ni and Ru model catalysts, Journal of Molecular Catalysis A: Chemical 163:9–18.
6. Dietzel PDC, Besikiotis V, Blom R (2009) Application of metal–organic frameworks with coordinatively unsaturated metal sites in storage and separation of methane and carbon dioxide, J. Mater. Chem. 19:7362–7370.
7. Demirbas A (2008) Hydrogen Production from Carbonaceous Solid Wastes by Steam Reforming, Energy Sources, Part A 30:924–931.
8. Tao X, Bai M, Li X, Long H, Shang S, Yin Y, Dai X (2010) $CH_4$-$CO_2$ reforming by plasma - challenges and opportunities. Prog Energ Combust 37:113-124.
9. Schütze A, Jeong JY, Babayan SE, Park J, Selwyn GS, Hicks RF (1998)The Atmospheric-Pressure Plasma Jet: A Review and Comparison to Other Plasma Sources, IEEE Transaction on Plasma Science 26:1685-1694.
10. Snowdon LR (2001) Natural gas composition in a geological environment and the implications for the processes of generation and preservation, Organic Geochemistry 32:913–931.
11. Zhou LM, Xue B, Kogelschatz U, Eliasson B (1998) Nonequilibrium Plasma Reforming of Greenhouse Gases to Synthesis Gas, Energy & Fuels 12:1191-1199.
12. Hilkiah Igoni A, Ayotamuno MJ, Eze MJ, Ogaji SOT, Prober SD (2008) Designs of anaerobic digesters for producing biogas from municipal solid-waste, Applied Energy 85:430–438.
13. Graf F, Bajohr S (2011) Biogas - Erzeugung, Aufbereitung, Einspeisung, Oldenburgischer Industrieverlag GmbH, München.
14. Byrne K (1997) Environmental Science, Thomas Nelson & Sons Ltd., Cheltenham.
15. Fitzke B (2006) Entwicklung eines anaeroben Membran-Bio-Reaktors zur Reinigung schwach belasteter Abwässer, Dissertation TU Clausthal.
16. Rasi S, Veijanen A, Rintala J (2007) Trace compounds of biogas from different biogas production plants, Energy 32:1375–1380.
17. Goujard V, Tatibouet J-M, Batiot-Dupeyrat C (2011) Carbon Dioxide Reforming of Methane Using a Dielectric Barrier Discharge Reactor: Effect of Helium Dilution and Kinetic Model, Plasma Chem Plasma P 31:315-325.
18. Rico VJ, Hueso JL, Cotrino J, González-Elipe AR (2010) Evaluation of Different Dielectric Barrier Discharge Plasma Configurations As an Alternative Technology for Green C1 Chemistry in the Carbon Dioxide Reforming of Methane and the Direct Decomposition of Methanol. J. Phys. Chem. A 114:4009–4016.
19. Sentek J, Krawczyk K, Młotek M, Kalczewska M, Kroker T, Kolb T, Schenk A, Gericke K-H, Schmidt-Szałowski K (2010) Plasma-catalytic methane conversion with carbon dioxide in dielectric barrier discharges. Appl Catal B 94:19–26.
20. Istadi N, Amin AS (2006) Co-generation of synthesis gas and $C_{2+}$ hydrocarbons from methane and carbon dioxide in a hybrid catalytic-plasma reactor: A review. Fuel 85:577–592.
21. Zhang K, Eliasson B, Kogelschatz U (2002) Direct Conversion of Greenhouse Gases to Synthesis Gas and C4 Hydrocarbons over Zeolite HY Promoted by a Dielectric-Barrier Discharge, Ind Eng Chem Res 41:1462-1468.
22. Song HK, Lee H, Choi J-W, Na B (2004) Effect of Electrical Pulse Forms on the CO2 Reforming of Methane using Atmospheric Dielectric Barrier Discharge Plasma, Chem Plasma Process 24:57-72.

23. Liu CJ, Mallison R, Lobban L (1998) Nonoxidative Methane Conversion to Ethine over Zeolite in a Low Temperature Plasma, Journal of Catalysis 179:326–334.
24. C.-J. Liu, B. Xue, B. Eliasson, F. He, Y. Li, G.-H. Xu (2001) Methane Conversion to Higher Hydrocarbons in the Presence of Carbon Dioxide Using Dielectric-Barrier Discharge. Plasmas Plasma Chem Plasma P 21:301-310.
25. B. Eliasson, C.-J. Liu, U. Kogelschatz (2000) Direct Conversion of Methane and Carbon Dioxide to Higher Hydrocarbons Using Catalytic Dielectric-Barrier Discharges with Zeolites. Ind. Eng. Chem. Res. 39:1221-1227.
26. Li X-S, Zhua A-M, Wang K-J, Xu Y, Song Z-M (2004) Methane conversion to C2 hydrocarbons and hydrogen in atmospheric non-thermal plasmas generated by different electric discharge techniques, Catalysis Today 98:617–624.
27. Wang B, XU G (2002) Conversion of natural gas to C2 hydrocarbons through dielectric-barrier discharge plasma catalysis, Sci China: Chem 45:299-310.
28. Martin NS, Savadkoohi HA, Feizabadi SY (2010) Methane Conversion to C2 Hydrocarbons Using Dielectric-barrier Discharge Reactor: Effects of System Variables, Plasma Chem Plasma Process 28:189-02.
29. Li Y, Liu C-J, Eliasson B, Wang Y (2002) Synthesis of Oxygenates and Higher Hydrocarbons Directly from Methane and Carbon Dioxide Using Dielectric-Barrier Discharges: Product Distribution, Energy Fuels 16:864-870.
30. Larkin DW, Lobban LL, Mallinson RG (2001) The direct partial oxidation of methane to organic oxygenates using a dielectric barrier discharge reactor as a catalytic reactor analog, Catalysis Today 71:199–210.
31. Baowei W, Xu Z, Yongwei L, Genhui X (2008) Conversion of CH4, steam and O2 to syngas and hydrocarbons via dielectric barrier discharge, J Nat Gas Chem 18:94–97.
32. Pietruszka B, Heintze M (2004) Methane conversion at low temperature: the combined application of catalysis and non-equilibrium plasma, Catalysis Today 90:151–158.
33. Mfopara A, Kirkpatrick MJ, Odic E (2009) Dilute Methane Treatment by Atmospheric Pressure Dielectric Barrier Discharge: Effects of Water Vapor, Plasma Chem Plasma P 29:91–102.
34. Kroker T (2011) Qualitative und Quantitative Produktanalyse der Katalytischen Konvertierung von Biogas in Plasmagestützten Rohrströmungsreaktoren, Dissertation TU Braunschweig.
35. Kroker T, Kolb T, Schenk A, Krawczyk K, Młotek M, Gericke K-H (2012) Catalytic Conversion of Simulated Biogas Mixtures to Synthesis Gas in a Fluidized Bed Reactor Supported by a DBD, Plasma Chem. Plasma Process 32:565–582.
36. Kroker T, Kolb T, Krawczyk K, Mlotek M, Schenk A, Gericke K-H (2010) Catalytic Conversion of Biogas in a Fluidized Bed Reactor Supported by a DBD, Front Appl Plasma Technol 3:69-73.
37. Bruchmann N (2010) Plasmagestützte Konvertierung von Biogas zu C2-Kohlenwasserstoffen, Bachelor Thesis.
38. Haak K (2010) Katalytische Konvertierung von Biogas in plasmagestützten Rohrströmungsreaktoren – Quantitative Analyse von Acetylen, Bachelor Thesis.
39. Schmidt I (2010) Konvertierung von Biogas in plasmagestützten Rohrströmungsreaktoren, Bachelor Thesis.
40. Schäfer K (2011) Ethan – Ein Produkt der plasmagestützten Konvertierung von Biogas in einem DBD-Reaktor bei einem Eduktstrom von 800 sccm, Bachelor Thesis.
41. Wilharm N (2011) Methanolausbeute bei der plasmagestützten Konvertierung von Biogas in Abhängigkeit vom Wasseranteil, Bachelor Thesis.
42. Song T (2011) Synthesegasproduktion bei der Plasmagestützten Konvertierung von Biogas in einem DBD Reaktor in Abhängigkeit von der eingeleiteten Wassermenge, Bachelor Thesis.
43. Homolya G (2012) Analyse der plasmagestützten Konvertierung von Biogas zu Sauerstoffhaltigen Kohlenwasserstoffen in Abhängigkeit vom Sauerstoffanteil, Bachelor Thesis.
44. Langmuir I(1928) Oscillations in Ionized Gases, Proceedings of the National Academy of Sciences14:627- 637.
45. Capitelli M, Grose C (1992) Plasma Technology – Fundamentals and Applications, Plenum Press, New York.

46. Goldston RJ, Rutherford PH (1998) Plasmaphysik – Eine Einführung, Vieweg Verlag, Braunschweig/Wiesbaden.
47. Kegel WH (1998) Plasmaphysik, Springer Verlag, Berlin Heidelberg.
48. Hipler R, Pfau S, Schmidt M, Schoenbach KH (2001) Low Temperature Plasma Physics – Fundamental Aspects and Applications, Wiley-VCH, Berlin.
49. von Keudell A (2007), Einführung in die Plasmaphysik, Vorlesungsskript Ruhr Universität Bochum.
50. Dinu EG (2005), Dielektrisch behinderte Barrierenentladungen für großflächige Plasmabehandelungen, Dissertation TU Wuppertal.
51. Janzen G (1992) Plasmaphysik, Hüthig, Heidelberg.
52. Roth JR (1995) Industrial Plasma Engineering Volume 1: Principles, Institute of Physics Publishing, London.
53. Paschen F (1889) Ueber die zum Funkenübergang in Luft Wasserstoff und Kohlensäure bei verschiedenen Drucken erforderliche Potentialdiffernz, Annalen der Physik 273:69-96.
54. Raizer YP (1991) Gas Discharge Physics, Springer-Verlag, Berkin-Heidelberg.
55. Kogelschatz U, Eliasson B, Egli W (1997) Dielectric-barrier discharges. Principle and applications, Journal de Physique IV 7:C4/47-C4/66.
56. Siemens W (1857) Ueber die elektrostatische induction und die verzogerung des stroms in flaschendraten, Annalen der Physik und Chemie 102:66-122.
57. Kogelschatz U (2003) Dielectric-barrier Discharges: Their History, Discharge Physics, and Industrial Applications, Plasma Chemistry and Plasma Processing 23:1-46.
58. Roth JR (2001) Industrial Plasma Engineering Volume 2: Applications to Nonthermal Plasma Processing, Institute of Physics Publishing, London.
59. deB. Darwent B (1970) Bond Dissociation Energies in Simple Molecules NBSDS-NBS 31.
60. NIST Chemistry WebBook, http://webbook.nist.gov/chemistry (27.08.2012).
61. Kolb T (2010) IR spektroskopische Produktanalyse von plasmakonvertiertem Biogas, Diplomarbeit TU Braunschweig.

# 8 Conversion of biogas like mixtures to $C_2$ hydrocarbon in a plug flow reactor supported by a DBD at atmospheric pressure

**Torsten Kolb, Thorsten Kroker, Karl-Heinz Gericke**

**Institut für Physikalische und Theoretische Chemie**

Braunschweig, 38106, Germany

**ABSTRACT**

*The conversion of biogas like mixtures of methane and carbon dioxide was studied in a plug flow reactor with a dielectric barrier discharge. A 13.56 MHz power supply generated the atmospheric plasma discharge. Studied concentration of methane ranged from 0 to 100%, with missing part filled up with carbon dioxide. This mixture was diluted with helium to 2.5% with small part of the product stream monitored online at a total pressure of 100 mbar by a Fourier transform infrared spectrometer supported by a White-cell and a quadrupole mass spectrometer. The reactor was driven at different flow rates. This DBD reactor produces all three hydrocarbons, with ethane being the major compound. The concentration of ethane increases when the power in the plasma region increases from 30 to 65 W. This product concentration also grows up, if the fraction of methane in the inlet flow is increased. The highest amount of ethane (5.4%) is produced, when the gas stream consist of 2.5% Methane and 97.5% helium at a flow rate of 200 sccm.*

**KEYWORDS**: DBD, Biogas, Ethane, C2 hydrocarbons, Atmospheric pressure discharge, Online monitoring

## 8.1 Introduction

C2 hydrocarbons (ethane, ethene and ethine) are important basic chemicals, especially the unsaturated one. Thermal cracking to ethene is an important range of application for ethane. This compound is also used as a fuel gas. Ethene is the starting material for industrial manufacturing of Ethanol or for the production of plastics like polyethylene [1]. Organic syntheses are the main application area of ethine. This compound is often used to prepare base material for most plastics.

The starting point for industrial manufacturing of ethane, ethene and ethine is natural gas or crude oil. New technologies are needed to prepare C2 hydrocarbon. One way is to convert a mixture of Methane and Carbon dioxide in a dielectric barrier discharge (DBD). The advantage for such type of plasma is the potential to activate thermodynamically unfavorable reactions through energy rich plasma electrons. In a DBD is the entire electrode area effectively used for generating the discharge. [2]

Intense research with DBDs have been done in the last years to convert methane and carbon dioxide to other useful chemicals like synthesis gas [3], [4], hydrocarbons [5], [6] or oxygenated hydrocarbons [7], [8]. Different techniques have been used. T. Kroker et al. [9] analyzed the produced amount of formaldehyde in a DBD reactor at a 100 mbar. The highest quantity of this product (1.25%) has been observed at low investigated plasma power (ca. 25 W). A Palladium catalyst increases the yield of formaldehyde at higher plasma power from 0.9% (without a catalyst) to 1.05%.

There are many sources for the starting material which is used in this process. Mixtures of methane and carbon dioxide are for example known as biogas or landfill gas. Biogas is independent from natural gas, because animal and vegeTable materials are used for this process, i.e. corn, sugar beets, grain or slaughterhouse waste. These materials are manly transformed in an anaerobe microbial mineralization to methane and carbon dioxide. The biogas composition can be actuated by using different starting materials or varying the process conduct.

This work focuses on the conversion of methane and carbon dioxide to C2 hydrocarbons in a 13.56 MHz DBD reactor. The plasma power, flow rate and the mixture of the inlet flow have been varied. Additionally the influence of high frequencies to generate the plasma has been studied.

## 8.2 Experimental procedure

The schematic setup of the current experiment is shown in Figure 8.1. This setup can be divided into two parts. The first part is the area of operation which works at am-

bient pressure. The reaction chamber with the DBD reactor is there located. The gas stream is analyzed by fourier transform infrared spectrometer (FTIR) at a pressure of 100 mbar in the analysis domain and by a quadrupole mass spectrometer (QMS).
The gas flow for this experiment consists of methane and carbon dioxide. Helium was used as a carrier gas to dilute the gas mixture to 2.5%. These three components were adjusted by three mass flow controllers. The influence of different compositions of the gas mixture (0 - 2.5% methane and 0 - 2.5% carbon dioxide) and flow rates (200 – 800 sccm) on the product distribution were analyzed. The cylindrical Duran glass DBD reactor is located in a cubic reaction chamber. The reactor has a length of 150 mm, an external diameter of 8 mm and an internal diameter of 5.8 mm.

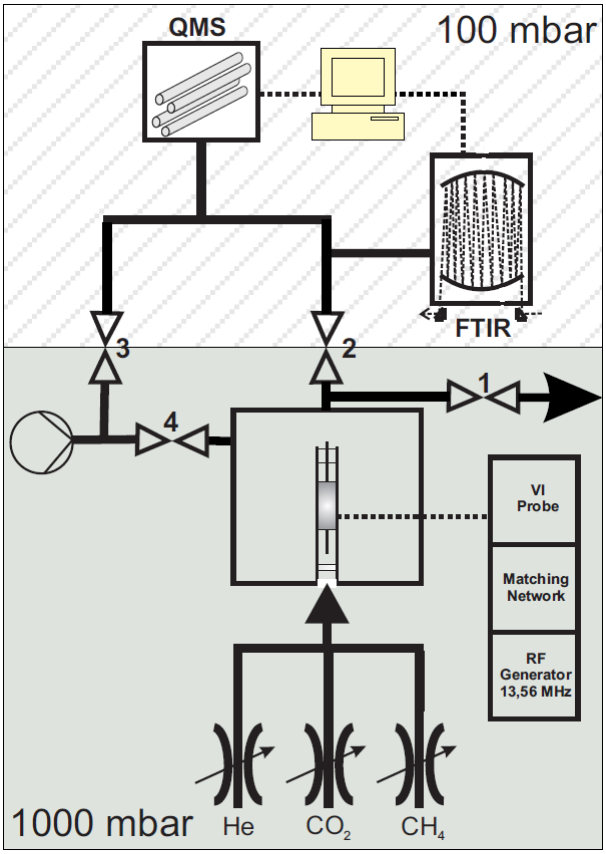


**Figure 8.1:** Schematic setup; FTIR: fourier transform infrared spectrometer; QMS: quadrupole mass spectrometer; → gas flow system; dotted line: electrical interface.

A 140 mm long welding rod with a diameter of 3 mm forms the inner electrode for igniting the plasma. This electrode is fixed on the top with two glass frits and on the bottom with glass wool. The reactor is covered over the length of 50 mm with a conductive silver varnish to create the outer electrode. A RF-generator (ENI ACG-6B) and a matching network (ENI MW-10D) come in operation to generate 13.56 MHz

plasma at atmospheric pressure. The input power has been adjusted in 5 W steps between 30 and 65 W. The reactor is driven for 15 minutes until the power is increased by 5 W.

Most of the gas flow leaves the reaction chamber through valve 1. A small stream is sidelined by the needle valve 2 to analyze the starting material and the product distribution. This occurs online at 100 mbar in the analysis domain. The pressure is realized with a XDS 10 dry scroll pump (Edwards) and valve 3. All IR active species have been researched in the FTIR spectrometer (Equinox 55, Bruker) in a White Cell with a path length of 6 meters. The resolution of this application is 0.5 $cm^{-1}$. All spectra consist of 16 scans (double sided, forward-backward). IR inactive or substances which have no characteristic IR peak were studied in the QMS (Balzer, QMS 200 Prisma). The measuring range is between m/z = 0 (mass per charge) to m/z = 90. All m/z would be measured for 2 seconds.

## 8.3 Results and discussion

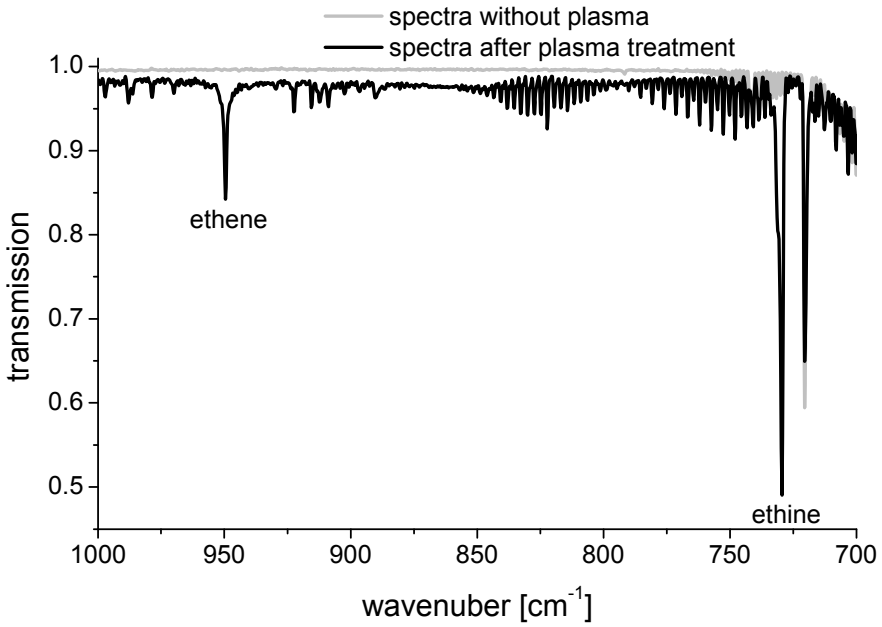


**Figure 8.2:** Spectra of the inlet flow (7 sccm $CH_4$, 3 sccm $CO_2$, 390 sccm He) and the product stream (generator power: 65 W).

In a previous work [9] we analyzed the recorded IR spectra between 500 and 5000 $cm^{-1}$. The present paper focuses on C2 hydrocarbons. Ethene (949.5 $cm^{-1}$) and ethine (729,4 $cm^{-1}$) have isolated IR peaks. They are shown in Figure 8.2. It is not possible to analyze ethane via IR spectroscopy, because this compound has a cha-

racteristic peak around 3000 $cm^{-1}$. All hydrocarbons have their CH-valance vibration in this region. Therefore, ethane and the conversion of methane are quantitatively analyzed by mass spectroscopy. For the representation of the produced amount of the C2 hydrocarbon the buffer gas helium is ignored.

The produced amounts of the three C2 hydrocarbons as a function of the power which is adjusted on the RF generator are illustrated in Figure 8.3. The inlet flow for this measurement consists of 1.75% methane, 0.75% carbon dioxide and 97.5% helium. Ethane is the main and ethene the lowest C2 product. The concentration ratio between ethane and ethene (and between ethane and ethine) is approximately 13.

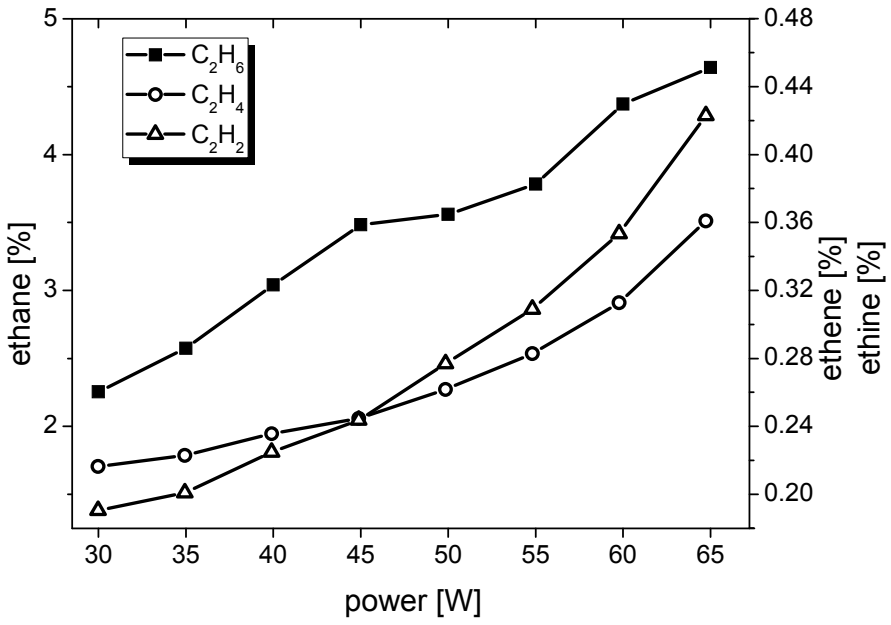


**Figure 8.3:** Produced amount of C2 hydrocarbons as a function of the adjusted generator power. The 400 sccm inlet gas stream consists of 1.75% methane, 0.75% carbon dioxide and 97.5% helium. The produced amount of ethane is illustrated on the left axis (solid points) and the right axis shows the produced amount of ethene and ethine (open points).

These results can be explained by the mechanism [5] for this reaction. The bond between hydrogen and carbon in a methane molecule are broken during the plasma treatment. The following reactions continue during this process:

$CH_4 + e^- \rightarrow CH_3 + H + e^-$ (8.1)

$CH_3 + e^- \rightarrow CH_2 + H + e^-$ (8.2)

$CH_2 + e^- \rightarrow CH + H + e^-$ (8.3)

The required energy to start these reactions is moderately, 4.37 – 4.90 eV [10]. The CH radical of reaction (8.3) can dissociate to form carbon black. However, no carbon black has been observed for this kind of measurements.

The produced radicals ($CH_3$, $CH_2$, CH) have to undergo a non elastic collision with the most abundant methane molecule to form ethane, ethene or ethine.

$$CH_4 + CH_3 \rightarrow C_2H_6 + H \quad (8.4)$$

$$CH_4 + CH_2 \rightarrow C_2H_4 + 2H/H_2 \quad (8.5)$$

$$CH_4 + CH \rightarrow C_2H_2 + H + H_2 \quad (8.6)$$

There are two reasons why ethane is the major C2 product. First only two steps (Reaction 8.1 and 8.4) are required to get this product. At least three collisions are necessary to form ethene (reaction 8.1, 8.2 and 8.5). The formation of ethine requires at least four reactions (reaction 8.1, 8.2, 8.3 and 8.6). The generated methyl radical (reaction 8.1) has to collide one or rather two times with energy rich electrons to form the starting material for reaction (8.5) and (8.6). The dwell time of the compounds in the DBD reactor is approximately 0.3 s and, thus, the probability of the collision of electrons with methane is rather low.

The second reason is that the average energy of one electron is between 0 and 10 eV for our plasma reactor. More energy is required (15.06 eV or rather 19.87 eV [11]) to create $CH_2$ or CH in one step from methane.

The reaction of two similar radicals for example two $CH_3$ radicals to ethane is thinkable but plasma in a DBD reactor has a small degree of ionization. The probability of a collision of two radicals is smaller than the collision of a radical and a molecule like in reaction 4 to 6.

There are not only reactions which generates C2 hydrocarbons. It is also possible to destroy these compounds in the plasma region (reaction 8.7 to 8.9).

$$C_2H_6 + e^- \rightarrow 2\ CH_3 + e^- \quad (8.7)$$

$$C_2H_4 + e^- \rightarrow C_2H_3 + H + e^- \quad (8.8)$$

$$C_2H_2 + e^- \rightarrow C_2H + H + e^- \quad (8.9)$$

To dissociate ethine via reaction 8.9 more energy is needed (5.72 eV [12]) as for reaction 8.8 (4.60 eV [12]) to destroy ethene. Thus ethine is in the plasma region more sTable than ethene. The amount of ethine is for this reason higher than the amount of ethene for power above 45 W.

The produced amount of the three C2 hydrocarbons increases with the adjusted generator power as shown in Figure 8.3. The ethane amount rises from 2.25% to 4.64%. There is an elevation of the ethene amount from 0.22% to 0.36% and 0.19%

to 0.42% for ethine. These results can be explained by the conversion of methane. Figure 8.4 illustrates the conversion of methane as a function of the adjusted generator power. The conversion of methane increases with the input power. The methane conversion has a value of 11.8% at a plasma generator power of 30 W and rise to 36.5% at the highest power. The number of electron increases with the power, which means a greater number of micro filaments. A larger number of micro filaments imply also a larger volume in which the starting material has been converted. A higher conversion of the starting material stands for more reactive species like $CH_3$, $CH_2$ or CH. These radicals collide with other methane molecules to form C2 hydrocarbons. The fraction of these products rises, if the concentration of the radical increases.

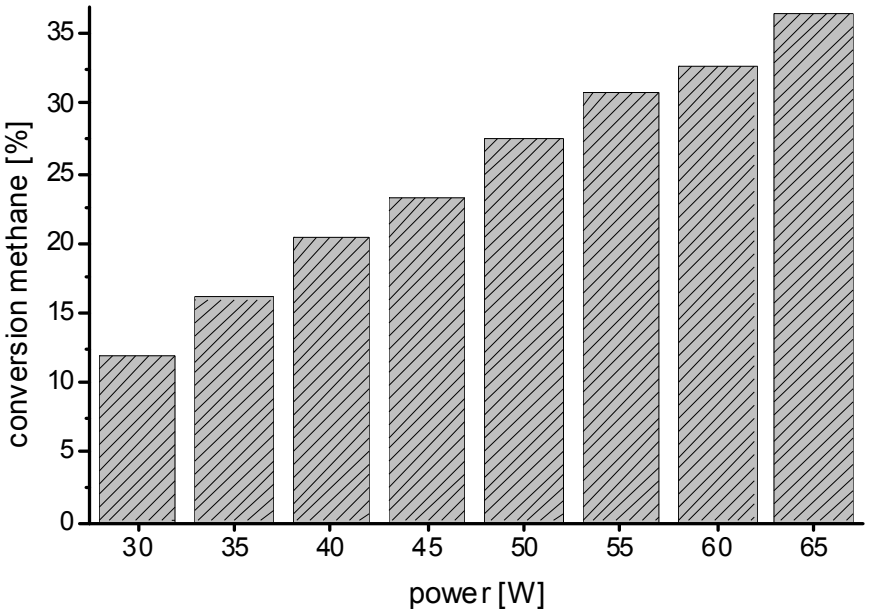


**Figure 8.4:** Conversion of methane as a function of the adjusted generator power.

The first paragraphs of this section have shown the produced amount of C2-hydrocarbons at a flow rate of 400 sccm. Figure 8.5 illustrates the dependence of the ethane yield on the velocity of the gas stream. The starting streams for these experiments consist of 1.75% methane and 0.75% carbon dioxide and the gas flow was variegated between 200 and 800 sccm. If the flow is decreased, the amount of ethane increases from 3.0% (800 sccm) to 5.4% (200 sccm) at a power of 60 W. This result can be explained by the dwell time of the compounds in the plasma region. A shorter flow implies a longer time to convert methane by energy rich plasma electrons in the reactor. The concentration of the required $CH_3$ radicals increases in this case and reaction (8.4) becomes more likely.

The dwell time of the particles in the 1.06 $cm^3$ plasma volume has been variegated between 80 ms (800 sccm) and 320 ms (200 sccm). If the power of the plasma generator reaches 65 W and the gas flow has a value of 200 sccm, an arc is and, thus, no ethane is shown in Figure 8.5. No measurements are done at these parameters to protect the reactor.

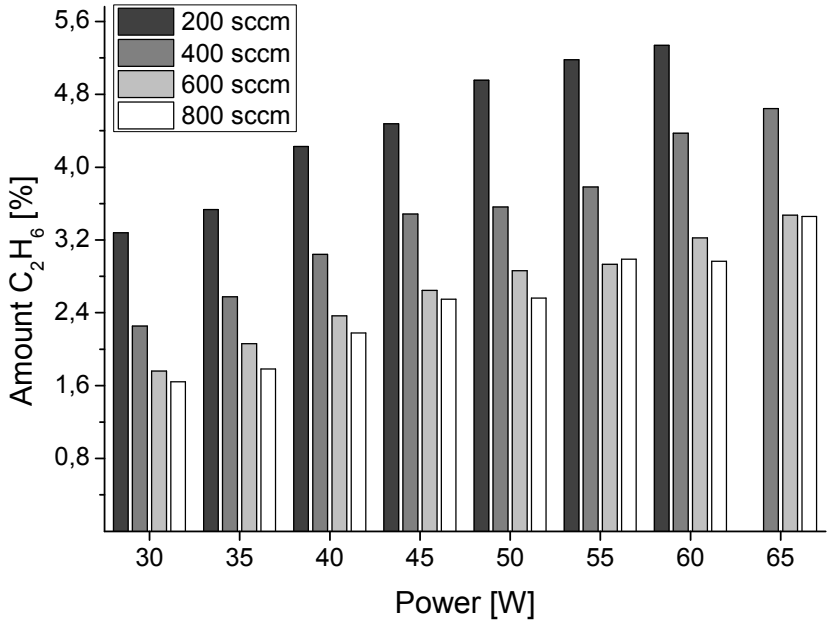


**Figure 8.5:** Influence of the flow velocity on the ethane yield. The gas stream consists of 1.75% Methane and 0.75% carbon dioxide.

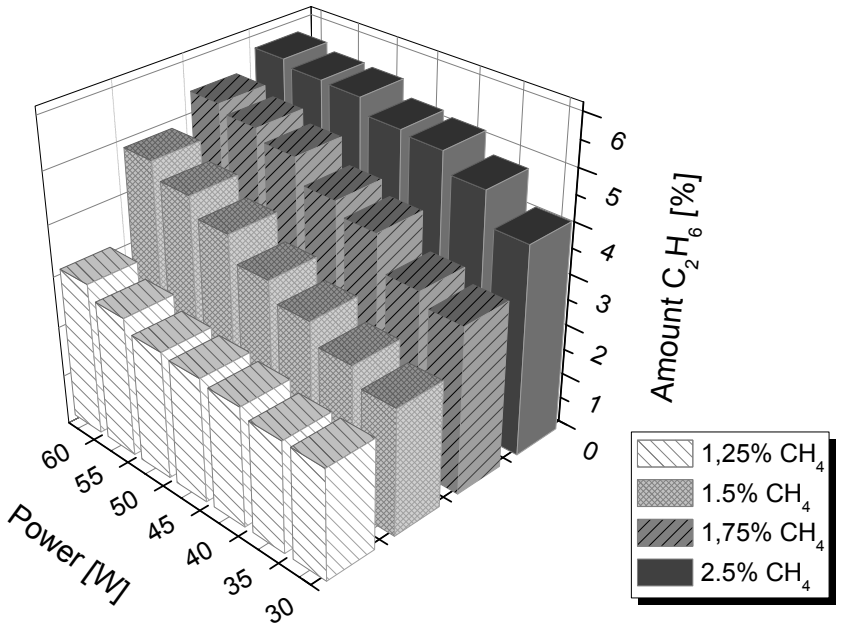


**Figure 8.6:** Produced amount of ethane as a function of the adjusted generator power for different inlet mixtures at a flow rate of 200 sccm.

The following results have been originated at a flow rate of 200 sccm. The dependence of the produced amount of ethane from the composition of the inlet flow is shown in Figure 8.6. The concentration of methane was changed from 1.25% to 2.5%. The highest concentration (5.7%) of ethane is produced, if the flow of the starting material consists of 5 sccm methane and 195 sccm of the buffered gas helium and the power of the plasma has a value of 60 W. In this case the concentration of the needed methyl radicals (reaction 8.6) is higher than for inlet flows which have, in addition to methane, a small amount of carbon dioxide. The probability of a collision of one methyl radical with a methane molecule increases, if the concentration of methane in the starting flow increases. This Figure shows an increasing of the ethane concentration with increasing power of the plasma generator to higher values.
Ethene and ethine show similar results, if the flow rate and the composition of the starting material have been varied.

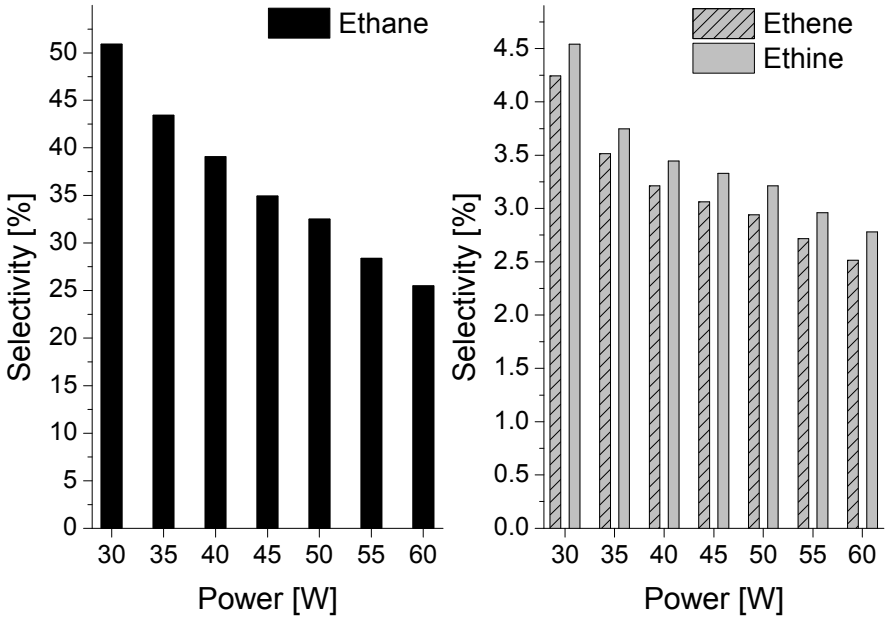


**Figure 8.7:** Selectivity of this reactor for the three C2 hydrocarbons as a function of the inlet power. The left graph shows the selectivity for this reaction to ethane and the right the selectivity of ethene and ethine.

The results for the selectivity of this reactor to the three C2 hydrocarbons (Figure 8.7) are shown for a starting stream which consists of 5 sccm methane and 195 sccm helium.

Selectivity of a reaction is another important factor to characterise the DBD reactor. For the C2 hydrocarbons it is calculated by the following formula:

$$S_{CH_x} = \frac{2 \cdot n_{C_2H_X}(\text{produced})}{n_{CH_4}(\text{converted})}$$

(8.10)

An increase of the inlet power leads to a decrease of the ethane selectivity from 50.9% at 30 W to 24.5% at 65 W. Similar results have been observed for ethene and ethine. The reaction selectivity for these two products is lower than for ethane; the values range between 2.5% and 4.5%. Two effects explain the decline of the selectivity: 1) Higher hydrocarbons are created at a higher power and 2) it is easier to create hydrogen at a higher input power. The selectivity of ethene is lower than the selectivity of ethane by about a factor of ten. The reason is the number of reactions to get the compounds. Ethane needs at least two and the other two products need three or rather four different reactions.

## 8.4 Conclusion

1) This DBD reactor generates the three C2 hydrocarbons. The main component of these three compounds is ethane. The relative amount of ethene and ethine is less than 1%.

2) The produced amount of three hydrocarbons is dependent on the adjusted generator power. There is an increase of the concentration, if the power rises.

3) A lower flow stream leads to a higher generated amount of the C2 hydrocarbons.

4) An increase of the amount of methane in the starting stream results in an increase of the produced amount of ethane, ethene and ethine.

5) The highest amount of ethane (5.4%) has been generated, if the inlet flow consists of 5 sccm methane and 195 sccm helium.

4) The selectivity of the three interesting products reaches a high value at a low plasma power in the DBD reactor. The selectivity for the plasma assisted reaction of methane to ethane reaches a value of 51% at 30 W, if the stream consists of 2.5% methane and 97.5% helium at a flow rate of 200 sccm.

5) A higher input plasma power raises the conversion of methane.

**Acknowledgements**

This project is part of the framework of the European Research Area (ERA) Chemistry call. This work is financially supported by the Deutsche Forschungs-Gesellschaft

(DFG). Support by the IGSM Braunschweig is gratefully acknowledged. We acknowledge K. Krawczyk and M. Młotek for fruitful discussions.

## 8.5 References for section 8

1. Ziegler K, Holzkamp E, Breil H, Martin H (1955) Das Mülheimer Normaldruck-Polyäthylen-Verfahren, Angew Chem 67:541-47.
2. Martin NS, Savadkoohi HA, Feizabadi SY(2010) Methane Conversion to C2 Hydrocarbons Using Dielectric-barrier Discharge Reactor: Effects of System Variables, Plasma Chem Plasma Process 28:189-02.
3. Zhou LM, Xue B, Kogelschatz U, Eliasson B (1998) Nonequilibrium Plasma Reforming of Greenhouse Gases to Synthesis Gas, Energy & Fuels 12:1191-99.
4. Sentek J, Krawczyk K, Młotek M, Kalczewska M, Kroker T, Kolb T, Schenk A, Gericke K-H, Schmidt-Szałowski K (2010) Plasma-catalytic methane conversion with carbon dioxide in dielectric barrier discharges, Appl Catal, B 94:19–26.
5. Wang B, Cao X, Yang K, Xu G (2008) Conversion of methane through dielectric-barrier discharge plasma, Front Chem Eng China 2:373-78.
6. Bogaerts A, Gijbels R (2003) Numerical modelling of gas discharge plasmas for various applications, Vacuum 69:37-52.
7. Larkin DW, Lobban LL, Mallinson RG (2001) The direct partial oxidation of methane to organic oxygenates using a dielectric barrier discharge reactor as a catalytic reactor analog, Catal Today 71:199-10.
8. Kroker T, Kolb T, Krawczyk K, Mlotek M, Schenk A, Schmidt-Schalowski K, Gericke K-H (2009) Catalytic Conversion of Biogas in a Fluidised Bed Reactor Supported by a DBD, Adv Appl Plasma Sci 7:187-90.
9. Kroker T, Kolb T, Krawczyk K, Mlotek M, Schenk A, Gericke KH (2010) Catalytic Conversion of Biogas in a Fluidized Bed Reactor Supported by a DBD, Frontier Appl Plasma Techn 3:69-73.
10. deB. Darwent B(1970) Bond Dissociation Energies in Simple Molecules. NBSDS-NBS 31.
11. Plessis P, Marmet P, Dutil R (1983) Ionisation and appearance potentials of $CH_4$ by electron impact, J Phys B: At, Mol Opt Phys 16:1283-94.
12. Wang B, XU G (2002) Conversion of natural gas to C2 hydrocarbons through dielectric-barrier discharge plasma catalysis, Sci China: Chem 45:299-10.

# 9 Wet conversion of methane and carbon dioxide in a DBD reactor

**Torsten Kolb, Thorsten Kroker, Jan H. Voigt, Karl-Heinz Gericke**

**Institut für Physikalische und Theoretsiche Chemie**

Braunschweig, 38106, Germany

**ABSTRACT**

*The influence of water on the plasma assisted conversion of methane and carbon dioxide in a dielectric barrier discharge (DBD) plug flow reactor was studied. The plasma at atmospheric pressure was ignited by a power supply at a frequency of 13.56 MHz. Product formation was studied at a power range between 35 W and 70 W. The concentrations of the three gases were altered and diluted with helium to 3%. FTIR spectroscopy and mass spectroscopy were applied to analyze the inlet and the product streams. The main product of this process are hydrogen, carbon monoxide and ethane. Ethene, ethine, methanol and formaldehyde are generated beside the main products in this DBD in lower concentrations. The conversion of methane, the ratio of the synthesis gas components ($n(H_2):n(CO)$), and the yield of oxygenated hydrocarbons and hydrogen increases by adding water. The total consumed energy reaches lower values for small amounts of water. Additional water does not influence the generated amount of C2 hydrocarbons and of CO, but decreases the carbon dioxide conversion.*

**KEYWORDS**: dielectric barrier discharge, cold plasma, water, methane, carbon dioxide

## 9.1 Introduction

The basic chemicals for the production of nearly all organic compounds are nowadays extracted from fossil fuels like crude oil or natural gas. These sources will run out in the future and new techniques are required to obtain the starting material for most organic synthesis. The conversion of methane and carbon dioxide mixtures might be one solution for this problem. This gas mixture is a well known regenerative source, because it is produced from renewable resources like biomass, waste or sludge. These solid compounds are converted in the absence of air by an anaerobic degradation or digestion process where organic carbon is subsequently oxidized and reduced to its most oxidized state ($CO_2$) and its most reduced state ($CH_4$) [1]. Gas mixtures generated from biomass (animal dung or plants like corn) are called biogas [2]. Digester gas [3] originates from sewage, and waste is transformed in landfills to landfill gas [2]. These three kinds of gas mixtures consist mostly of methane (37 - 75%) and carbon dioxide (30 – 45%) and to a minor amount of nitrogen, hydrogen, oxygen and hydrogen sulfide [2,3].

Methane and carbon dioxide are very unreactive compounds, which have to be activated in order to increase the reactivity. One way is the ignition of a cold plasma using for example corona discharge, dielectric barrier discharge (DBD), gliding arc, glow discharge or microwave discharge. This paper focuses on the conversion of methane and carbon dioxide in a DBD reactor. The dielectric barrier prevents the formation of sparks or arcs [4]. The slightly higher electron temperature [5] is another advantage of this device in comparison to the other named techniques.

Intense research is performed to convert methane and carbon dioxide in a DBD reactor. The main products are synthesis gas [6-9] C2 hydrocarbons [10], [11] and oxygenated hydrocarbons, [12],[13] like methanol or formaldehyde. Mfopara et al. [14] analyzed the effect of water on the methane conversion in an atmospheric pressure dielectric barrier discharge. Methane was added in deficient proportion and the amount of water was changed up to 10%. This set up generated mainly hydrogen and carbon dioxide.

In a previous work we [15] analyzed the conversion of biogas like mixtures in a DBD to C2 hydrocarbons, so here ethane was found to be the main hydrocarbon. The concentration of all above mentioned products increases with increasing plasma power at low inlet flows (200 sccm) and the absence of carbon dioxide.

In contrast to Mfopara, this work focuses on the effect of small amounts of water on the product distribution when methane and carbon dioxide are converted in a DBD reactor. The amount of water, the power, and the composition of the inlet flow were varied. Increasing the conversion of the starting material and the amount of the products is the aim of this research.

## 9.2 Experimental setup

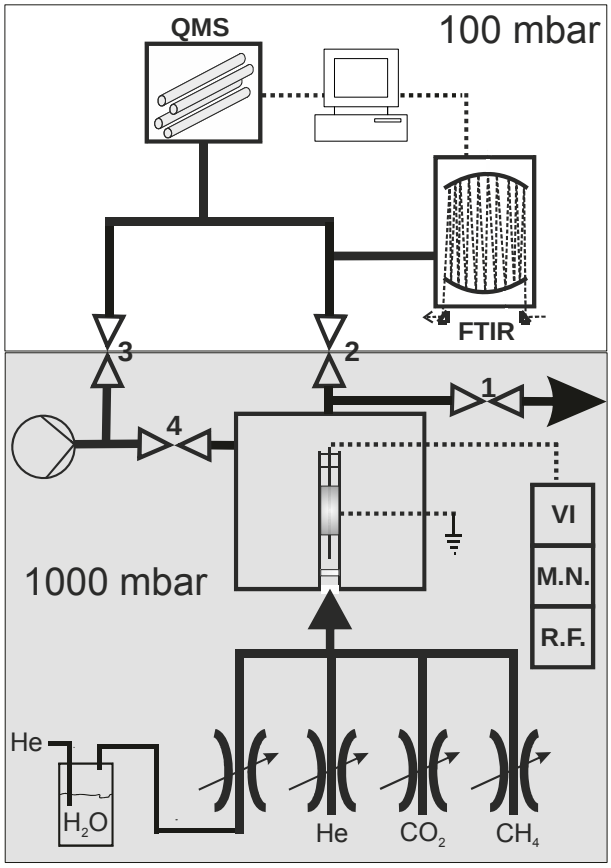


**Figure 9.1:** Schematic setup of the current experiment. QMS: quadropole mass spectrometer; FTIR: Fourier transform interferometer; VI: Octiv VI probe; M.N.: matching network; R.F. radio frequency generator (13.56 MHz); 1,4 Valves; 2,3 precision valves.

The experimental setup of this project is shown in Figure 9.1. Four mass flow controllers (MFC) adjusting the gas flow are controlled by a multi gas controller (MFC). The compositions of the inlet flow consist of different amounts of methane, carbon dioxide and water vapor and the buffer gas helium to dilute this mixture to 3%. The water vapor is created by bubbling helium through a tank of liquid distilled water at ambient conditions. The concentration of water vapor generated in the bubbling tank depends on the temperature and is adjusted by using another MFC (helium). This second MFC (helium) regulates the total flow of 200 sccm. The concentration of water is de-

termined by the flow of the two helium mass flow controllers. All gases are mixed before they reach the reaction chamber. The dielectric barrier discharge reactor is located inside a stainless steel cube. One side of this chamber has a transparent plexiglas wall to observe the process.

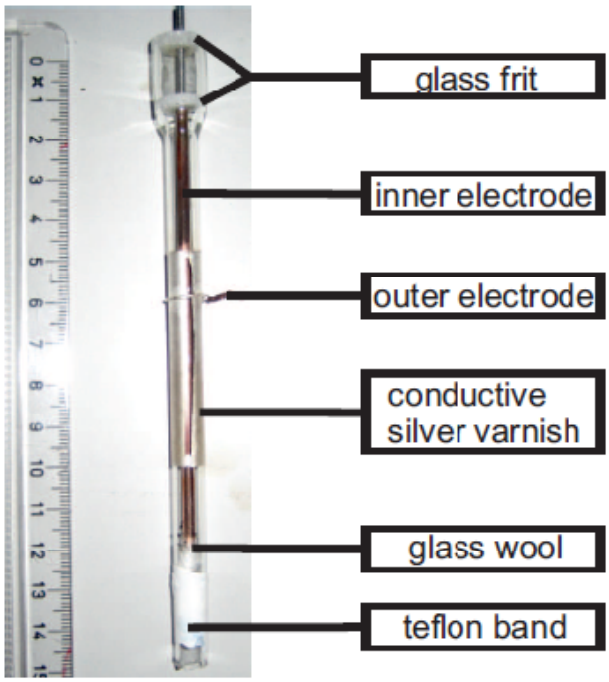


**Figure 9.2:** The DBD reactor used in this experiment.

The reactor (Figure 9.2) consists of a 15 cm long Duran glass cylinder with an inner diameter of 5.9 mm and an outer diameter of 8.0 mm. The inner working iron electrode with a diameter of 3.0 mm is fixed on the top by two glass frits and on the bottom by glass wool. The outer part of the glass body is covered over a length of 50 mm with a conductive silver varnish to create the outer grounded counter electrode. The outer electrode has over the whole length a slit of about one millimeter width to monitor the plasma. The plasma is generated by a 13.56 MHz radio frequency generator (ENI ACG-6B) and a matching network (ENI RFC 5M) at atmospheric pressure. The power of this device can be adjusted in one watt steps to a maximum power of 600 W. An Octiv VI probe (Impedans) is installed between the reactor and the plasma generator unit to measures the voltage, the current and the phase between them. These data are necessary to calculate the total consumed energy. The reactor temperature changes from room temperature to about 100°C after increasing the power. The details for this measurement are explained in a previous work [8]. Therefore, the plasma is in the low temperature region.

The stream of the reactants and the products leaves the reaction chamber through valve 1 (Figure 9.1). A small gas stream is sidelined through the precision valve 2 to be analyzed online in a FTIR spectrometer and a quadrupole mass spectrometer. The FTIR spectrometer (Bruker Equinox 55) is equipped with a long path white cell at a total pressure of 100 mbar. The quadrupole mass spectrometer (Balzer QME 200) operates at a pressure of $10^{-5}$ mbar. The pressure for the FTIR spectrometer is adjustable by a precision valve 3 and a dry scroll pump (Edwards XDS 10). This pump is also used to evacuate the reaction chamber through valve 4. The White cell increases the optical path length up to 6 m. The IR spectra are recorded with a resolution of 0.5 $cm^{-1}$ between 500 and 5000 $cm^{-1}$. The detection limit of this setup is approximately 5 ppm. [16]

The QMS continuously records spectra between m/z=1 to m/z=90 and is used to analyze IR inactive species like hydrogen or substances which have no characteristic IR peaks like ethane. For this spectrometer the detection limit is 3 ppm. The pressure is generated by a turbo molecular drag pumping station (Pfeiffer TSU 071E) consisting of a diaphragm pump (Pfeiffer MVP 015) and a turbo molecular pump (Pfeiffer TMU 071P).

The FTIR spectrometer and the QMS are calibrated with the starting material and the exact identified products to determine the conversion of the raw material and the yield of the products. The details for this procedure are discussed in a previous paper [8].

## 9.3 Results and discussion

A qualitative analysis of this process has been done in a previous work [12]. The products carbon monoxide, ethene, ethyne, formaldehyde, and methanol are clearly identified via IR spectroscopy. Mass spectroscopy is applied to identify ethane and hydrogen and to determine the conversion of methane and carbon dioxide.

The conversion of the starting materials is calculated according to:

$$C_x = \frac{n_{x,conv.}}{n_{x,0}}, \quad \text{were x represents } CO_2 \text{ or } CH_4; \qquad (9.1)$$

$$n_{x,conv} = n_{x,0} - n_{x,end}$$

The selectivity of the particular products is given by:

$$S_{H_2} = \frac{n_{H_2}}{2 \cdot n_{CH_4,conv.}} \qquad (9.2)$$

$$S_{CO} = \frac{n_{CO}}{n_{CH_4,conv.} + n_{CO_2,conv.}} \tag{9.3}$$

$$S_{C_2H_b} = \frac{2 \cdot n_{C_2H_b}}{n_{CH_4,conv.}} \qquad \text{with b = 2, 4 or 6} \tag{9.4}$$

$$S_{CH_3OH} = \frac{n_{CH_3OH}}{n_{CH_4,conv.} + n_{CO_2,conv.}} \tag{9.5}$$

$$S_{CH_2O} = \frac{n_{CH_2O}}{n_{CH_4,conv.} + n_{CO_2,conv.}} \tag{9.6}$$

The yield of the particular products is calculated by:

$$Y_i = \frac{n_i}{\sum n_P + \sum n_S} \tag{9.7}$$

i …. particular product
P …. product
S …. starting material

The buffer gas helium will be neglected for the following. Two different types of measurements are discussed in each sub section. In the first series of measurements the concentration of the water flow was varied between 0 and 19%. Here, the undiluted gas flow without water consisted of 80% methane and 20% carbon dioxide. A fixed plasma power of 60 W was applied. The second kind of experiments concentrated on the influence of the plasma power (35 – 70 W). The amount of water vapor was adjusted to 17%, the concentration of methane ranged between 41.5% and 83% and carbon dioxide was accordingly added to reach 100%.

### 9.3.1 Conversion of the starting material

Figure 9.3 shows the conversion of methane and carbon dioxide as a function of added water vapor. A raise of the added water fraction up to 19% increased the conversion of methane from 48% to 58% and decreased the conversion of carbon dioxide from 36% to 31%. This observation can be explained by the reactions occurring in the plasma volume through energy rich electrons.

$$CH_4 \xrightarrow{e^-} CH_3 + H \tag{9.8}$$

$$CO_2 \xrightarrow{e^-} CO + O \tag{9.9}$$

$$H_2O \xrightarrow{e^-} OH + H \tag{9.10}$$

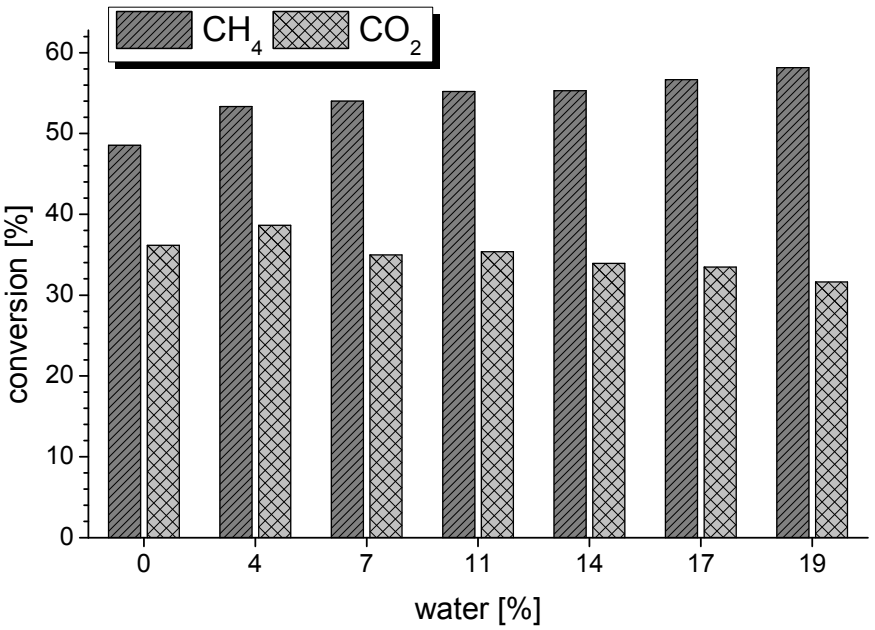


**Figure 9.3:** Conversion of methane and carbon dioxide as a function of the water proportion. The gas flow without water consisted of 80% methane and 20% carbon dioxide and was diluted to 2.5% with helium. The power was adjusted to 60 W.

Methane, carbon dioxide and water dissociate in this primary reaction to form methyl and hydrogen, carbon monoxide and oxygen or hydroxyl radicals. Thus, additional water in the DBD reactor increases the concentration of the OH radicals. The starting material for this process can be converted by metasTable helium according to a Penning dissociation phenomenon [17]. However, a significant amount of energy is required to form He* ($2^3$s: 19.8 eV and $2^1$s: 20.6 eV [18]) and, thus, it is not very likely the reaction with He* will occur. A DBD reactor generates a power of only 10 eV [23]. Secondary reactions of the generated radicals with the starting material have a high probability. Important examples for this operating condition are:

$$CH_4 + O \rightarrow CH_3 + OH \qquad (9.11)$$

$$CH_4 + HO \rightarrow CH_3 + H_2O \qquad (9.12)$$

Thus, reaction (9.12) has a higher probability when water is present and thus the conversion of methane rises.

There are no secondary reactions with OH to convert carbon dioxide. However, water consumes part of the energy which is needed to convert carbon dioxide. As a consequence, the conversion of this compound decreases. The dissociation energy of reaction (9.9) is (5.52 eV [19]) slightly higher than for reaction (9.10) (5.18 eV [19]). Methane is more easily dissociated by the electrons (4.45 eV [19]) than the other two

components. Therefore, the converted amount of methane is higher than that for $CO_2$.

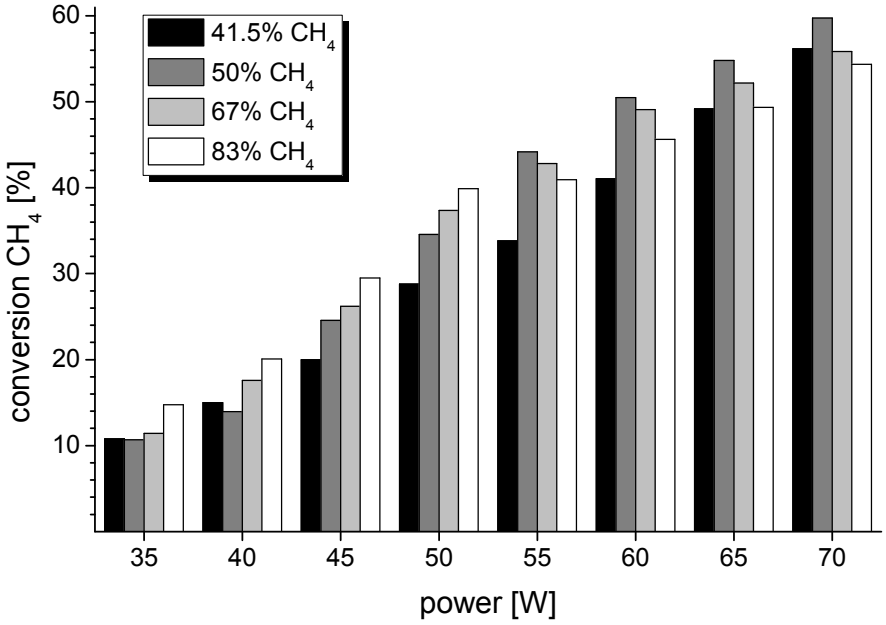


**Figure 9.4:** Conversion of methane as a function of plasma power and $CH_4$ composition of the inlet flow. The amount of water was fixed to 17% and the missing part is filled up with carbon dioxide. The gas mixture was diluted to 3% with helium.

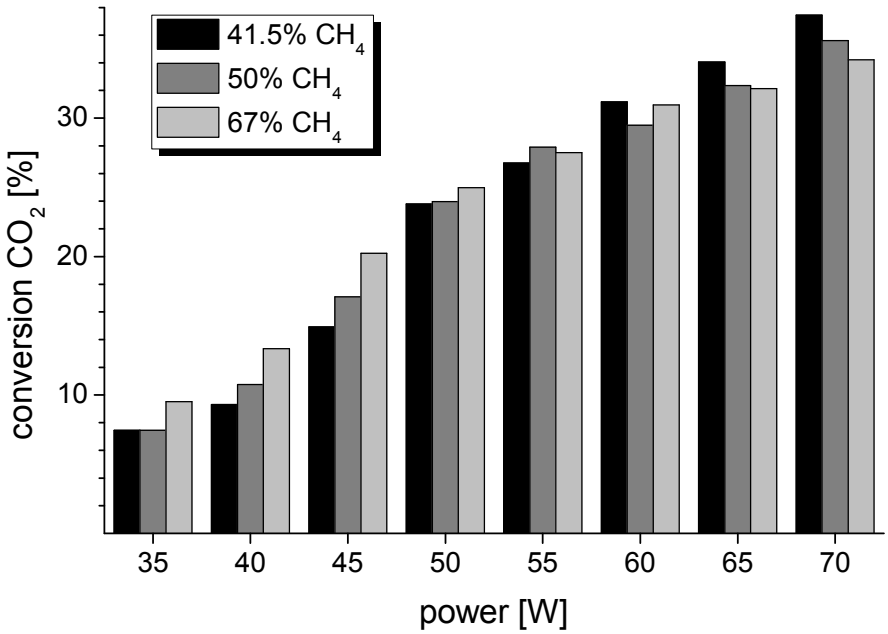


**Figure 9.5:** Conversion of carbon dioxide as a function of plasma power and $CH_4$ composition of the inlet flow. The amount of water was fixed to 17% and the missing part is filled up with carbon dioxide. The gas mixture was diluted to 3% with helium.

The dependency of the plasma power and the composition of the inlet flow on the conversion of methane and carbon dioxide is shown in Figure 9.4 and 9.5. The contribution of water was fixed to 17% for these measurements. The conversion of the starting material increased by a factor of approximately 5 for methane and by a factor of approximately 4 for carbon dioxide, when the power was changed from 35 W to 70 W.

For our plasma process the conversion of the biogas compounds reaches maximum values for high $CH_4$ and low $CO_2$ concentrations. A collision of methane with an energy rich plasma electron has a higher probability if the concentration of this molecule is high. The quenching reaction of carbon monoxide with oxygen radical reduces the conversion of carbon dioxide [20]:

$$CO + O \rightarrow CO_2 \qquad (9.13)$$

At a higher methane concentration reaction (9.13) is less probable compared to reaction (9.9), resulting in an overall higher carbon dioxide conversion.

The conversion of methane reaches a maximum for an inlet stream consisting of 50% $CH_4$ if the power was elevated above 50 W. The power is now high enough to convert more carbon dioxide via reaction (9.9) and the products are able to convert methane by the secondary reactions (9.11) and (9.12). The concentration of the needed O radicals and methane molecules reaches an optimum value for an inlet flow consisting of 50% $CH_4$ and 33% $CO_2$.

Essentially no conversion of water was observed: The reactive species generated through reaction (9.9) and (9.10) are mainly recombined to water via reaction (9.11) and (9.12). The use of additional water in the DBD reactor reduces the concentration of the polluting greenhouse gas methane, but it increases the amount of oxygenated hydrocarbons and of hydrogen as described in the following section.

### 9.3.2 Oxygenated hydrocarbons

Oxygenated hydrocarbons are an important class of organic chemicals. Their generation is influenced by an additional amount of water. Methanol and formaldehyde are major oxygenated products in this study. Figure 9.6 illustrates the influence of water on the produced amount of methanol and formaldehyde. The concentration of both components increases with an extra amount of $H_2O$. The formaldehyde concentration rises from 0.2% (without water) to 0.6% (19% water). The formation of methanol increases from 0.1% to 0.4%. The mechanisms [21, 22] for the generation of these two products explain the observed results:

$$CH_3 + O \rightarrow H_2CO + H \quad (9.14)$$

$$CH_2 + OH \rightarrow H_2CO + H \quad (9.15)$$

$$CH_3 + OH \rightarrow CH_3OH \quad (9.16)$$

The needed methylene radical for reaction (9.15) is generated by dissociating the generated methyl radicals (reaction (9.8)) through energy rich plasma electrons. Additional water increases the concentration of the needed OH radicals in the reactor and thereby the amount of the two identified oxygenated hydrocarbons (methanol and formaldehyde). There are two reasons why the methanol and formaldehyde yield is fairly small. Firstly, reactions (9.14) to (9.16) are recombination's of two radicals. The ionization rate and the number of reactive radicals are very low in such a plasma source and the probability of collisions between two radicals are also low [23]. Secondly, methanol and formaldehyde exhibits a high reactivity with the generated radicals OH, O or H.

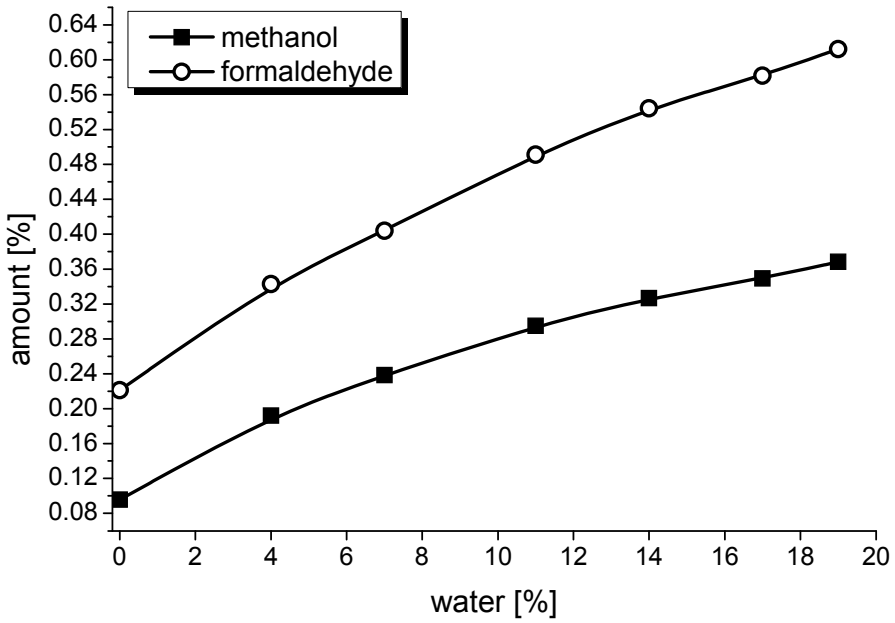


**Figure 9.6:** Methanol and formaldehyde yield as a function of added water. The gas flow without water consisted of 80% methane and 20% carbon dioxide and was diluted to 2.5% with helium. The power was adjusted to 60 W.

The amount of these two oxygenated compounds is relatively small without water because the needed OH radical is then only generated through carbon dioxide (reaction (9.9)).

The selectivity of this reactor to form methanol or formaldehyde for different water concentrations is shown in Figure 9.7. Water increases the selectivity of methanol

formation by a factor of 3 and for formaldehyde a doubling for its selectivity is observed. The higher concentration of OH (from water) is responsible for the higher selectivity.

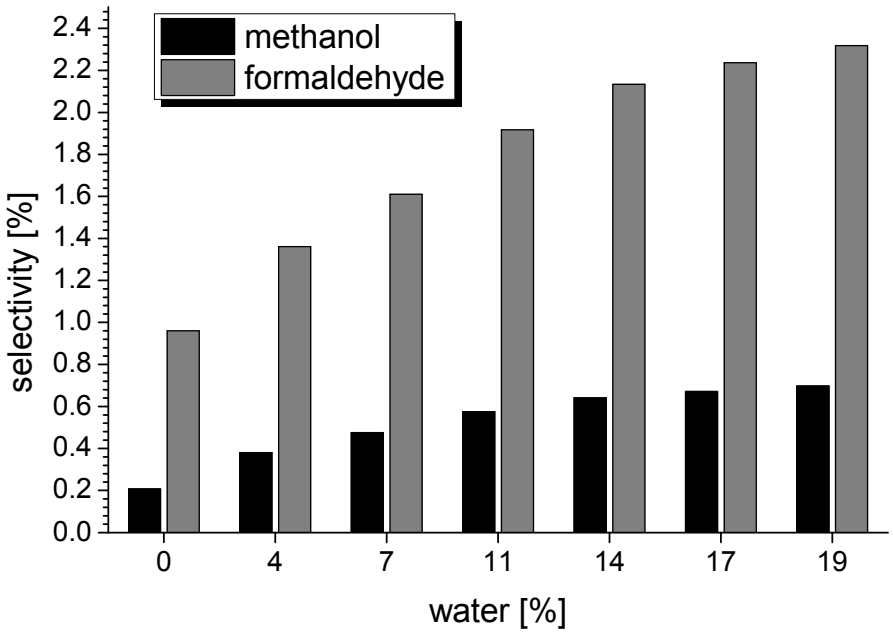


**Figure 9.7:** Selectivity of the two oxygenated hydrocarbons for different amounts of water. The gas flow without water consisted of 80% methane and 20% carbon dioxide and was diluted to 2.5% with helium. The power was adjusted to 60 W.

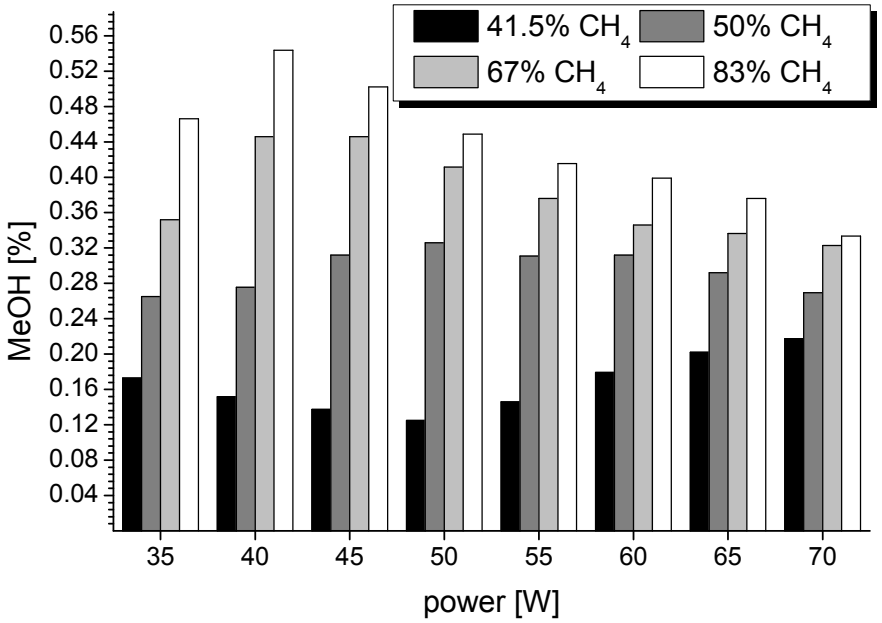


**Figure 9.8:** Methanol yield for different plasma powers and $CH_4$ composition of the inlet flow. The amount of water was fixed to 17% and the missing part is filled up with carbon dioxide. The gas mixture was diluted to 3% with helium.

Figures 9.8 and 9.9 display the methanol and formaldehyde yield for different inlet stream compositions and plasma powers.

The amount of methanol increases if the stream of the starting material contains more methane. A high concentration of methane generates a higher amount of $CH_3$ radicals in the reactor, resulting in a higher collision frequency to collide with the generated OH radicals which origin from water to form methanol (reaction 15). The methanol yield reached a maximum at intermediate power values if the power of the plasma generator was altered from 35 W to 70 W and at least 50% methane was inserted. At low power levels the concentration of the radicals is fairly low resulting in low product formation and at very high power levels the concentration of the products becomes reduced due to radical reactions. The maximal received amount of MeOH at a power of 40 W and an inlet stream consisting of 83% $CH_4$ and water is 0.54%.

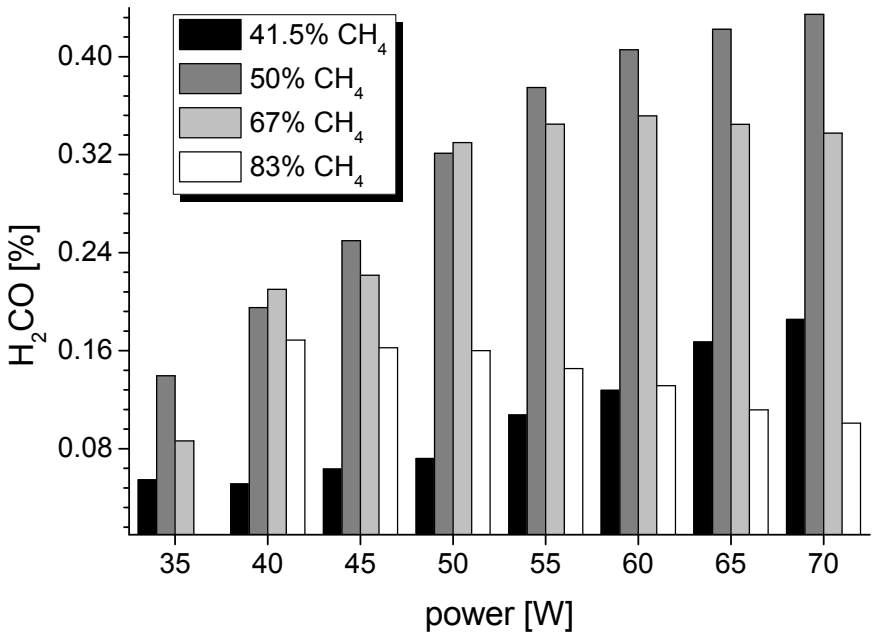


**Figure 9.9:** Formaldehyde yield for different plasma powers and $CH_4$ composition of the inlet flow. The amount of water was fixed to 17% and the missing part is filled up with carbon dioxide. The gas mixture was diluted to 3% with helium.

In contrast to methanol the generated amount of formaldehyde reaches the highest concentration at medium methane concentrations. The generated oxygen, hydroxyl and methyl radicals react via reaction (9.14) or (9.15) to generate formaldehyde. Too few oxygenated radicals are generated in the case of a methane rich inlet stream. There are not enough methyl radicals created if the starting flow is rich of carbon dioxide.

The formaldehyde yield rises for high amounts of carbon dioxide and decreases for $CO_2$ poor inlet composition with increasing of the plasma power to 70 W. The highest formaldehyde value (0.4%) was observed at 70 W and a reactant stream consisting of 50% methane, 33% $CO_2$ and 17% water. The oxygen radicals which are required to form formaldehyde are generated from carbon dioxide, and the probability of a collision of an electron with $CO_2$ increases with higher $CO_2$ concentration. The formation of O radicals for reaction (9.14) is more likely at higher velocities of the free electrons which can be achieved at higher plasma powers.

The second required $CH_3$ radical for the formation of formaldehyde (reactions (9.14) or (9.15) reacts rather with methane to form C2 hydrocarbons (see below) than with the oxygenated radicals. The methyl radicals can also undergo another dissociation reaction with other plasma electrons at a higher power resulting in a decrease of the formaldehyde concentration.

### 9.3.3 Synthesis gas

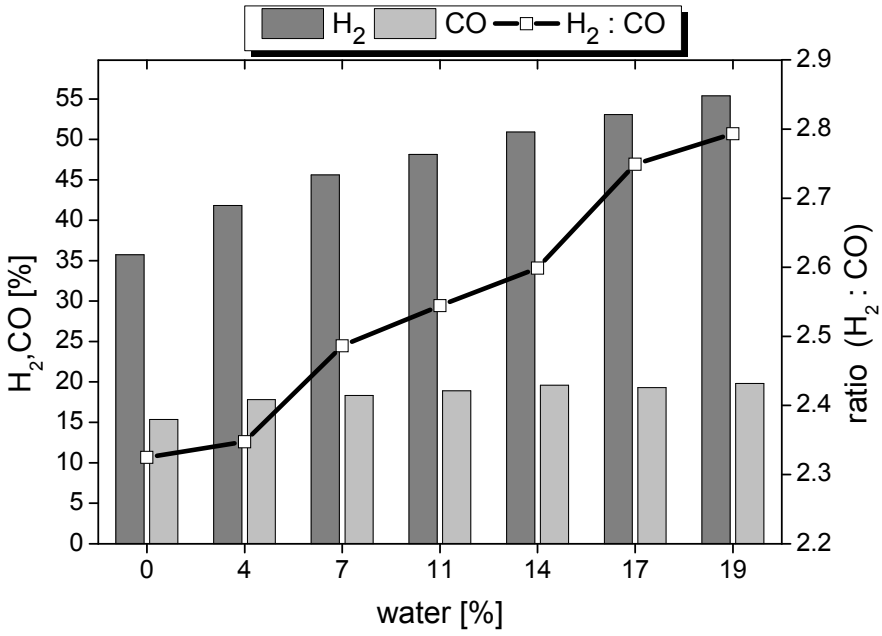


**Figure 9.10:** Dependency of the yield of the synthesis gas components on the amount of water and the ratio of hydrogen to carbon monoxide. The gas flow without water consisted of 80% methane and 20% carbon dioxide and was diluted to 2.5% with helium. The power was adjusted to 60 W.

The synthesis gas components are generated from the starting material in the absence of water by the following overall reaction:

$$CH_4 + CO_2 \rightarrow 2H_2 + 2CO \qquad (9.17)$$

This is a well known reforming reaction. However, it is not an elementary reaction which we will focus on in the following.

In our experiments hydrogen and carbon monoxide are the main products which, as an ensemble, are called synthesis gas. The formation of these components and their ratio for different water amounts are shown in Figure 9.10. The hydrogen concentration increases while the carbon monoxide concentration stays constant with increasing water concentrations. As a consequence the ratio of hydrogen to CO rises.

There are different ways to generate a hydrogen molecule. One possibility is the three body collision of two hydrogen radicals with another particle or with the reactor wall:

$$H + H + M \rightarrow H_2 + M \qquad (9.18)$$

Since the concentration of methane is higher than the amount of the generated reactive H radicals reaction (9.19) is the more likely reaction:

$$H + CH_4 \rightarrow H_2 + CH_3 \qquad (9.19)$$

Water is, due to reaction (9.10), an additional hydrogen source for this process. The yield of molecular hydrogen increases by a factor of approximately 1.5 from 36% (without water) to 55% (19% water).

Carbon monoxide is generated via the primary plasma reaction (9.9). This process is independent of water and its contribution is about 18%. If the concentration of hydrogen rises with the amount of water and the carbon dioxide concentration stays constant, the $H_2$:CO ratio has to increase. This ratio is important for industrial applications like Fischer Tropsch Synthesis [24] or hydroformylation [25]. A $H_2$:CO = 2 is needed to generate alkenes or methanol via Fischer Tropsch Synthesis. A ratio of one is used for hydroformylation reactions of alkenes. The ratio of $H_2$ to CO is not only shifted by changing the composition and the power (see below); additional water is also a possible alternative solution.

Figure 9.11 illustrates the selectivity of hydrogen and carbon monoxide as a function of the water amount. They reach high values. The selectivity of CO (≈ 38%) stays constant while the selectivity of $H_2$ increases from 46% (without water) to 60% (19% water). These results are explained by the additional hydrogen source (water). The selectivity of CO doesn't change by adding water when the amount of $CO_2$ and the power are kept constant.

In principle, water gas shift reaction can explains the increase of the hydrogen yield and selectivity and constant values for carbon monoxide beside the above specified reason. The following reaction illustrates this process:

$$CO + H_2O \rightarrow CO_2 + H_2 \qquad (9.20)$$

Both components are in the apparatus. Water is a starting material and carbon monoxide is generated in the DBD reactor. Reaction (9.20) is an exothermic process. A catalyst and a temperature of at least 180°C are used for industrial applications [26]. Our reactor has a maximum temperature of about 100°C. Therefore, reaction (9.20) should have only a small influence on the contribution of the synthesis gas products and its selectivity.

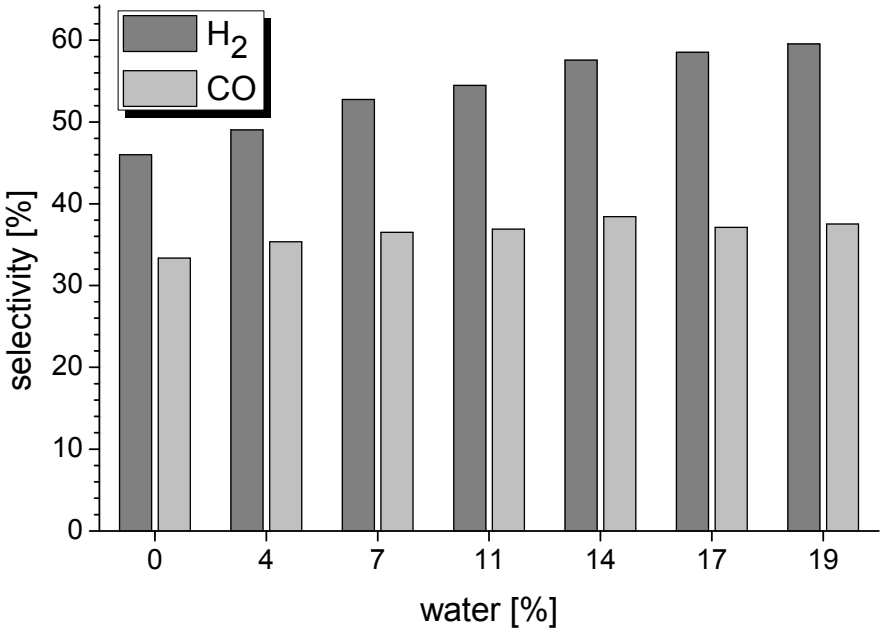


**Figure 9.11:** Selectivity of the synthesis gas components for different amounts of water. The gas flow without water consisted of 80% methane and 20% carbon dioxide and was diluted to 2.5% with helium. The power was adjusted to 60 W.

Figure 9.12 shows the product distribution of hydrogen and carbon monoxide and the ratio of these two products ($H_2$:CO) for different plasma powers. The amount of methane was incresed from Figure 9.12a to 9.12d. The concentrations of $H_2$ and CO increase with the power in these four types of measurements. A higher power implies a higher potential difference between the two electrodes and the free plasma electrons need a shorter mean path to reach the needed energy for dissociating the starting material. The result is a higher concentration of hydrogen and carbon monoxide.

Three effects are observed by changing the inlet flow to higher methane concentrations. Firstly, the concentration of the $H_2$ increases. The reason is the higher amount of hydrogen sources ($CH_4$) so that reaction (9.19) becomes more likely. The biggest amount of hydrogen (53%) was generated at a power of 70 W and an inlet flow consisting of methane and water in the absence of $CO_2$. Secondly, there is a decrease of the carbon monoxide amount. More methane reduces the source for CO via reaction (9). 51% is the highest observed amount of CO. The results shown in Figure 12d were achieved without any carbon dioxide; nevertheless, the amount of CO reaches a value of about 4%. The following reactions [21] are possible to form this product in absence of $CO_2$ and presence of water:

$$H_2CO + OH \rightarrow CHO + H_2O \quad (9.21)$$

$$CHO + OH \rightarrow CO + H_2O \quad (9.22)$$

This is not a one step mechanism and, therefore, the concentration of carbon monoxide is low.

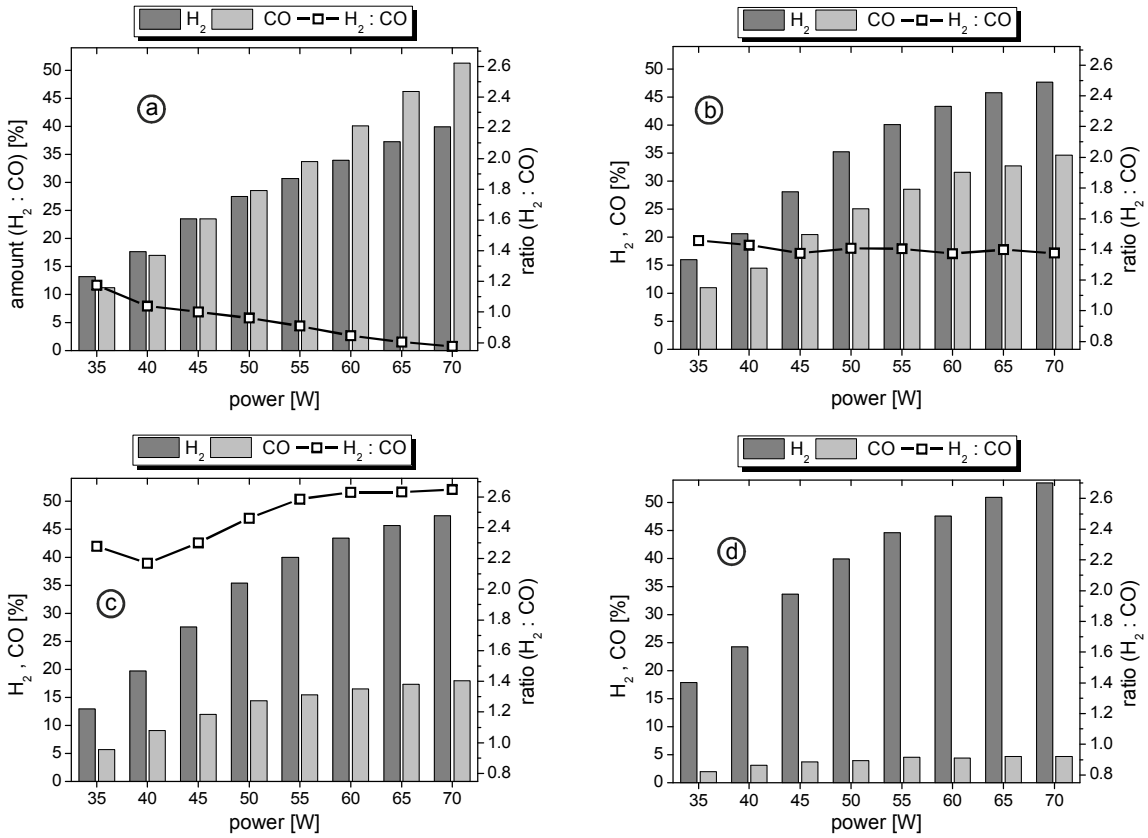


**Figure 9.12:** Yield of the synthesis gas components and their ratio ($H_2$:CO) on the plasma power for different composition of the inlet flow at a fixed amount of water (17%). a) 41.5% $CH_4$ and 41.5% $CO_2$ b) 50% $CH_4$ and 33% $CO_2$ c) 67% $CH_4$ and 16% $CO_2$ d) 83% $CH_4$ and 0% $CO_2$. All gas flows were diluted with helium to 3%.

Thirdly the ratio of the synthesis gas components decreases with the methane concentration, because the $H_2$ concentration increases and the CO concentration decreases with a higher methane concentration in the inlet flows. The ratio ranges from 0.8 to 2.7. The CO amount is for the measurements without carbon dioxide very low and the $H_2$:CO ratio is therefore very high (7 to 11). This is for clarity reasons not displayed in Figure 9.12d. The value is also beyond the limits for industrial applications. With the following parameters it is possible to convert the generated synthesis gas in a hydroformylation reaction: 41.5% $CH_4$, 41.5% $CO_2$ and 17% water; flow rate: 200 sccm; power: 50 W. The amount of water has to be changed to use the generated synthesis gas in a Fischer Tropsch reactor.

### 9.3.4 C2 hydrocarbons

Beside the already discussed products other clearly identified compounds are C2 hydrocarbons. This reactor also generates hydrocarbons with more than two carbon atoms. However, these species do not have characteristic peaks in an IR- or mass spectra. Therefore, it is not possible to determine any quantitative amounts for these substances.

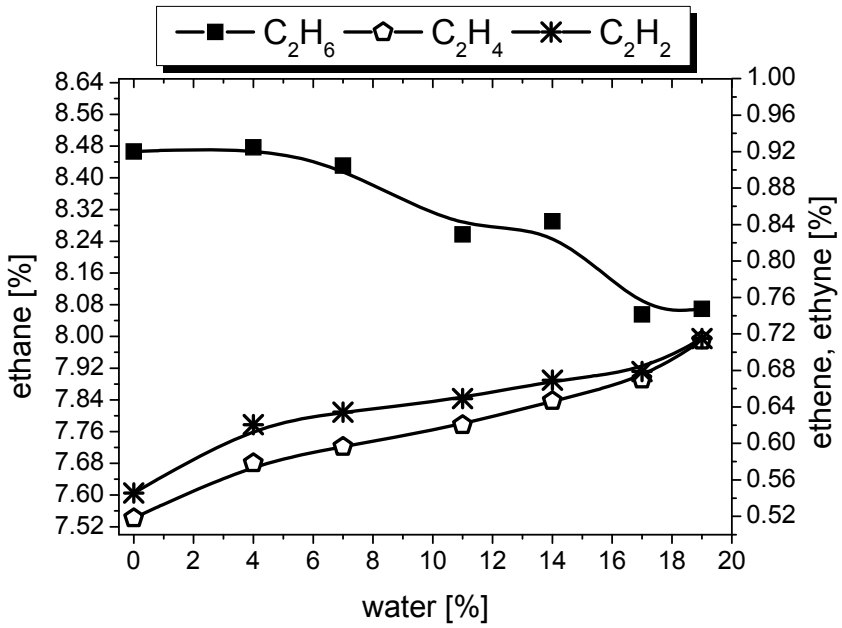


**Figure 9.13:** Yield of C2 hydrocarbons in a DBD reactor. The gas flow without water consisted of 80% methane and 20% carbon dioxide and was diluted to 2.5% with helium. The power was adjusted to 60 W.

Figure 9.13 shows the produced amount of C2 hydrocarbons as a function of the introduced amount of water. Ethane is the major organic compound produced. Ethyne

and ethene concentrations are one order of magnitude lower. Two steps are required to form ethane in comparison to three or four steps to form ethene or ethyne. The details are discussed in a previous article [15]. Water has a very small effect on the yield of these three hydrocarbons. Since the creation of these three products requires only the collision of methane and a $CH_x$ radical. No radicals originating from water are required for this process. The fluctuation of ethane concentration in Figure 9.13 is arranged in the range of error.

### 9.3.5 Total consumed energy

The energy required to convert one mole of substance is important to get information about an industrial application. Formula (9.23) is used to calculate the total consumed energy (SE) of this process.

$$SE = \frac{P}{\dot{n}[CO_2],conv + \dot{n}[CH_4],conv} \tag{9.23}$$

with P = measured power (VI Probe) [W]

$\dot{n}[x],conv$ = molar flow rate of reactant x converted [mol/s]

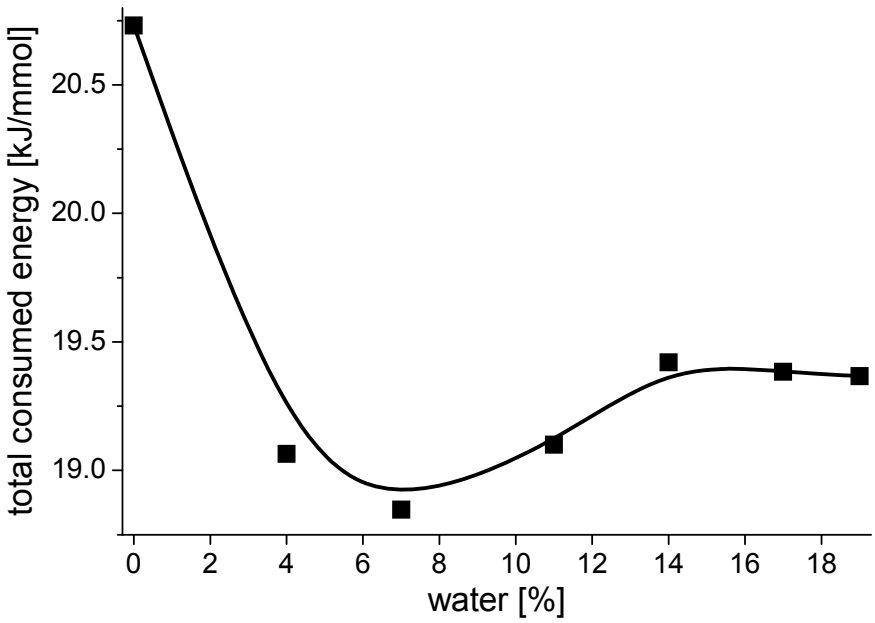


**Figure 9.14:** Total consumed energy for the conversion in this DBD reactor for different water amounts. The gas flow without water consisted of 80% methane and 20% carbon dioxide and was diluted to 2.5% with helium. The power was adjusted to 60 W.

Figure 9.14 illustrates the trend of the total consumed energy as a function of the introduced amount of water. A small amount of additional water decreases the SE for this process from 20.7 kJ/mmol to 18.8 kJ/mmol if the additional water increases up

to 7%. The energy to dissociate water via reaction (9.10) is slightly lower than for carbon dioxide by reaction (9.9). The result is a higher concentration of OH radicals which will convert methane (Reaction (9.12)). The SE rises if the amount of water increases above 7%. The reached value is below the value for measurements without water.

In comparison to our experiment Tao et al [5] reported in their review article from 2011 a total consumed energy of a DBD reactor between 7.3 kJ/mmol and 10.4 kJ/mmol. The present work doesn't focus on reaching low energy consumptions, but to observe relative trends when water is added. The SE differences could be received by using different frequencies (high frequency vs. radio frequency).

## 9.4 Conclusion

The current work focuses on the influence of water on the plasma assisted conversion of methane and carbon dioxide. The water amount was altered between 0% and 19%. The main products are the synthesis gas components $H_2$ and CO and ethane. Ethene, ethyne, formaldehyde and methanol are observed in lower concentrations. Water has a positive effect on:

- the conversion of methane. Additional water increases the conversion of this product from 48% to 58%.
- the yield of the oxygenated hydrocarbons. The generated amount of formaldehyde rises by a factor of 3 and methanol by a factor of 4.
- the yield of hydrogen. Water is an additional source for the production of this molecule.
- the $H_2$:CO ratio. This ratio is important for industrial applications like Fischer Tropsch reactions or hydroformylations. This parameter is adjusTable by using wet conditions with different amounts of water.
- the total consumed energy. A small amount of water decreases the total consumed energy from 20.7 kJ/mmol to 18.8 kJ/mmol, i.e. almost 10%.

Water has a negative influence on:

- the conversion of carbon dioxide. The conversion of $CO_2$ decreases from 36% to 31%.

The following substances are nearly unaffected by water:

- carbon monoxide
- C2 Hydrocarbons

A numerical summery of the effect of water in this experiment is shown in Table 9.1.

The second part of this work focused on the effect of the power and the composition at a constant water amount on the conversion of the starting material and the product distribution. The conversion of methane and carbon dioxide as well as the concentration of the synthesis gas components rises with increasing plasma power. The oxygenated compounds like methanol and formaldehyde reach their maximum at medium power levels.

**Table 9.1:** Summery of the wet conditions.

| What? | Observation | Situation |
|---|---|---|
| Conversion methane | +17% | Increasing $H_2O$ amount (0% to 19%) |
| Conversion $CO_2$ | -12% | |
| Yield formaldehyde | +64% | |
| Yield methanol | +74% | |
| Yield hydrogen | +36% | |
| Yield CO | ≈ constant | |
| $H_2$:CO | +17% | |
| Yield C2 hydrocarbons | ≈ constant | |
| Total energy consumption | -9% | Increasing $H_2O$ amount |

Methane rich streams increase the yield of methanol and hydrogen and the $H_2$:CO ratio. A higher amount of $CO_2$ has a positive effect on the produced amount of CO. The concentration of formaldehyde reaches its maximum for nearly the same amount of CO and $CH_4$.

To sum up, additional water increases the conversion of methane, the yield of $H_2$ and oxygenated hydrocarbons (methanol and formaldehyde) and reduces the total consumed energy.

**Acknowledgement**

This project is part of the framework of the European Research Area (ERA) Chemistry call. This work is financially supported by the Deutsche Forschungs-Gemeinschaft (DFG). Support by the IGSM Braunschweig is gratefully acknowledged. We acknowledge K. Krawczyk and M. Młotek for fruitful discussions.

## 9.4 References for section 9


1. Angelidaki I, Ellegaard L, Kioer Ahring B (2003) Applications of the Anaerobic Digestion Process. Adv Biochem Eng Biot 82:1-33
2. Hilkiah Igoni A, Ayotamuno MJ, Eze CL, Ogaji SOT, Probert SD (2008) Designs of anaerobic digesters for producing biogas from municipal solid-waste. Appl Energ 85:430–438
3. Rasi S, Veijanen A, Rintala J (2007) Trace compounds of biogas from different biogas production plants. Energy 32:1375–1380
4. Moreau M, Orange N, Feuilloley MGJ (2008) Non-thermal plasma technologies: New tools for bio-decontamination. Biotechnol Adv 26:610–617
5. Tao X, Bai M, Li X, Long H, Shang S, Yin Y, Dai X (2010) $CH_4$-$CO_2$ reforming by plasma - challenges and opportunities. Prog Energ Combust 37:113-124
6. Sentek J, Krawczyk K, Młotek M, Kalczewska M, Kroker T, Kolb T, Schenk A, Gericke K-H, Schmidt-Szałowski K (2010) Plasma-catalytic methane conversion with carbon dioxide in dielectric barrier discharges. Appl Catal B 94:19–26
7. Istadi N, Amin AS (2006) Co-generation of synthesis gas and C2C hydrocarbons from methane and carbon dioxide in a hybrid catalytic-plasma reactor: A review. Fuel 85:577–592
8. Kroker T, Kolb T, Schenk A, Krawczyk K, Młotek M, Gericke K-H (2012) Catalytic Conversion of simulated Biogas mixtures to Synthesis Gas in a Fluidized Bed Reactor Supported by a DBD. Plasma Chem Plasma P 32:565–582
9. Rico VJ, Hueso JL, Cotrino J, González-Elipe AR (2010) Evaluation of Different Dielectric Barrier Discharge Plasma Configurations As an Alternative Technology for Green C1 Chemistry in the Carbon Dioxide Reforming of Methane and the Direct Decomposition of Methanol. J. Phys. Chem. A 114:4009–4016
10. Eliasson B, Liu CJ, Kogelschatz U (2000) Direct Conversion of Methane and Carbon Dioxide to Higher Hydrocarbons Using Catalytic Dielectric-Barrier Discharges with Zeolites. Ind. Eng. Chem. Res. 39:1221-1227
11. Liu C-J, Xue B, Eliasson B, He F, Li Y, Xu G_H (2001) Methane Conversion to Higher Hydrocarbons in the Presence of Carbon Dioxide Using Dielectric-Barrier Discharge. Plasmas Plasma Chem Plasma P 21:301-310
12. Kroker T, Kolb T, Krawczyk K, Mlotek M, Schenk A, Gericke K-H (2010) Catalytic conversion of biogas in a fluidized bed reactor supported by a DBD. Front Appl Plasma Technol 3:69-73
13. Zhang Y-P, Li Y, Wang Y, Liu C-J, Eliasson B (2003) Plasma methane conversion in the presence of carbon dioxide using dielectric-barrier discharges. Fuel Process Technol 83:101-109
14. Mfopara A, Kirkpatrick MJ, Odic E (2009) Dilute Methane Treatment by Atmospheric Pressure Dielectric Barrier Discharge: Effects of Water Vapor. Plasma Chem Plasma P 29:91–102
15. Kolb T, Kroker T, Gericke K-H (2012) Conversion of Biogas like Mixtures to C2 Hydrocarbon in a Plug Flow Reactor Supported by a DBD at Atmospheric Pressure, Vaccum doi: 10.1016/j.vacuum.2012.01.013
16. Kroker T (2010) Qualitative und Quantitative Produktanalyse der Katalytischen Konvertierung von Biogas in Plasmagestützten Rohrströmungsreaktoren. PHD Thesis TU Braunschweig
17. Goujard V, Tatibouet JM, Batiot-Dupeyrat C (2011) Carbon Dioxide Reforming of Methane Using a Dielectric Barrier Discharge Reactor: Effect of Helium Dilution and Kinetic Model, Plasma Chem Plasma P 31:315-325
18. Drake GWF (2002) Progress in helium fine-structure calculations and the fine-structure constant, Can. J. Phys. 80:1195-1212
19. deB. Darwent B (1970) Bond Dissociation Energies in Simple Molecules. NBSDS-NBS 31
20. Wang Q, Yan BH, Jin Y, Cheng Y (2009) Investigation of Dry Reforming of Methane in a Dielectric Barrier Discharge Reactor. Plasma Chem Plasma P 29:217–228
21. Liu CJ, Mallinson R, Lobban L (2009) Nonoxidative Methane Conversion to Ethine over Zeolite in a Low Temperature Plasma. J Catal B 179:326–334
22. Tsang W, Hampson RF (1986) Chemical kinetic data base for combustion chemistry. Part I. methane and related compounds. Journal of Physical and Chemical Reference Data 15:1087-1279

23. Kogelschatz U (2003) Dielectric-barrier Discharges: Their History, Discharge Physics, and Industrial Applications. Plasma Chem Plasma P 23, 2003,1-46
24. Iglesia E (1997) Design, synthesis, and use of cobalt-based Fischer-Tropsch synthesis catalysts. Appl Catal A 161:59-78
25. Beller M, Cornils B, Frohning CD, Kohlpaintner CW (1995) Progress in hydroformylation and carbonylation. J of Mol Catal A 104:17-85
26. Pasel J, Samsun RC, Schmitt D, Peters R, Stolten D (2005) J. Power Sources 152:189-195

# 10 Conversion of methane and carbon dioxide in a DBD reactor – influence of oxygen

**Torsten Kolb, Jan H. Voigt, Karl-Heinz Gericke**

**Institut für Physikalische und Theoretsiche Chemie**

Braunschweig, 38106, Germany

**ABSTRACT**

A continuous plug flow reactor supported by a dielectric barrier discharge (DBD) is used to study the conversion of methane, carbon dioxide, and oxygen at different compositions. The three studied gases were diluted with helium to 3% with an overall flow rate of 200 sccm. The 13.56 MHz plasma was ignited at atmospheric pressure. The product stream and the inlet flow were analyzed by a FTIR spectrometer equipped with a White-cell and by a quadrupole mass spectrometer. The DBD reactor generates hydrogen, carbon monoxide, ethane, ethene, ethine, formaldehyde, and methanol. Additional oxygen in the feed has positive effects on the yield of methanol, formaldehyde and carbon monoxide and reduces the total consumed energy. The hydrogen yield reaches its maximum at medium amounts of oxygen in the inlet flow. The conversion of methane increases to a limiting value of about 35%. Methane rich feeds increase the yield of hydrogen, ethane and methanol. On the other hand, additional oxygen has a negative influence on the produced amount of C2 hydrocarbons. The conversion of methane and carbon dioxide as well as the yield of synthesis gas components and C2 hydrocarbons increases by changing the plasma power to higher values.

**KEYWORDS**: cold plasma, dielectric barrier discharge, methane, oxygen, online monitoring

## 10.1 Introduction

Fossil fuels like crude oil or natural gas will be exhausted in the near future. These substances are not only used as a power fuel or to generate heat or electricity, but also source for producing organic basic chemicals via thermal or fluid catalytic cracking [1]. Our work deals with the development of a new technique to generate synthesis gas and basic organic chemicals like C2 hydrocarbons and oxygenated hydrocarbons i.e. methanol and formaldehyde from alternative sources.

The conversion of gas mixtures of the dangerous gases carbon dioxide and methane is one solution for this problem. $CO_2$ is obtained by burning fossil fuels while methane is the main component of natural gas. A mixture of both gases is generated in biogas, landfill or sewage plants by anaerobic microbial mineralization of organic compounds. The regenerative starting material for this process is organic solids. The main products are methane (40%-70%) and carbon dioxide (30%-50%) with oxygen, hydrogen, nitrogen and hydrogen sulfide being generated in minor concentration [2, 3].

To effectively convert methane and carbon dioxide, their reactivity has to be increased. One way to achieve that is the use of a non thermal plasma like a dielectric barrier discharge (DBD), a gliding arc, a corona discharge or a microwave discharge. Here, the low temperature of the molecules and ions and the high energy of the free electrons (up to 10 eV) is an advantage [4]. In this work a DBD reactor powered by a RF generator was used to ignite the plasma. Advantages of this plasma source are the absence of sparks and arcs, the flexibility of the reactor geometry, and the scale up [5].

The conversion of methane and carbon dioxide in a DBD reactor has been studied in many research projects. Synthesis gas components [6-10] (hydrogen and carbon monoxide), hydrocarbons [11, 12] and oxygenates [13, 14] have been obtained as products. Some research groups [15-21] have already studied the influence of oxygen on the plasma assisted conversion of $CH_4$ and $CO_2$ mixtures in a DBD reactor in the low and high frequency (40-5000 Hz) range. However, no investigations at radio frequencies were performed. Thus, our research concentrates on the radio frequency range at 13.56 MHz. However, no investigations at radio frequencies were performed.

In our current research the effect of oxygen on the conversion of methane and carbon dioxide mixtures is analyzed. For this study the amounts of the three inlet gases

and the plasma power have been altered. The primary aim of this work is to increase the conversion of the reactants and the yield of the products.

## 10.2 Experimental Setup

The experimental setup has been described in detail in a previous paper [12]. A fourth mass flow controller (MFC) has been used in this research in comparison to the previous work. These four MFCs have been used to adjust the 200 sccm gas flow consisting of methane (1.25-2.5%), carbon dioxide (0-1.25%) and oxygen (0-1%). The remaining volume is our carrier gas, helium. These gas mixtures have been converted in a cylindrical DBD reactor at atmospheric pressure. A RF-generator and a matching network have been used to ignite the 13.56 MHz plasma. An Octive VI probe has been used to measure the voltage, the current and the phase shift between them in order to calculate the total consumed energy. This device is located between the plasma generating unit and the reactor. The reactor has a capacity of 32 nF which has been determined via impedance spectroscopy.

The reactor temperature reaches about 100°C at the highest plasma power (70 W). The details for this measurement are explained in an article representing previous work [6].

For the analysis of the inlet gas and the product stream of IR active species a FTIR spectrometer has been used at a resolution of 0.5 $cm^{-1}$ and a pressure of 100 mbar equipped with a White - Cell providing an optical path length of up to 6 meter. All compounds which do not show a characteristic IR peak or are IR inactive have been monitored by a quadrupole mass spectrometer at a pressure of $10^{-5}$ mbar.

## 10.3 Results and discussion

We have analyzed the recorded IR spectra between 5000 and 500 $cm^{-1}$ and identified carbon monoxide, formaldehyde, methanol, ethene and ethine [13]. Hydrogen, methane, ethane, oxygen and carbon dioxide have quantitatively been studied in the mass spectrometer. Methane and carbon dioxide have characteristic IR peaks, but they absorb too intensively and for methane the C-H stretch around 3000 $cm^{-1}$ is characteristic for all hydrocarbons.

Helium has been used for dilution and to facilitate the ignition of the plasma. Hence, this gas is neglected in the following discussion. Nevertheless, it should be mentioned, that helium is a very important reagent in DBD condition. Many molecules are

generated from helium. This noble gas can transfer energy to the molecules methane and carbon dioxide after a collision.

Two different kinds of measurements have been performed to study the influence of oxygen on the plasma assisted conversion of methane and carbon dioxide (see Section 10.3.1). The concentration of oxygen has been altered between 0 and 29% in the first set of measurements. In that case, the undiluted gas flow without oxygen has consisted of 100% methane and the power has been fixed to 35 W.

At this plasma power the concentration of the oxygenated products reached the highest values (see Section 10.3.2). In the second part of this work the power (0-70 W) and the composition of the inlet stream have been varied (see Section 3.2). The concentration of methane has been altered between 41.5 and 83% at a fixed amount of oxygen (17%) and carbon dioxide has accordingly been added to reach 100%.

All measurements were carried out three times in order to access reproducibility and experimental errors. The product yields, conversions of the starting material, selectivities and the total consumed energy were averaged, and the error bars represent the standard deviation of the three measurements.

The following formulas were used to calculate the conversion (C) of the starting material and the selectivity (S) of the particular products:

$$C_x = \frac{n_{x,conv.}}{n_{x,0}} \quad \text{, where x represents } CO_2, CH_4 \text{ or } O_2; \; n_{x,conv} = n_{x,0} - n_{x,end} \tag{10.1}$$

$$S_{H_2} = \frac{n_{H_2}}{2 \cdot n_{CH_4,conv.}} \tag{10.2}$$

$$S_{CO} = \frac{n_{CO}}{n_{CH_4,conv.}} \tag{10.3}$$

$$S_{C_2H_b} = \frac{2 \cdot n_{C_2H_b}}{n_{CH_4,conv.}} \qquad \text{with b = 2, 4 or 6} \tag{10.4}$$

$$S_{CH_3OH} = \frac{n_{CH_3OH}}{n_{CH_4,conv.}} \tag{10.5}$$

$$S_{CH_2O} = \frac{n_{CH_2O}}{n_{CH_4,conv.}} \tag{10.6}$$

The total consumed energy (TCE) is calculated by the following formula:

$$TCE = \frac{P}{\dot{n}_{CH_4,conv.} + \dot{n}_{CO_2,conv.} + \dot{n}_{O_2,conv.}} \qquad (10.7)$$

with P = measured power (VI Probe) [W]

$\dot{n}_{x,conv.}$ = molar flow rate of reactant x converted [mol/s]

### 10.3.1 Influence of oxygen on the conversion of methane and on the product distribution

The conversion of methane and oxygen as a function of the added amount of oxygen is shown in Figure 10.1. The conversion of oxygen reaches a maximum value of 79% for measurements with at least 19% oxygen in the inlet gas. Oxygen dissociates in the plasma zone via reaction (10.8) into two O radicals. For low $O_2$ concentrations the probability for a collision of an energy rich electron with an oxygen molecule is lower than for high concentrations, resulting in a smaller conversion for low amounts of oxygen. The conversion reaches a limiting value, because the mean free paths of the electrons are not sufficiently large to dissociate all oxygen molecules upon a collision. Molecular oxygen has a large electron affinity. Thus, this molecule easily captures electrons in the plasma region and reduces their number. In turn, the negatively charged ion ($O_2^-$) with a high reactivity is able to enhance the conversion of methane.

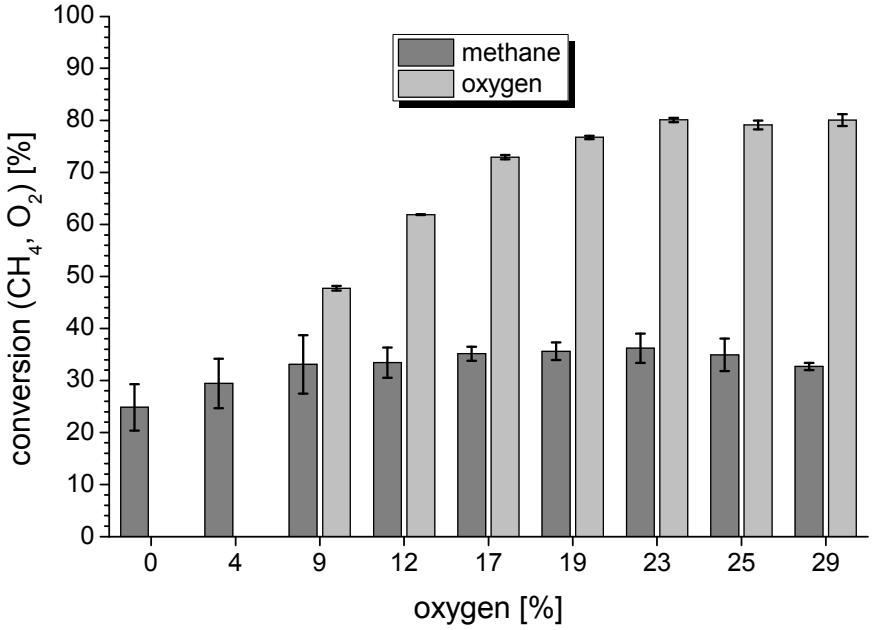


**Figure 10.1:** Conversion of methane and oxygen as a function of the oxygen portion. The undiluted gas flow without oxygen consisted of 100% methane. The power was adjusted to 35 W.

Additional $O_2$ increases the conversion of methane from 25% (without $O_2$) to 35% (17% $O_2$). For higher oxygen concentrations the conversion also approaches a limiting value. These results are explainable by the following reactions occurring as a primary or a secondary reaction in the plasma region.

$$O_2 \xrightarrow{e^-} O + O \tag{10.8}$$

$$CH_4 \xrightarrow{e^-} CH_3 + H \tag{10.9}$$

$$CH_4 + O \rightarrow CH_3 + OH \tag{10.10}$$

$$CH_4 + HO \rightarrow CH_3 + H_2O \tag{10.11}$$

Methane is dissociated through energy rich plasma electrons to a methyl and hydrogen radical (reaction (10.9)), regardless of the presence or absence of oxygen. In the presence of oxygen, the generated O radicals (reaction (10.8)) are very reactive and form an OH radical after a collision with methane (reaction (10.10)). The OH radical can undergo another secondary reaction with methane to form water (reaction (10.11)). Reactions (10.10) and (10.11) become more probable by increasing the concentration of oxygen, resulting in a higher conversion of methane.

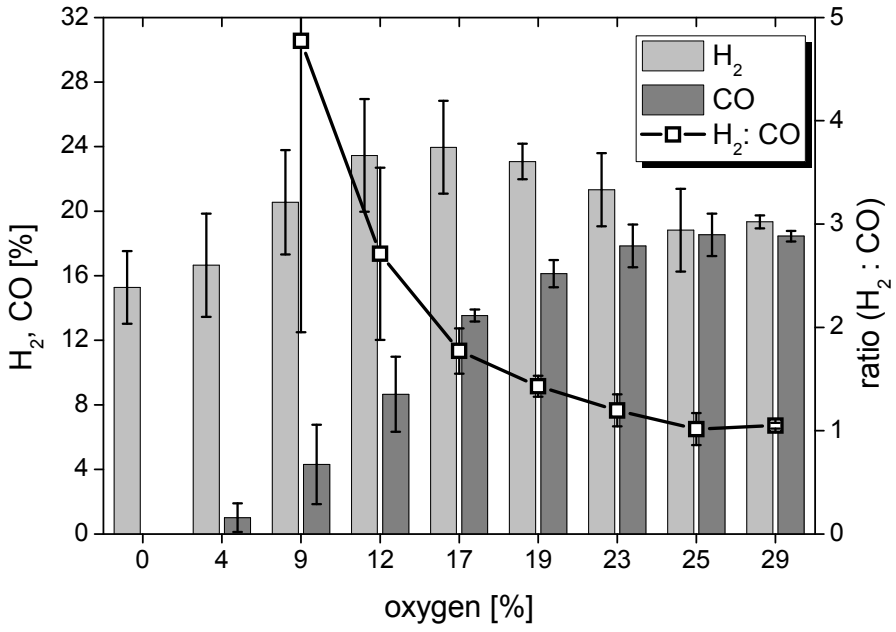


**Figure 10.2:** Product distribution of the synthesis gas components ($H_2$ and CO), left scale, and their ratio ($H_2$:CO), right scale, for different amounts of oxygen in the inlet gas. The undiluted gas flow without oxygen consists of 100% methane. The plasma power was fixed to 35 W at a total flow rate of 200 sccm.

Figure 10.2 to 10.4 illustrate the yields of the identified products as a function of the amount of oxygen in the inlet gas. The main products are hydrogen and carbon monoxide (Figure 10.2), together known as synthesis gas. The generated amount of carbon monoxide grows from 1% to 18% if the oxygen concentration in the inlet gas increases. The hydrogen yield (24%) reaches a maximum at medium oxygen concentrations (17%). These observations are explainable by the reactions (12-14) that lead to the formation of molecular hydrogen.

$$H + H + M \rightarrow H_2 + M \qquad (10.12)$$

M represents another particle or the reactor wall.

$$H + CH_4 \rightarrow H_2 + CH_3 \qquad (10.13)$$

$$CH_2 + O \rightarrow CO + H_2 \qquad (10.14)$$

Molecular hydrogen can either be generated in a three body collision of two hydrogen radicals with another particle or the reactor wall (reaction (10.12)) or via reaction (10.13) following a collision of a hydrogen radical with a methane molecule. Reaction (10.14) comes into play for samples containing additional oxygen where $CH_2$ radicals are generated in a collision of the methyl radical with a plasma electron. This reaction requires an activation energy of 4.9 eV [26]. Since the free electrons of the plasma source have a temperature up to 10 eV [4] this is sufficient for an effective $CH_2$ generation. Reaction (10.14) becomes more relevant with increasing amount of oxygen in the feed resulting in an enhancement of the synthesis gas yield.

The hydrogen yield decreases again at even higher oxygen concentrations because oxygen is then able to react with methane to water (reaction (10.10) and (10.11)).

Another minor pathway is the formation of carbon dioxide following the collision of carbon monoxide with a hydroxyl radical forms carbon dioxide.

$$CO + OH \rightarrow CO_2 + H \qquad (10.15)$$

The generated amount of carbon dioxide is small and therefore not illustrated in Figure 10.2.

In addition to the yields of the synthesis gas components Figure 10.2 also shows their ratio ($n(H_2):n(CO)$). The $H_2$:CO ratio decreases with the addition of oxygen mainly because of the increase of the generated amount of carbon monoxide. Synthesis gas is needed in hydroformylations [22] of unsaturated alkenes or in Fischer Tropsch reactions [23] to produce hydrocarbons. For these reactions particular ratios are required. A $H_2$:CO ratio of 1 is required for hydroformylation while a ratio of 2 is

necessary to produce alkenes. Our results provide the opportunity to adjust this ratio in a simple way by adding the required amount of oxygen.

The very large $H_2$:CO ratio at four percent oxygen content in the starting material is out of the relevant range for industrial applications and is therefore not displayed in Figure 10.2.

Ethane is the third important product in the conversion process beside the two synthesis gas components. Figure 10.3 shows the product distribution of the three C2 hydrocarbons (ethane, ethene, ethine) for different amounts of oxygen.

A small amount of oxygen does not noticeably influence the product concentrations of these compounds as oxygen is not needed at all to generate these products. The detailed mechanism has been discussed in a previous publication [12]. The starting point for this process is methane, dissociating via reaction (10.9) to $CH_3$. In order to form ethane, the methyl radical has then to collide with another methane molecule. For the generation of at ethene and ethine, additional steps are required in which $CH_3$ radicals have to collide one or several times with an energy rich electron to be dissociated to a $CH_2$ or CH radical. Those radicals will then undergo a reaction with methane to form ethene or ethine. Since multiple steps are required to generate the unsaturated hydrocarbons, this concentration is generally low.

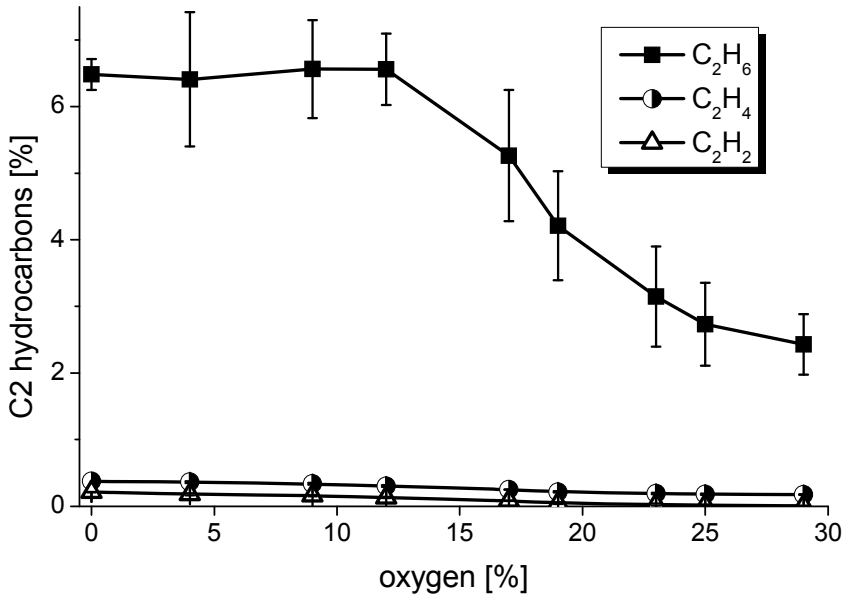


**Figure 10.3:** Yield of C2 hydrocarbons as a function of the amount of oxygen. The undiluted gas flow without oxygen consists of 100% methane. The plasma power was fixed at 35 W at a total flow rate of 200 sccm.

A higher percentage of oxygen has a negative effect on the production of ethane, ethene and ethine. Two processes contribute to the inhibition of C2 hydrocarbons generated upon by adding oxygen. Firstly, oxygen reduces the concentration of methane (water is formed) by reactions (10) and (11). Secondly, the C2 hydrocarbons themselves can be destroyed in reactions with oxygen.

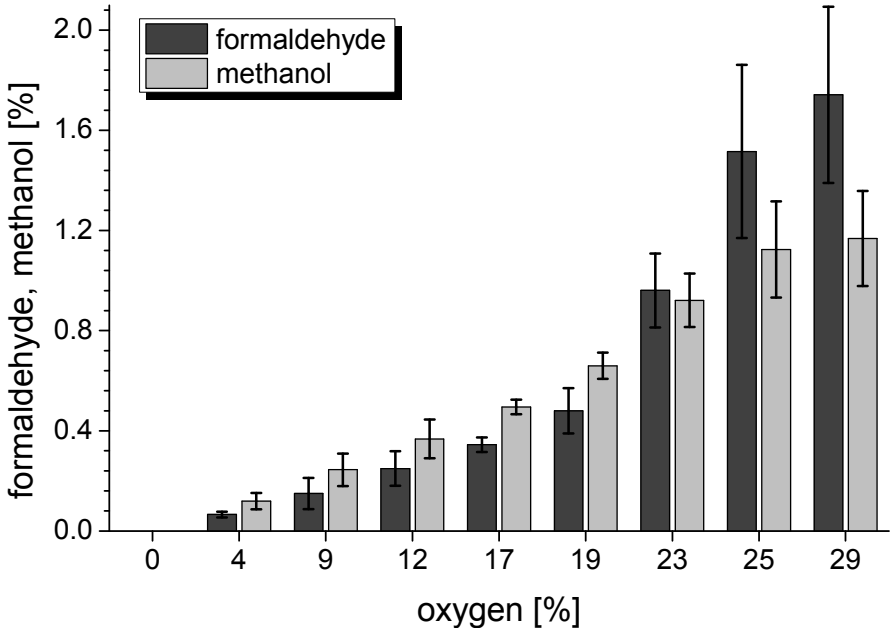


**Figure 10.4:** Methanol and formaldehyde yields as a function of the amount of oxygen. The undiluted gas flow without oxygen consists of 100% methane. The plasma power was fixed at 35 W at a total flow rate of 200 sccm.

The striking contrast, oxygen has a large and positive effect on the produced amount of oxygenated hydrocarbons (methanol or formaldehyde). Our reactor generates maximally 3% of these two products. Figure 10.4 illustrates the dependency of the methanol and formaldehyde yields on the concentration of oxygen in the inlet gas. The amounts of both oxygenated products rise to 1.2% (MeOH) and 1.7% (formaldehyde) by increasing the amount of oxygen to 29%. The generation of these two products can be understood by the following reactions are [24, 25]:

$$CH_3 + O \rightarrow H_2CO + H \qquad (10.16)$$

$$CH_3 + OH \rightarrow CH_3OH \qquad (10.17)$$

Both reactions are collisions of two radicals originating from methane and oxygen, respectively $CH_3$ radicals are generated via the primary reaction (10.9) or via the secondary reaction (10.10) which simultaneously generates the needed OH radical for reaction (10.17). O radicals are created via the primary reaction (10.8) by the ac-

tion of plasma electrons. The concentration of each of the oxygenated products is less than 2% because the radical concentration in weakly ionized plasmas is also low [5] and, therefore, the collision of two radicals is less likely. In addition, oxygenated products are easily destroyed because they are a highly reactive with radicals like OH, O, and H which are formed in large abundance in the DBD reactor during the plasma process.

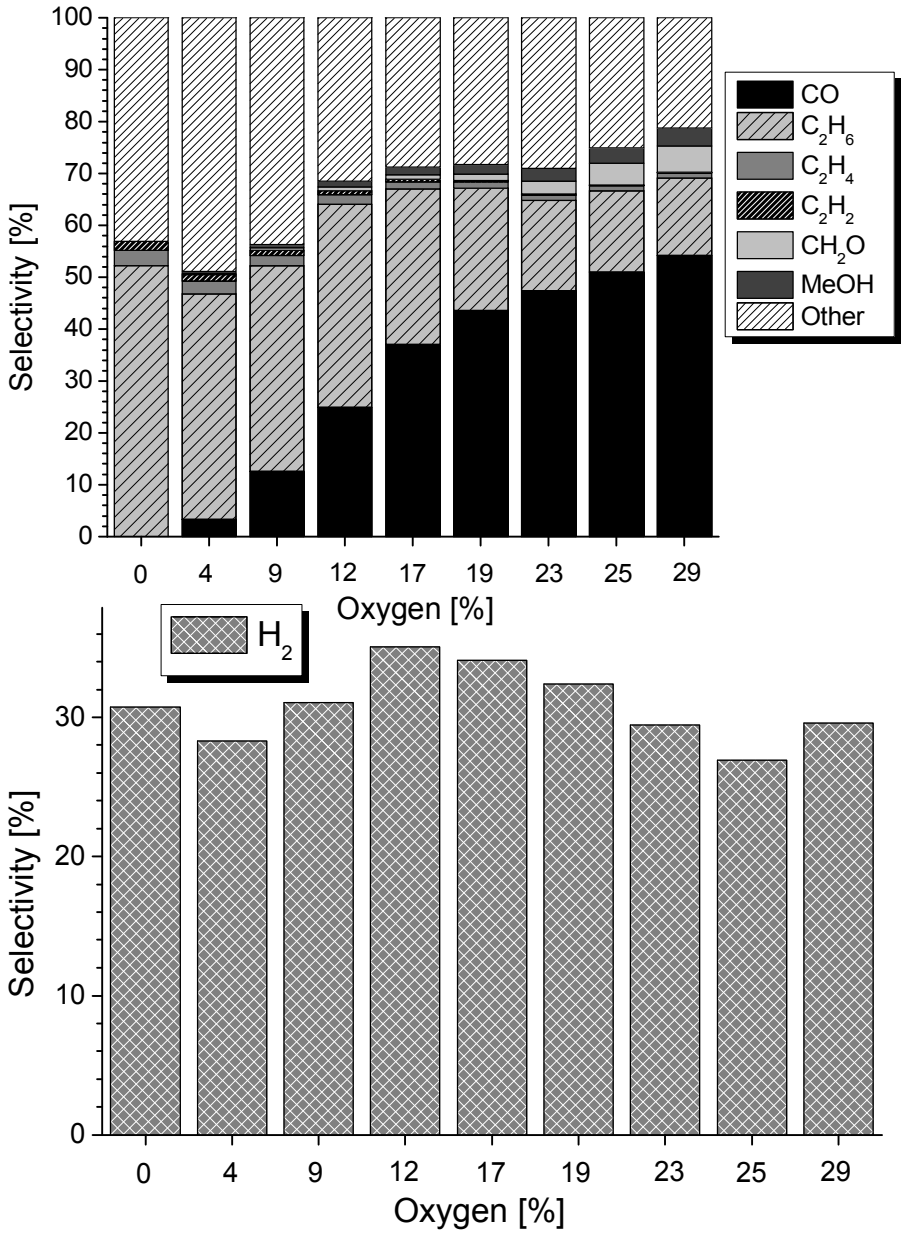


**Figure 10.5:** Above: Selectivity calculated from C balance as a function of the added oxygen. Below: Selectivity of methane to hydrogen. The plasma power was fixed at 35 W at a total flow rate of 200 sccm. a) 0% oxygen, b) 12% oxygen, c) 19% oxygen, d) 29% oxygen.

Larger amounts of oxygen in the inlet gas lead to a higher conversion of the starting material in the DBD reactor; resulting in higher concentrations of the required radicals

for reactions (10.16) and (10.17). As a consequence an increase in the concentration of oxygenates is observed if the oxygen amount in the inlet gas is increased.

Another important aspect which is discussed in the following subsection is the selectivity of the relevant plasma processes. Figure 10.5 illustrates the dependence of the selectivity for methane conversion on the amount of oxygen in the inlet gas. The missing fraction to 100% selectivity being calculated from C-balance is assumed to be due to the generation of higher hydrocarbons which cannot identified quantified with the used FTIR and mass spectrometer. All together, five selectivity effects are observed upon adding oxygen. Firstly, the selectivity for hydrogen formation remains constant with the experimental error. Since no additional reactions generating hydrogen occur after adding oxygen. Secondly, the selectivity for CO increases because of reaction (10.14). Thirdly, the selectivity to form ethane reaches a maximum at a low oxygen concentration. The reason is that starting radicals for the ethane generation are produced from reactions with O radicals with methane and that high concentrations of oxygen combust the methane, resulting in a decrease of the ethane selectivity. Fourthly, the selectivity of the unsaturated C2 hydrocarbons decreases after adding oxygen. Fifthly, the selectivity of the oxygenated hydrocarbons (methanol and formaldehyde) reaches a maximum at a high concentration of oxygen because O radicals are needed to form those products.

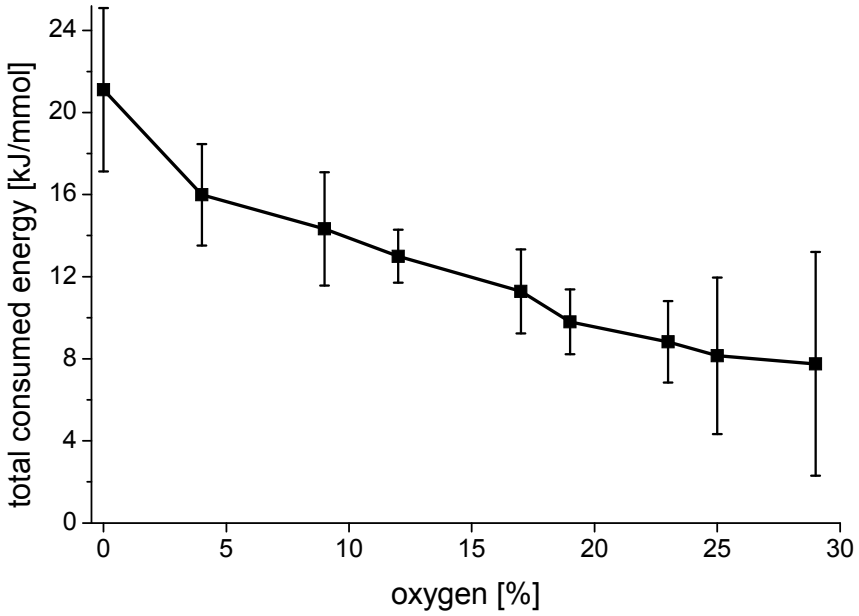


**Figure 10.6:** Total consumed energy for different concentration of oxygen. The undiluted gas flow without oxygen consists of 100% methane. The plasma power was fixed at 35 W at a total flow rate of 200 sccm.

The influence of oxygen in the inlet gas on the total consumed energy is shown in Figure 10.6. Additional oxygen decreases the consumed energy from 21 kJ/mmol to 8 kJ/mmol. Even one oxygen molecule that is dissociated in the DBD reactor via reaction (10.8) into two O radicals will convert four methane molecules via reaction (10.10) and (10.11). Thus, the increase in the conversion effencey goes along with a decrease of the total consumed energy. Similar values of 5 to 10 kJ/mmol have been reported in the literature [4, 16] for a DBD reactor. However, the present work has not focused on minimizing the energy consumption, but instead to investigate and understand relative trends in product composition when oxygen is added.

### 10.3.2 Influence of methane, carbon dioxide, and plasma power on the product distribution.

In Section 10.3.1 we have analyzed the influence of different concentrations of oxygen on the conversion of methane and the product distribution in the DBD reactor at a fixed power (35 W). In this Section we will discuss the influence of different concentrations of methane, carbon dioxide and the variation of the plasma power on the conversion process at a fixed amount of oxygen in the inlet gas (17%).

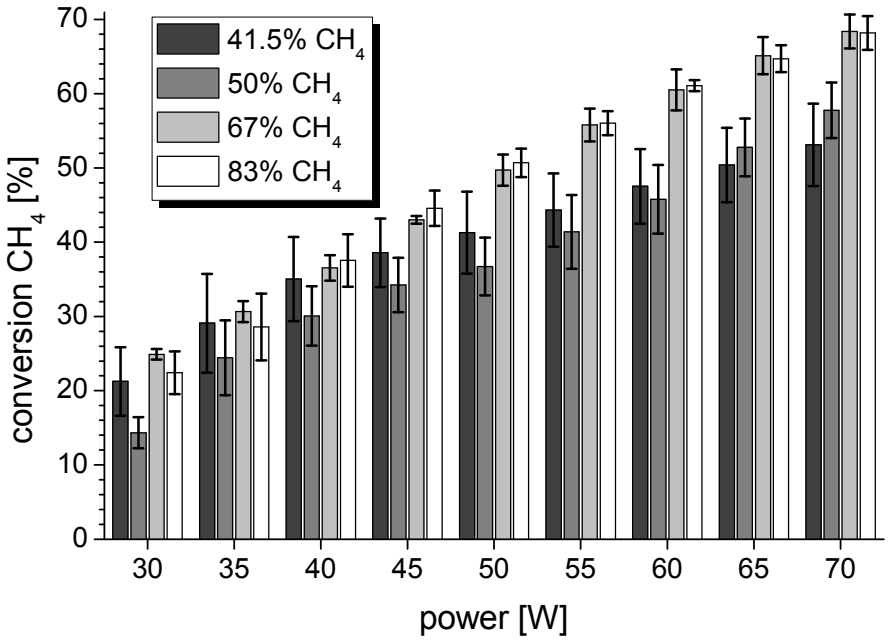


**Figure 10.7:** Conversion of methane as a function of the concentration of the starting material ($CH_4$, $CO_2$ and $O_2$) and the plasma power. The amount of oxygen was fixed at 17%.

Before discussing the product distribution the conversion of the starting materials will be analyzed. The conversion of methane and carbon dioxide as a function of the

plasma power for different compositions of the inlet gas is shown in Figures 10.7 and 10.8. As the number of micro filaments in the reactor rises by increasing the power in the plasma region, the conversion of both components also increases with increasing power.

Generally, the conversion of methane is always larger than the conversion of carbon dioxide. Methane is fragmented by plasma electrons via reaction (10.9), while carbon dioxide is converted by the following process:

$$CO_2 \xrightarrow{e^-} CO + O \qquad (10.18)$$

For the electron assisted dissociation of $CO_2$ (5.52 eV [26]) more energy is required than for the fragmentation of $CH_4$ (4.45 eV [26]), reaction (10.9). Moreover, the additional oxygen from reaction (10.8) is another source to accomplish the conversion of methane via reaction 10.10 while there are no additional reactions of carbon dioxide with oxygen.

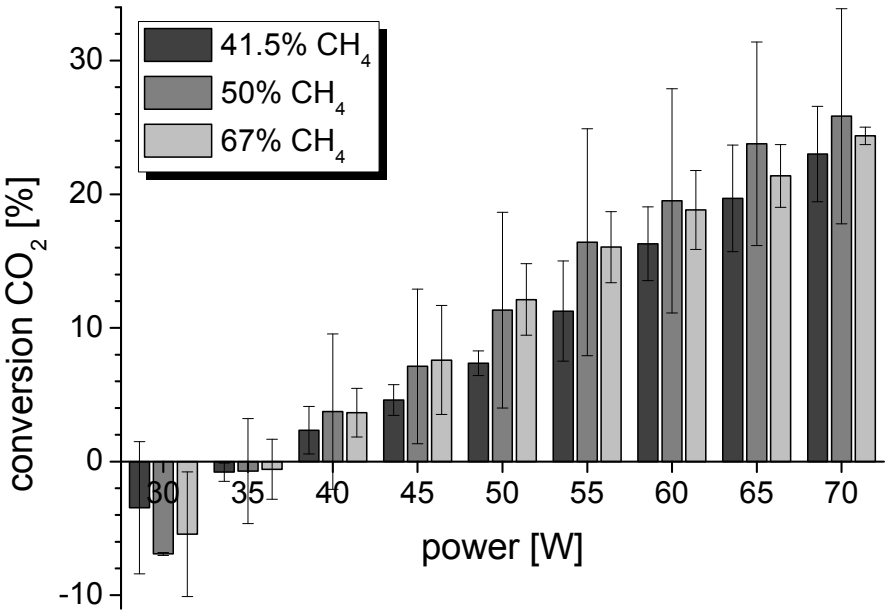


**Figure 10.8:** Conversion of carbon dioxide as a function of the concentration of the starting material ($CH_4$, $CO_2$ and $O_2$) and the plasma power. The amount of oxygen was fixed at 17%.

Negative conversions are observed for carbon dioxide at a power of 30 W and 35 W, i.e. a production of $CO_2$ takes place. Carbon dioxide production occurs either via reaction (10.15) or via back reaction of reaction (10.18). For reaction (10.15) to occur, oxygen needs to form an OH radical first after a collision with methane (reaction (10.10)), which can then collide with CO to form carbon dioxide. The back reaction of reaction (10.18) becomes more likely because additional oxygen increases the con-

centration of O radicals significantly. At low plasma power, the energy of the plasma is not high enough to counter balance this $CO_2$ production by the conversion process. For any fixed plasma power, the highest conversion of methane is reached at the highest concentration of methane and for low amounts of carbon dioxide. For this starting material composition, a collision of a methane molecule with a plasma electron, an O, or an OH radical is most probable.

The conversion of oxygen for different compositions of the inlet gas and the plasma power is listed in Table 10.1. The composition of the inlet gas does not significantly affect the conversion of oxygen because the amount of $O_2$ was fixed only for very large plasma powers a high methane concentration significantly increases the oxygen conversion. At low plasma power (30 W) little more than 50% of $O_2$ is converted. An increase in the power above 30 W generally increases the conversion to a limiting value of around 75% because the plasma electrons cannot dissociate all oxygen within the short residence time of only 320 ms of the starting material in the reactor. Only if the power was increased to 65 W with 83% methane, and at 70 W for the measurement with 67% methane all oxygen molecules could be converted. Under these conditions the concentration of hydrogen radicals in the reactor is very large which react with molecular oxygen to an oxygen radical and a hydroxyl radical.

**Table 10.1:** Conversion of oxygen as a function of the concentration of the starting material ($CH_4$, $CO_2$) and the plasma power. The amount of oxygen was fixed at 17%.

| Power [W] | conversion of oxygen [%] | | | |
|---|---|---|---|---|
| | 41.5% $CH_4$<br>41.5% $CO_2$<br>17% $O_2$ | 50% $CH_4$<br>33% $CO_2$<br>17% $O_2$ | 67% $CH_4$<br>16% $CO_2$<br>17% $O_2$ | 83% $CH_4$<br>0% $CO_2$<br>17% $O_2$ |
| 30 | 64.3 | 54.8 | 58.2 | 65.1 |
| 35 | 64.4 | 70.9 | 65.4 | 72.0 |
| 40 | 74.7 | 74.3 | 70.0 | 74.1 |
| 45 | 76.2 | 74.7 | 71.5 | 74.3 |
| 50 | 76.5 | 74.7 | 72.1 | 75.1 |
| 55 | 76.6 | 74.7 | 72.0 | 75.2 |
| 60 | 77.0 | 75.3 | 72.5 | 75.6 |
| 65 | 77.3 | 75.5 | 73.9 | 100 |
| 70 | 77.6 | 77.8 | 100 | 100 |

The following part of this Section addresses the product distribution. The components are discussed in the order of the influence of additional oxygen.

The influence of different compositions of the inlet gas and of the plasma power on the formaldehyde yield is shown in Figure 10.9. The produced amount of formalde-

hyde reaches the highest values at the lowest power and decreases by increasing the power from 30 to 45 W. The mechanism for the formaldehyde generation has been discussed in Section 10.3.1. The collision of a methyl with an oxygen radical is the final reaction to form formaldehyde (reaction (10.16)) where carbon dioxide is another source for oxygen radicals.

Generally, radicals like OH, H, and O will destroy the formed formaldehyde. As the concentration of these radicals increases with the plasma power, the formaldehyde yield decreases. For plasma powers larger than 40 W and methane pure and rich inlet gas mixtures the $H_2CO$ yield is independent of the plasma power. Here, the formaldehyde yield remains constant because the formation and decay reactions are in equilibrium: with increasing power more O radicals are available to produce CO, but at the same time the concentration of the destructive radicals increases in the same way. For the measurements with 50% or 67% methane the concentration of formaldehyde slightly rises again after increasing the power to values beyond 45 W. Now, reaction (10.18) occurs with a higher probability because the electric field in the reactor rises with the plasma power. The result is a higher concentration of the O radicals which are required for reaction (10.16).

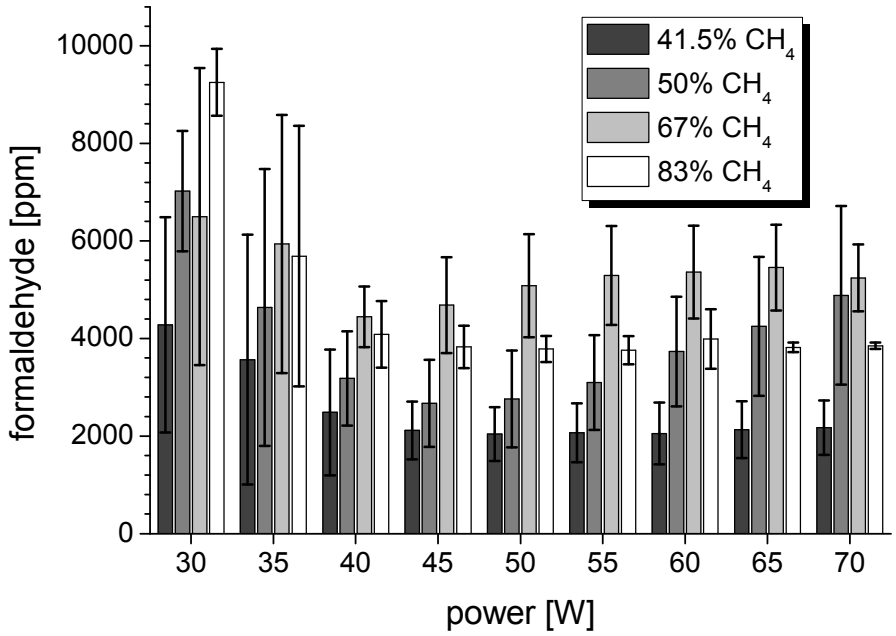


**Figure 10.9:** Formaldehyde yield for different compositions of the inlet gas and plasma power. The amount of oxygen is fixed at 17%.

In general, the highest formaldehyde yield is found for measurements with 67% methane, 16% $CO_2$ and 17% $O_2$ for any fixed plasma power. Only for the lowest power, a higher methane concentration leads to a higher formaldehyde concentration.

The concentration of the methanol product decreases with the power as shown in Figure 10.10 for different compositions of the inlet stream. The formation process in this case is a collision of two radicals ($CH_3$ and OH) via reaction (10.17). The decrease of the methanol yield is explained by the formation of other reactive radicals in the DBD reactor. The details are discussed in the formaldehyde paragraph above.

In contrast to the case of formaldehyde the production of methanol increases with increasing concentration of methane in the inlet gas at any fixed plasma power. The concentration of $CH_3$ radicals in the DBD reactor is larger at a higher methane concentration. Thus, the collision of an OH radical with a $CH_3$ radical becomes more probable.

The highest concentration of methanol (7100 ppm) is generated at a power of 30 W and for a carbon dioxide free inlet gas consisting of 83% methane and 17% oxygen only.

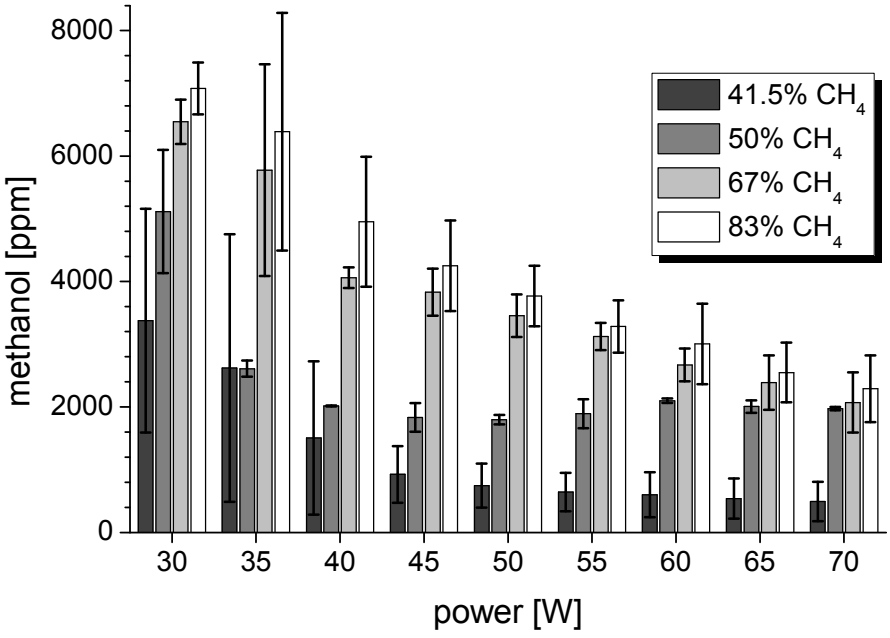


**Figure 10.10:** Influence of the plasma power and the composition of the inlet gas on the concentration of methanol. The amount of oxygen is fixed at 17%.

Figure 10.11 illustrates the dependency of the hydrogen and carbon monoxide yields on the composition of the inlet gas. For all inlet gas compositions, the yield of the synthesis gas components (hydrogen and carbon monoxide) increases when the

plasma power rises from 30 W to 70 W. The mechanism for the generation of these products is discussed in Section 3.1 for measurements without carbon dioxide. Carbon monoxide is generated via the primary plasma (reaction (10.18)), via reaction (10.14) reaction or by a collision of methanol or formaldehyde with an oxygen or hydroxyl radical. Reaction (10.19) and (10.20) illustrate the latter pathway for the example of the collision of formaldehyde with an O radical.

$$H_2CO + O \rightarrow CHO + OH \quad (10.19)$$

$$CHO + O \rightarrow CO + OH \quad (10.20)$$

If the application of energy is increased by increasing the power, the number of micro filaments is accordingly increasing resulting in a higher amount of radicals generated via reaction (10.8), (10.9) and (10.18). Some of the formed species are the starting point to form synthesis gas.

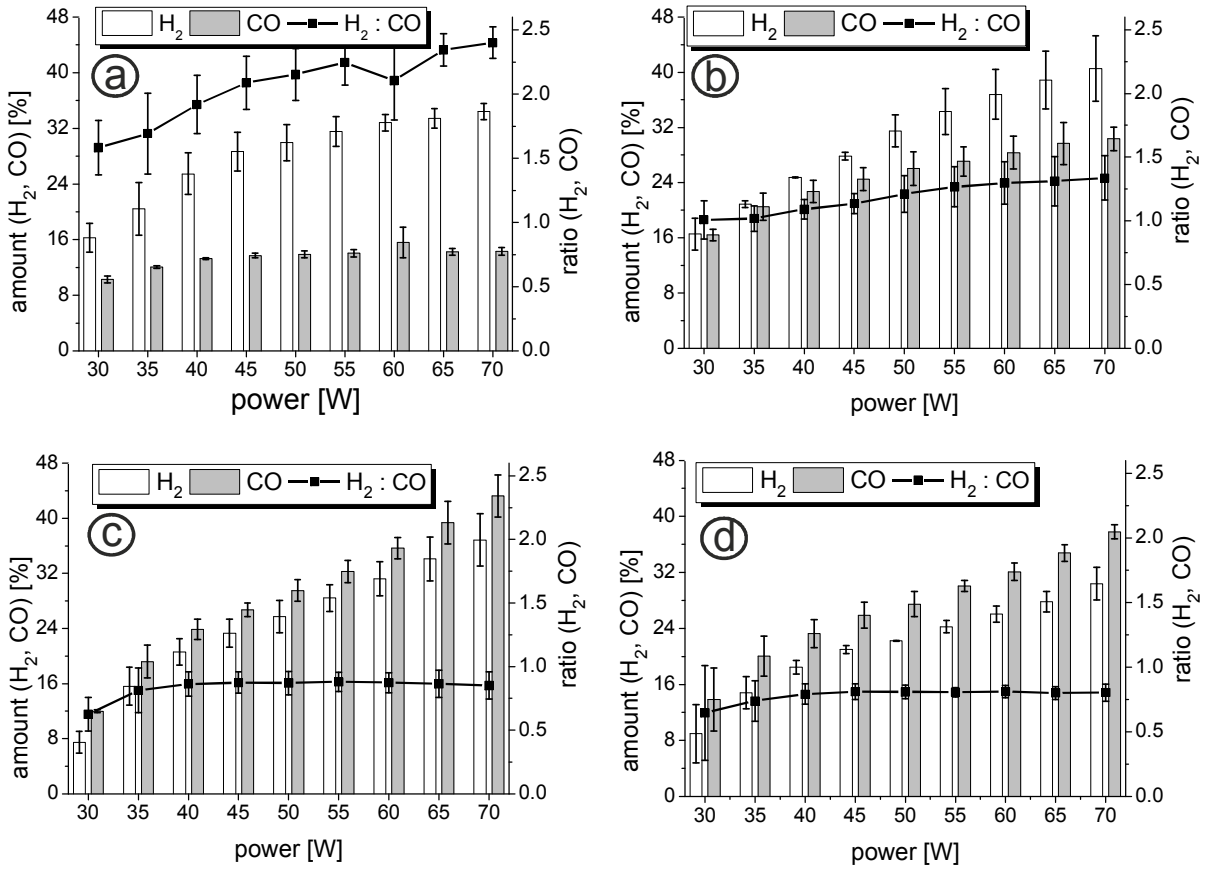


**Figure 10.11:** Yield of the synthesis gas components as a function of the power and the composition of the inlet gas at a fixed amount of oxygen (16%) a) 83% $CH_4$, 17% $O_2$ b) 67% $CH_4$, 16% $CO_2$, 17% $O_2$ c) 50% $CH_4$, 33% $CO_2$, 17% $O_2$ d) 41.5% $CH_4$, 41.5% $CO_2$, 17% $O_2$.

Figure 10.11a-d shows the synthesis gas formation for decreasing the concentration of methane in the inlet gas. The produced amount of hydrogen reaches a maximum

for 67% $CH_4$, 16% $CO_2$, 17% $O_2$ (see Figure 10.11b). The formation of $H_2$ in the absence of carbon dioxide is discussed in Section 10.3.1 resulting from reaction (10.13) (collision of H with $CH_4$) and (10.14) ($CH_2$+O). Additional $CO_2$ in the reaction mixture forms formaldehyde which is able to react with hydrogen radicals to form molecular hydrogen:

$$CH_2O + H \rightarrow HCO + H_2 \qquad (10.21)$$

This reaction reaches the highest probability at low concentrations of carbon dioxide (Figure 10.11b).

The concentration of product carbon monoxide does not reach its maximum for the highest concentration of reactant carbon dioxide. The CO product can be produced by one or more of the following mechanism:

1) Dissociating of $CO_2$ via plasma electrons (reaction 18)
2) The reaction of a $CH_2$ radical with an O radical (reaction (14))
3) The destruction reaction of formaldehyde and methanol via O or OH radicals (reaction (19) and (20)).

The optimum for the CO yield is achieved for a composition consisting of 50% $CH_4$, 33% $CO_2$, and 17% $O_2$.

The ratio of the two synthesis gas components ($H_2$:CO) is an important factor for industrial application. This parameter decreases by increasing the amount of carbon dioxide in the inlet gas. In that case, the amount of hydrogen decreases, while the concentration of CO increases. The ratio is independent of the plasma power for measurements with a large carbon dioxide concentration in the inlet gas (Figure 10.11c and d). A methane rich inlet stream generates a ratio of $H_2$:CO that increases by increasing the plasma power (Figure 11a and b).

The highest concentration of hydrogen (41%) is generated in a mixture, consisting of 67% $CH_4$, 16% $CO_2$, and 17% $O_2$ at a power of 70 W. 44% is the highest produced amount of CO for the same concentration. The $H_2$:CO ratio of 2 (Fischer Tropsch synthesis to methanol or alkenes) is reached for the following parameters: 83% $CH_4$, 17% $O_2$ and 45 W. Hydroformylation ($H_2$:CO=1) reactions are realizable at a power of 30 W and an inlet gas consisting of 67% $CH_4$, 16% $CO_2$, 17% $O_2$. For higher power, the methane concentration has to be slightly reduced as can be concluded from Figure 10.11b and c.

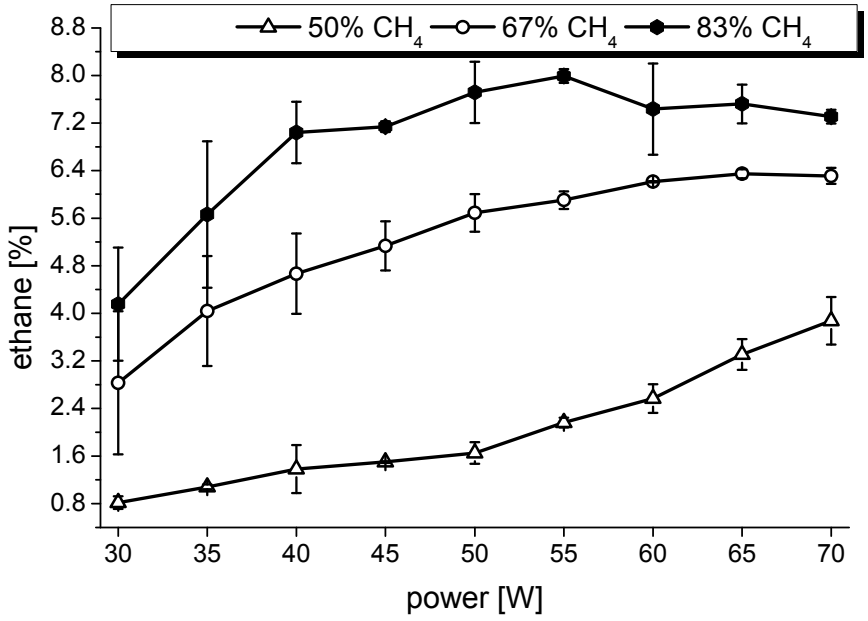


**Figure 10.12:** Influence of the plasma power and the composition of the inlet gas on the ethane yield. The amount of oxygen is fixed at 17%.

The amount of ethane rises with increasing the power from 30 W to 70 W (Figure 10.12). A higher plasma power represents a higher concentration of the required $CH_3$ radicals which are needed to form ethane:

$$CH_4 + CH_3 \rightarrow C_2H_6 + H \qquad (10.22)$$

A higher concentration of methane in the inlet gas increases the concentration of ethane at any fixed plasma power. Higher concentrations of the $CH_3$ radicals are generated in a reaction mixture consisting of mostly methane to undergo reaction (10.22). No ethane at all has been detected for measurements consisting of 41.5% or less methane in the inlet gas. The unsaturated C2 hydrocarbons are not discussed in this Section because their yield is smaller than 0.7% and oxygen has only a minor effect on the distribution of these products.

## 10.4 Conclusion

The current work discusses the influence of oxygen on the plasma assisted conversion of methane and carbon dioxide in a DBD reactor. The main products for this conversion process are hydrogen and carbon monoxide (synthesis gas), and ethane. The DBD reactor also generates ethene, ethine, formaldehyde, and methanol in minor concentrations. The inlet and the product flow compositions have been analyzed

by quadrupole mass spectrometry and FTIR spectroscopy supported by a White - cell.

Oxygen increases the yield of methanol by a factor of 10 and the yield of formaldehyde by a factor of 26 at a fixed plasma power of 35 W. The methane conversion rises from 25% under oxygen free conditions to a limiting value of approximately 35% with oxygen. The hydrogen concentration reaches a maximum at 17% of oxygen in the inlet gas. Additional $O_2$ is able to combust methane to carbon monoxide, thus increasing the amount of CO. In contrast, the yield of C2 hydrocarbons drops by adding oxygen. While not in the focus of this work it is worth to note that the total consumed energy is reduced by almost a factor of three by adding oxygen to the inlet gas flow.

In this work we have also analyzed the influence of the plasma power and of different concentrations of methane and carbon dioxide on the product distribution at a fixed amount of oxygen (17%). The yield and the conversion of nearly all products are increased by changing the power to higher values. Only the concentrations of methanol and formaldehyde decrease under these conditions, with the latter approaching a lower limiting value. The concentrations of methanol, hydrogen and ethane rise with increasing concentrations of methane in the inlet gas, while carbon dioxide rich inlet gas increase the amount of produced CO.

It is possible to adjust the composition of the generated synthesis gas such that it can either be used for hydroformylation ($H_2$:CO=1) or for Fischer Tropsch synthesis of alkenes ($H_2$:CO=2) by changing the amount of oxygen, methane and carbon dioxide in the inlet gas mixture and by controlling the plasma power.

The influence of water on the plasma assisted conversion of methane and carbon dioxide has been analyzed in a previous publication [27]. The $H_2$:CO ratio can be controlled by adding water to the inlet gas mixture. The ratio increases upon addition of water. The product gas composition in biogas conversion depends on the experimental conditions. Since the starting material for the conversion of $CH_4$ and CO originating from different regenerative sources (biogas, landfill, or sewage plants) has variable compositions, a required product ratio ($H_2$:CO) is adjustable by adding water or oxygen to mixtures of methane and carbon dioxide.

In addition, it is shown, that an oxygen free apparatus is not necessary for this DBD reactor, thus facilitating its use in every day applications.

**Acknowledgement**

This project is part of the framework of the European Research Area (ERA) Chemistry call. The work is financially supported by the Deutsche Forschungsgemeinschaft (DFG). Support by the IGSM Braunschweig is gratefully acknowledged. We acknowledge T. Kroker for measuring the impedance spectra of our reactor and C. Maul for critically reading the manuscript.

## 10.5 References for section 10

1. Harding RH, Peters AW, Nee JRD (2001) Appl Catal, A 221:389-396.
2. Rasi S, Veijanen A, Rintala J (2007) Energy 32:1375–1380.
3. Rasi S, Läntelä J, Veijanen A, Rintala J (2008) Waste Manage 28:1528–1534.
4. Tao X, Bai M, Li X, Long H, Shang S, Yin Y, Dai X (2011) Prog Energ Combust 37:113-124.
5. Kogelschatz U, Eliasson B, Egli WJ (1997) Phys IV France 07:47-66.
6. Kroker T, Kolb T, Schenk A, Krawczyk K, Młotek M, Gericke K-H (2012) Plasma Chem. Plasma Process 32:565–582.
7. Sentek J, Krawczyk K, Młotek M, Kalczewska M, Kroker T, Kolb T, Schenk A, Gericke K-H, Schmidt-Szałowski K (2010) Appl Catal B 94:19–26.
8. Zhang K, Eliasson B, Kogelschatz U (2002) Ind Eng Chem Res 41:1462-1468.
9. Song HK, Lee H, Choi J-W, Na B (2004) Plasma Chem Plasma Process 24:57-72.
10. Wang Q, Yan BH, Jin Y, Cheng Y (2009) Energy Fuels 23:4196–4201.
11 Li X-S, Zhua A-M, Wang K-J, Xu Y, Song Z-M (2004) Catalysis Today 98:617–624.
12. Kolb T, Kroker T, Gericke K-H (2012) Vaccum doi:10.1016/j.vacuum.2012.01.013.
13. Kroker T, Kolb T, Krawczyk K, Mlotek M, Schenk A, Gericke K-H (2010) Front Appl Plasma Technol 3:69-73.
14. Li Y, Liu C-J, Eliasson B, Wang Y (2002) Energy Fuels 16:864-870.
15. Pietruszka B, Heintze M (2004) Catalysis Today 90:151–158.
16. Larkin DW, Lobban LL, Mallinson RG (2001) Catalysis Today 71:199–210.22.
17. Aghamir FM, Matin NS, Jalili AH, Esfarayeni MH, Khodagholi MA, Ahmadi R (2004) Plasma Sources Sci Technol 13:707–711.
18. Zhou LM, Xue B, Kogelschatz U, Eliasson B (1998) Plasma Chem Plasma Process 18:375-393.
19. Nozaki T, Goujard V, Yuzawa S, Moriyama S, Agiral A, Okazaki K (2011) J Phys D: Appl Phys 44:1-6.
20. Larkin DW, Caldwell TA, Lobban LL, Mallinson RG (1998) Energy Fuels 12:740-744.
21. Baowei W, Xu Z, Yongwei L, Genhui X (2008) J Nat Gas Chem 18:94–97.
22. Beller M, Cornils B, Frohning CD, Kohlpaintner CW (1995) J Mol Catal A: Chem 104:17-85.
23. Iglesia E. (1997) Appl Catal A 161:59-78.
24. Liu C-J, Mallinson R, Lobban LJ (2009) Catal 179:326–334.
25. Tsang W, Hampson RF (1986) J Phys Chem Ref Data 15:1087-1279.
26. deB. Darwent B (1970) Bond Dissociation Energies in Simple Molecules NBSDS-NBS 31.
27. Kolb T, Kroker T, Voigt JH, Gericke K-H (2012) Plasma Chem Plasma Process, DOI 10.1007/s11090-012-9411-y.

# 11 Conclusion

The research work presented in this thesis focuses on the conversion of biogas mixtures in a dielectric barrier discharge (DBD) reactor at atmospheric pressure. The gas mixture was diluted with helium to improve the ignition behavior of the starting material. The yield and the distribution of C2 hydrocarbons products and the influence of reactant additives such as water and oxygen are in the main focus of this work. In addition, the conversion efficiency, the selectivity and the total consumed energy were determined. The analysis of the starting material and the products was proper used in a Fourier transform infrared spectrometer (FTIR) supported by long path cell and in a quadrupole mass spectrometer.

Numerous products are generated during the plasma assisted biogas conversion. Seven important products were analyzed quantitatively. The main products are the synthesis gas components (hydrogen and carbon monoxide) and ethane. Ethene, ethine, formaldehyde and methanol are generated in lower concentrations.

The results of the three research aspects (C2 hydrocarbons as products, water and oxygen as an additive) are described in detail in section 8 to 10.

In summary, the composition of the starting material, the plasma power and the velocity of the gas stream were altered to study the conversion of methane and carbon dioxide to C2 hydrocarbons with ethane being the main C2 hydrocarbon. A low velocity of the gas stream (200 sccm) and a methane rich composition of the inlet flow (2.5% methane and 97.5% helium) yield the highest concentrations of ethane, ethene and ethine in the used DBD reactor. Consequently, all subsequent experiments were carried out at a low volume stream of 200 sccm.

Below, the results of the studies with water and oxygen as additives are summarized together. Experiments were performed at different amount fractions of methane, carbon dioxide and additives and at different plasma power. Both additives increase the yield of methanol and formaldehyde. With respect to synthesis gas composition, the exact ratio of the amount of hydrogen to the amount of carbon monoxide ($n(H_2):n(CO)$) is very important for industrial applications. Synthesis gas compositions can be adjusted by suitable adding water or oxygen to the starting material. Generally, it decreases after adding oxygen and increases with additional water. On the contrary, the effect of the two additives on the C2 hydrocarbons is very low. The overall

conversion efficiency increases for methane and decreases for carbon dioxide after adding the extra substances.

To sum up, additional water and oxygen is another possibility to change the yield of the products and the conversion of the starting material beside the plasma power, the flow rate and the composition of the inlet flow. Carefully adjustment of the starting material with respect to the addition of water and/or oxygen allows one to manipulate the product yield and the product composition in a wide range. As an example, the synthesis gas yield is improved after adding water. Another example, the generated synthesis gas is the starting material for many organic syntheses like the Fischer Tropsch Synthesis or the hydroformylation. All in all, controlling starting material composition with or without carefully chosen additives is a powerful tool for optimizing the conversion process and tailing it to one's needs.

However, therefore aspects of the presented requirements can enter industrial applications, two main issues needed to be addressed which have remained unresolved. First, total energy needs to be further decreased in order for the method to be competitive. Second, the need for helium to improve the ignition behavior of the sample is impractical in industrial environments. Further research would therefore primarily focus on those two issues.

# 12 Acknowledgement

A number of people have generously given time, advice, encouragement and valuable information during the course of this research.

Therefore, I am particularly grateful to my mentor Prof Dr. Karl-Heinz Gericke not only for the interesting and challenging dissertation topic, the friendly integration into the working group, but also for his valuable guidance and patient supervision.

To Dr. Christof Maul I would like to express my gratitude about the helpful discussions and hints for my experiment. In addition, I am very glad that he agreed to accept the responsibility being the second reviewer of my thesis.

Special thanks also to the whole laser chemistry group for the professional working atmosphere. Not to forget the very good cooperation with numerous students who took over the operational part of this experiment for lab courses or final assignments.

Also, I would like to thank Thorsten Kroker for the excellent cooperation and discussions about this demanding project.

I am much indebted to Karl-Peter Ahrens, Thorsten Himstedt, Manfred Hilpert and Bernd Sladeczek for the fast and immediate help in uncountable technical orders.

My special thanks to the glassblower Mr. Schröpfer from the Institute of Inorganic and Organic Chemistry as he prepared the base body of reactors for my experiments.

Thanks are also due to my gratitude Dr. Erik Uhde from the Fraunhofer Wilhelm Klauditz Institute in Braunschweig for measuring the product distribution via gas chromatography.

Furthermore, I would like to thank all persons for reviewing earlier versions of this thesis (or parts of it) and for suggesting helpful improvements.

Finally, the thesis could never have been finished successfully without the understanding and backing of my family and friends, who supported and motivated me in challenging hours of my research and experiments.